#6780

Modeled and Measured Infiltration: Phase II

A Detailed Case Study of Three Homes

TR-102511

May 1993

Prepared by
Ecotope, Inc.
2812 E. Madison
Seattle, WA 98102

Principal Investigators
Larry Palmiter
Tami Bond

Sponsored by
Residential Ventilation Consortium
Current Members:
Electric Power Research Institute
Bonneville Power Administration
Honeywell, Inc.
Pacific Gas and Electric Company

Prepared for
Electric Power Research Institute
3412 Hillview Avenue
Palo Alto, CA 94304

EPRI Project Manager
John Kesselring

Residential Systems Division

ABSTRACT

The primary purpose of this work was to investigate the impacts of wind, temperature and mechanical systems on infiltration in real homes, with a view toward resolving infiltration modeling problems raised in recent studies. This report contains results from the second phase of an ongoing project. In phase I, detailed infiltration and pressure measurements were made by Lawrence Berkeley Laboratory on four homes in the Pacific Northwest. In this phase, similar measurents were made on an additional three homes, chosen for maximal wind exposure. For the reader's convenience the summary tables in this report contain data from all seven homes in a uniform format.

The predictions of two natural infiltration models (LBL and AIM-2) were compared in detail with one another and the measured data. The separate influences of stack- and wind-induced flow are analyzed. The LBL model predictions were about 30% greater than the AIM-2 model; the measured data fell within the range bounded by the two models, and the mean absolute percentage error of both models was about 15%. An improved method of calculating the height parameter for both models is proposed. A modification of the LBL wind model is also proposed.

A simple model is presented to incorporate the infiltration effects of exhaust and supply ventilation systems and unbalanced flows due to duct leakage. An unbalanced flow to the conditioned space induces approximately one-half of its magnitude in additional infiltration when it is small relative to natural infiltration. The measured data agreed reasonably well with the theoretical model.

Forced-air distribution systems were investigated in detail. Air handlers and associated duct leakage can have large effects on living-zone infiltration rates; for these homes the median increase in overall infiltration was 21%, based on a runtime of six hours per day. Closing even a single bedroom door can cause a major increase in infiltration when the air handler runs. Pressures measured across a single closed door ranged from 2-6 Pa. At one site, closing the bedroom door more than doubled the added infiltration produced by the air handler.

The bias due to use of a time-averaged concentration tracer technique (i.e., the perfluorocarbon (PFT) method) was assessed and found to be small for the living zones, and large for the wind-dominated, ventilated crawl space and attic zones.

CONTENTS

Section Page

LIST OF FIGURES

Figure **Page**

LIST OF TABLES

Table **Page**

EXECUTIVE SUMMARY

Air infiltration into residential buildings has important effects on both heat loss and indoor air quality. Recent emphasis by home buyers and builders on energy efficiency has resulted in the construction of tighter homes to reduce air infiltration; however, past assumptions that naturally induced infiltration provides adequate ventilation for a home are no longer valid for modern homes.

The growing attention to indoor air quality has led to the development of minimum ventilation standards and requirements for mechanical ventilation systems. This concern has also resulted in a need for models which accurately predict ventilation rates resulting from natural driving forces and from the operation of mechanical systems.

In 1990, the Residential Ventilation Consortium (RVC) initiated a study to perform detailed infiltration measurements on homes in the Pacific Northwest. The primary purpose of this study was to obtain sufficiently detailed data from a carefully selected sample of houses to resolve identified weaknesses in the LBL model and to enhance our understanding of the effects of mechanical ventilation systems. A previous report presented results from four homes tested during the first year of this project. During the second year, an additional three homes were tested; this report summarizes the methodology used and presents detailed results from the three homes.

For the convenience of the reader, and to enhance the interpretability of the testing done to date, the data from all seven homes are presented in the summary tables. The discussions in the main body of the report, as well as the findings and conclusions are also based on the evidence from all seven homes. A summary of the findings and conclusions is given below.

Suggested Improvements to LBL Model

The analysis to date supports several suggestions for improving the LBL model and the calculation of required inputs.

Throughout this project we have used an average stack height for the height parameter in both the LBL and AIM-2 models. This average stack height was also used for the

NORIS homes. For these 134 homes, the reduction in height was about 32% relative to the height between the lowest leak and the highest leak. The reduction in predicted infiltration is about 16%. For the seven homes tested for this project, the average reduction in height was about 18%, resulting in a 9% reduction in predicted infiltration.

The wind-effect portion of the LBL model produces more accurate results when modified to account more realistically for wind-generated pressures across the floor and ceiling in the case of ventilated attics and crawl spaces. Analysis of the data strongly suggests that the original assumptions made in the LBL model are not justified. The Ecotope-modified LBL wind model typically predicts infiltration rates 28% lower than the original model. The predictions of the modified model agree well with the wind portion of the AIM model which uses the same external pressure coefficient assumptions as the Ecotope modification.

For homes in the Pacific Northwest, the terrain and shielding coefficients should each be set to a value of 4, whereas original LBL defaults were each set at 3. In this study, the extrapolation of airport wind speed to the site was within 6% of the site-measured wind speed, on average.

It should be noted that even when the measured site wind speed is used it was still necessary to reduce the wind speed for best agreement with the tracer-measured infiltration. This may be because the fraction of the leakage in the walls is less than our default assumption of one-half.

Comparison of LBL and AIM-2 Models

The LBL and AIM-2 models differ systematically in their predictions of natural infiltration; the LBL model predictions were 26% greater for the stack effect, 61% greater for the wind effect, and 28% greater for the total natural infiltration. Most of the difference between the two models is due to the consistent use of the blower door C and n in the AIM-2 model.

The wind-effect infiltration predicted by the modified LBL model is about 28% less than that of the standard LBL model and about 16% greater than that of the AIM-2 wind model.

Comparison of Measured and Modeled Infiltration

For these seven homes, both the LBL model and the AIM model had mean absolute prediction errors of 16%, and the modified LBL model had a mean absolute prediction error of 15%.

Effects of Ventilation Systems

Air-to-air heat exchangers typically have two fans; a supply fan pumping outdoor air into a building and an exhaust fan pumping indoor air out. If the supply and exhaust flows are balanced, there is no interaction with natural infiltration. The added infiltration is simply the supply flow through the ventilation system.

If supply and exhaust flows are not balanced, the ventilation system pressurizes or depressurizes the home. Under these conditions, the induced flows interact in a complex fashion with natural infiltration. We have proposed a simplified model of this interaction which agrees reasonably well with the measured data in these homes.

For typical natural infiltration rates seen in energy-efficient all-electric homes, and a typically sized exhaust fan system (50 cfm), it is necessary to operate the system continuously in order to meet ASHRAE Standard 62, which requires a ventilation rate of 0.35 air-changes per hour. Intermittent operation of one to two hours in the morning and evening will produce almost no measurable increase in ventilation.

Effects of Forced-Air Distribution Systems

Forced air distribution systems and associated duct leakage can have large effects on pressures and whole-house infiltration rates. Assuming a standard runtime of 6 hours/day, the median infiltration due to duct leakage was 21% of the total. Infiltration rates are increased both when the fan is off and when it is on.

In these homes, the median increase in natural infiltration due to duct leakage was 14%, which compares with other recent studies indicating a 16 to 20% increase.

The increased infiltration when the fan is on tends to be much larger than the increase in natural infiltration, because the pressures produced by the air handler are much greater than natural pressures.

The measured data also show a large impact on infiltration due to closing one or more doors to bedrooms with supplies but no returns. Typical pressures measured across the bedroom doors were 4 Pascals.

The extension of the fan model to unbalanced flows due to duct leakage agrees reasonably well with the measured data.

Although a return leak and a supply leak of the same magnitude have the same effect on infiltration, supply leaks have much greater impacts on furnace efficiency than do return leaks.

Measured Natural Infiltration

The measured natural infiltration under winter conditions ranged from 0.14 to 0.66 air changes per hour, with an average of 0.37 ACH for the seven homes. Excluding Site 7 with its unusually windy location, the average was 0.32 ACH. Natural infiltration in three of the seven homes would fail to meet the 0.35 ACH minimum ventilation rate required by ASHRAE Standard 62, thus indicating the need for mechanical ventilation. With the exception of Site 7, natural infiltration in these homes is stack-dominated and the additional infiltration due to wind is small.

Time-Averaging Bias

The average bias due to the time-averaging as used in the PFT technique is 5% for living-zone infiltration, 12% for attic infiltration and 15% for crawl space infiltration. The measured data confirm the simulation results, which show that buildings in which the infiltration is totally wind-dominated can have substantial bias; the highest measured was 30% for the crawl space at Site 2. The bias which occurs under stack-dominated conditions is small.

Infiltration Rates in Attics and Crawl Spaces

All of these homes had well-ventilated crawl spaces, and, except for the two manufactured homes, they had ventilated attics. Crawl space infiltration rates averaged 4.6 ACH and attic infiltration rates averaged 6.9 ACH, compared with an average for the living space of 0.37 ACH. The infiltration into attics and crawl spaces is very wind-dominated.

Blower Door Tests

We performed precision blower door tests covering a range of pressures between 1-2 Pa and 60-70 Pa on six of the seven sites. At all sites, except for Site 4, the measured flows at low pressure were less than those obtained by extrapolating using the power law fit obtained from the data taken between 15 and 60 Pa. The exponents estimated from the low-pressure data (roughly 1-10 Pa) were higher in all cases; an average of 0.71 compared with the 0.65 for the conventional pressures.

These results are consistent with the Ethridge model of the pressure-flow relationship. However, in spite of trying to obtain optimum conditions, such effects could also be caused by bias due to pre-existing stack or wind pressures, or by systematic error when using the smallest orifice on the blower door. Similar low-pressure tests should be done on a large number of homes before drawing firm conclusions about the low-pressure relationship.

1

INTRODUCTION AND BACKGROUND

Air infiltration into residential buildings has important effects on both heat loss and indoor air quality. Recent emphasis by home buyers and builders on energy efficiency has resulted in the construction of tighter homes to reduce air infiltration; however, past assumptions that naturally induced infiltration provides adequate ventilation for a home are no longer valid for modern homes.

The growing attention to indoor air quality has led to the development of minimum ventilation standards and requirements for mechanical ventilation systems. This concern has also resulted in a need for models that accurately predict ventilation rates resulting from natural driving forces and from the operation of mechanical systems.

Previous studies in the Northwest compared measured infiltration using the passive tracer technique with predictions from a widely used infiltration model developed at Lawrence Berkeley Laboratory (LBL) (Sherman and Grimsrud, 1980). It was found that the LBL model consistently overpredicted the measured infiltration, and that the magnitude of the discrepancy correlated with amount of wind effect. The stack (temperature-driven) portion of the LBL model appeared to correlate well with the measured infiltration (Palmiter et al., 1991).

These studies also showed that homes with central forced-air heating systems had infiltration rates that averaged 17 to 36% greater than those without such systems and raised questions about the effectiveness of mechanical ventilation systems (Palmiter et al., 1991).

Results from Previous Testing

In 1990, the Residential Ventilation Consortium (RVC) initiated a study to perform detailed infiltration measurements on homes in the Pacific Northwest. The primary purpose of this study was to obtain sufficiently detailed data from a carefully selected sample of houses to resolve identified weaknesses in the LBL model and to enhance our understanding of the effects of mechanical ventilation systems.

During the first year of this study, which is referred to as Phase I, four homes were tested. In these homes, most of the infiltration resulted from the stack effect (pressures across the building envelope induced by indoor-outdoor temperature differences). The

amount of wind-driven infiltration was small. Exhaust fans produced very little overall effect.

Three of the Phase I homes had central forced-air heating systems. These systems can have large effects on living-zone infiltration rates and are still poorly understood, since differential pressures due to closed doors and unbalanced leakage interact with natural infiltration. Duct leakage was found at all three sites; at two of the homes, infiltration rates increased by more than 50% when the air handler was running.

The natural infiltration was predicted using two models: the LBL model and another model developed at the University of Alberta, known as the AIM-2 model (Walker and Wilson, 1990). The difference between the two models was systematic, with the LBL model predictions being greater than those from the AIM-2 model. It was found that the disparity in the two predictions was primarily due to the differing treatment of the envelope leakage function at low pressures.

Measured infiltration data agreed with the predictions of the AIM-2 model at one of the sites and with the LBL model predictions at two sites; at one site, the measured infiltration fell between the two predictions. Of the four homes studied in Phase I, only one had sufficient wind exposure to provide data on the effects of wind.

A simple model for combining the effects of ventilation fans and duct leakage was also developed. This model predicts that unbalanced flows to the conditioned space induce approximately one-half of their magnitude in additional infiltration. Measured infiltration rates from each of the sites agreed well with the predictions of the model. However, exhaust fan use was limited and several types of mechanical ventilation systems used in the Northwest were not represented in the homes measured.

Current Testing

In 1991, the RVC requested that detailed measurements be made on another three homes to clarify some of the questions raised during the first year of testing. The Phase II homes were to be selected to maximize information with regard to wind effects on infiltration and interaction of natural infiltration and mechanical systems.

The Phase II homes were selected for their high wind exposure; the lowest average wind speed among these homes was about the same as the highest average wind speed among the Site I homes. One site in particular, east of the Cascade mountain range, experienced extremely high wind speeds averaging over 11 mph.

The homes in Phase II all had central heating systems: one had a heat pump, one had a gas furnace, and one had an electric furnace. Two of the homes were built to utility energy-efficiency standards and had ventilation systems; one home had a balanced-flow air-to-air heat exchanger and one had a designated bath fan.

In the Phase I study, the most significant issue raised regarding infiltration modeling was the nature of the leakage function at low pressures. The testing for Phase II included low-pressure blower door testing, as well as return visits to the four Phase I homes to complete such tests.

Summary Data for Seven Homes

For the convenience of the reader, and to enhance the interpretability of the testing done to date, the data from all seven homes are presented in the summary tables. The discussions in the main body of the report, as well as the findings and conclusions are also based on the evidence from all seven homes.

The most pertinent characteristics of the homes are summarized in Table 1-1. Note that all but one home had forced air heating systems and four of the homes had designed ventilation systems. All of the homes were located within 100 miles of Seattle, and all but Site 7 were in the Puget Sound area. Most of the Phase I homes were occupied during the tracer tests, but the Phase II homes were not.

Table 1-1
Characteristics of seven homes

	Site 1	Site 2	Site 3	Site 4	Site 5	Site 6	Site 7
Year built	1988	1979	1984	1988	1988	1985	1990
Heating system	Wall htr	HP	Furn	Furn	HP	Furn	Furn
Floor area (ft^2)	1553	2213	1812	1182	3503	1695	1217
Volume (ft^3)	12367	17589	14226	9496	28510	14876	9746
Number of stories	2	2	1.5	1	2	2	1
Occupied for test?	Yes	Yes	Yes	No	No	No	No
Ventilation system	Multiport	None	None	Bath fan	AAHX	None	Bath fan
Air handler location	--	Garage	Garage	House	Closet	Garage	House
Supply duct location	--	Crawl	Crawl	Crawl	Crawl	Crawl	Crawl
Return duct location	--	Attic	House	None	Attic	Attic	None

Outline of Report

The main body of this report is organized in terms of the various factors that affect infiltration; conclusions are supported by data from the seven houses. Detailed information and measurement results for the three homes tested under Phase II are presented in Appendices A through C; these appendices are completely self-contained and can be read without reference to the main report. Similar information for the four homes tested during Phase I is given in appendices in the Phase I report.

In the main body of the report, a tutorial introduction to the principles of infiltration is given in Section 2. Measurement and analysis procedures used for the three homes are reviewed in Section 3. Section 4 contains an assessment of environmental conditions at the homes. In Section 5, the effects of wind on infiltration are discussed.

Results from low-pressure blower door testing on all seven homes are presented in Section 6. Section 7 contains a comparison of measured infiltration with that predicted by models. In Section 8, a discussion of bias caused by time-averaging of tracer concentrations is given. Effects of mechanical systems, including ventilation and heating systems, are described in Section 9. Section 10 contains our findings and conclusions, as well as a summary of suggested modifications to the LBL infiltration model.

After the appendices containing the detailed results from each home, wind pressure coefficients measured at each home are given in Appendix D. Appendix E contains graphical results from the low-pressure blower door tests. Equations for the LBL and AIM models are given in Appendix F.

Acknowledgements

This work could not have been accomplished without the help and cooperation of many people. The field work was done primarily by Darryl Dickerhoff of LBL with assistance from Brian Smith of LBL and the authors. Jim Bellamy of Tacoma City Light, Michael Lubliner of the Washington State Energy Office, and Shannon McCormick of Puget Power assisted with the recruitment of the Phase II homes. Ian Brown, Carolyn Roos, and Mark Frankel of Ecotope assisted in the preparation of this report. Final editing, layout, and administration were cheerfully provided by Michael Geffon of Ecotope. Max Sherman of LBL provided assistance with the theory and interpretation of the data. David Wilson of the University of Alberta assisted with the use and interpretation of the AIM-2 model. John Kesselring of EPRI, the project manager, provided support and encouragement throughout both phases of this work. It is a pleasure to thank all of them for their capable advice and support.

Last, but not least, we thank the homeowners who vacated their homes for almost a week so that the measurements could be done under controlled experimental conditions.

2

PRINCIPLES OF INFILTRATION

Natural infiltration stems from two driving forces: wind-generated pressures on the building exterior and buoyancy pressures due to density differences between the interior and exterior. In keeping with tradition, buoyancy effect is referred to as stack effect, so called because the equations are similar to those used to predict flow in a chimney or stack.

The two driving forces interact with each other and the leakage characteristics of the building in a complex fashion. Liddament gives a good elementary discussion of wind and stack pressures in homes (1986). Discussion of air flow around buildings, including wind pressure coefficients, is contained in Chapter 14 of the ASHRAE Handbook (1989c). In both the LBL and AIM-2 models, the wind and stack effects are calculated separately and then combined. Further details are given in a recent paper by Sherman (1990).

The magnitude of the induced pressures is generally small. Under typical Northwest heating-season conditions (a temperature difference of 23 F between indoors and outdoors), the stack-induced pressure across the floor or ceiling is about 1.2 Pa for a two-story home or 0.6 Pa for a one-story home. Assuming wall-averaged wind pressure coefficients of 0.5, a wind speed of 4 mph produces a pressure of about 1 Pa across the walls.

In spite of the mild climate, previous studies (RSDP, NORIS, and RCDP) have suggested that heating season infiltration in Northwest homes is stack dominated. One reason for this is that the stack effect is always present during the heating season and thus operates continuously. Another reason is the tendency for homes to have significant leaks in the ceiling due to fan, wiring, plumbing and access penetrations.

Stack Pressure and Neutral Level

Because the stack effect is so important, a review of some of the terminology of this effect is in order. A diagram of pressures due to stack effect in winter conditions is shown in Fig. 2-1. The bold lines show inside and outside pressures. Both of these pressures decrease with height in accordance with the hydrostatic equation. However, under these conditions the outdoor air is colder and thus more dense, so the rate of decrease with height of the outdoor pressure is greater than that for the warmer indoor

air. The point where the two lines cross is called the neutral level because the pressure across the walls at that height is zero.

The pressure data presented in this report are expressed as inside pressure minus outside pressure. As Fig. 2-1 shows, this gives negative delta pressures at the floor and positive delta pressures at the ceiling. The ceiling delta pressure minus the floor delta pressure gives a parameter called the stack pressure, which is positive under winter conditions.

The exact position of the interior pressure line, and therefore the neutral level, is determined by the location of the leaks. If there are more leaks in the ceiling, the neutral level moves closer to the ceiling. If the neutral level is halfway up, the pressure across

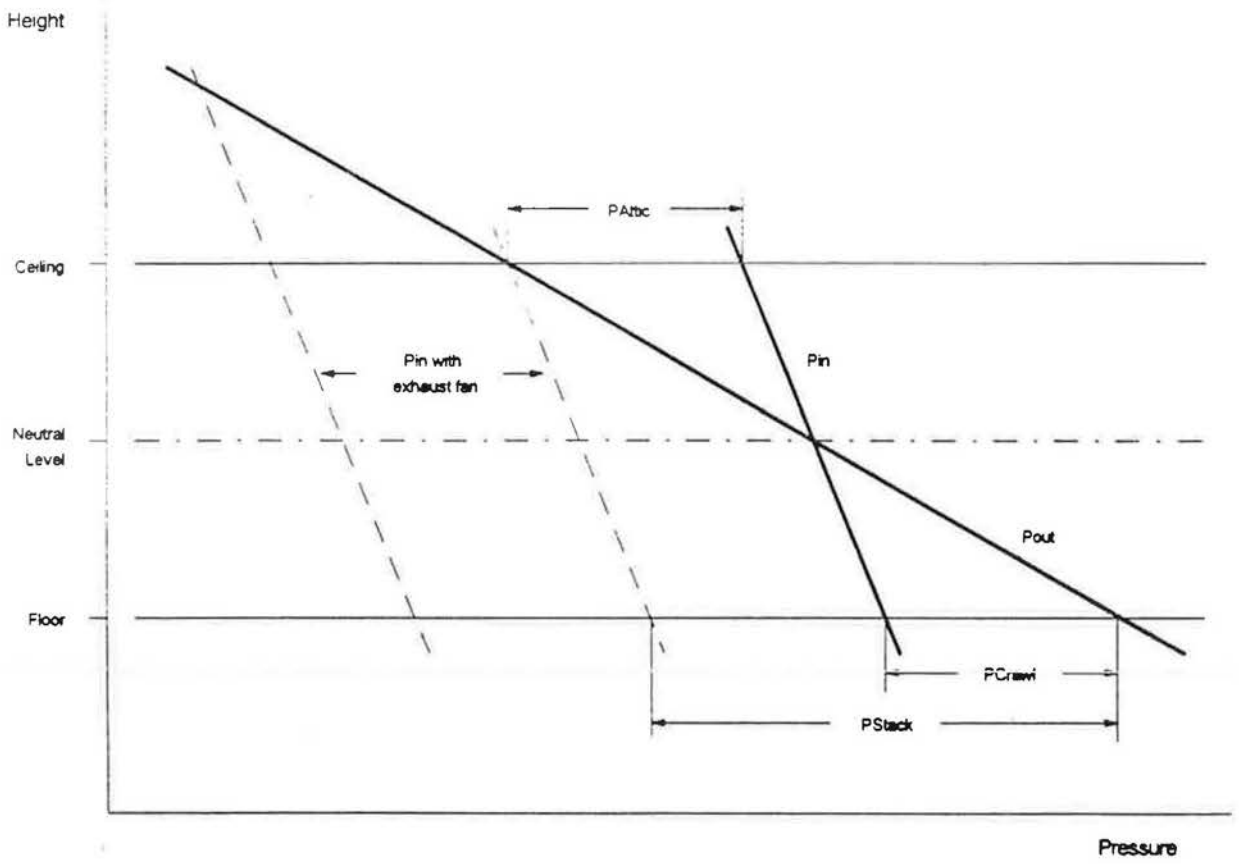

Figure 2-1
Pressures due to stack effect and exhaust fans

The graph is not to scale; for clarity, the pressure differences at the floor and ceiling have been exaggerated. The dashed lines show the change in internal pressure caused by two sizes of exhaust fan: one which just raises the neutral level to the ceiling and one which raises the neutral level above the ceiling.

the floor and ceiling are each half the stack pressure.

Under stack-only conditions, the neutral level can be no higher than the highest ceiling and no lower than the floor. In the case of a simple rectangular box, it is convenient to express it in dimensionless form as a fraction of the total height of the building.

The location of the interior pressure line or the neutral level is also affected by fans. When fans are operating, the neutral level can be far above the ceiling or far below the floor. As shown in the figure, an exhaust fan depressurizes the home, shifting the internal pressure line to the left and increasing the neutral level. It is important to note that the exhaust fan reduces the natural exfiltration through the ceiling. This effect is the basis of the fan infiltration model discussed in Section 9.

Wind can also shift the internal pressure line. Wind pressures are typically positive on one wall and negative on the other three walls. Therefore, the action of wind tends to depressurize the home, shifting the internal pressure line to the left.

Indoor and outdoor densities determine the slopes but not the positions of the pressure lines. The stack pressure is proportional to the density difference between outdoor and indoor air and to the height of the home, but is independent of the location of the leaks.

It is important to distinguish between the neutral level due to stack effect only and that resulting from stack effect combined with fans and wind effects. In Figure 2-1, the stack neutral level is 0.5, and with the small exhaust fan running the neutral level is 1.0. The neutral level referred to in the LBL model and in Sherman's recent paper (1990) is that due to stack effect only; this will be referred to as the stack neutral level.

Leakage Ratios

The infiltration rate due to stack and wind depends on both the total leakage area and on the distribution of leakage area. The infiltration models discussed later characterize the leakage distribution by the parameters R and X, where R is the fraction of total leakage in the floor plus ceiling (and 1-R is the fraction in the walls) and X is the ceiling leakage area minus the floor leakage area expressed as a fraction of the total.

Of the two parameters, R has the largest effect. Larger values of R enhance the stack effect and reduce the wind effect; smaller values have the opposite effect. Unfortunately, there is no known way to measure or accurately estimate the value of R for a given home. It has been traditional to assume a value of 0.5 for R. This assumption was also used for the model runs in this study.

The parameter X is closely related to the stack neutral level; in fact, one formulation of the LBL stack model uses X and R as the parameters. It is usually assumed that X=0, corresponding to a stack neutral level of 0.5. That is, the stack neutral level is halfway

between the floor and ceiling. The predicted infiltration is not very sensitive to variations of the stack neutral level in the range from 0.4 to 0.6.

The measured stack neutral levels of the four homes in Phase I of this study were close to midway between the lowest floor and the highest ceiling, suggesting that a value of 0.5 for the stack neutral level is reasonable.

Stack Height

Both infiltration models considered in this study use building height as a parameter in calculating stack-induced infiltration. The models assume that a home is a simple rectangular box; the height used in these models is measured from the lowest floor to the highest ceiling.

The simple box model is usually not valid for homes in the Northwest. The second floor is generally of a different size than the first floor. There are typically cantilevers and overhangs, and offsets between floors. The garage is usually either integral (part of the conditioned area is above or below it) or attached. Daylight basements with the lower floor partially below grade are common.

The use of an average stack height for this parameter has been proposed previously. This is defined as the average height of a column of warm air which displaces outdoor air. For example, consider a home of daylight basement construction in which the lower floor is half below grade and half of the lower floor is a two-car garage (a common home type in this area). By the standard rules (ASHRAE 1989b), the height is from the lowest leak above grade to the highest ceiling. This gives a full height of about 16 feet. However, because the lower floor is half below grade, it would count as only 4 feet high; because it is half unheated garage the height would be reduced to only 2 feet. The average stack height would then be 10 feet as opposed to 16 feet, a reduction of 38% in height and about half that in infiltration.

In the NORIS study, the average height of 134 homes from the field data was 17.3 feet, and the average stack height was 11.7 feet, a reduction of 32%. The heights of the seven homes in the present study are compared in Table 2.1. Using the concept of average stack height has reduced the heights in these homes by an average of 18%. This correction applies to both the AIM-2 and LBL models and was used in all of the model runs presented in this report.

This correction had no impact on the wind prediction in this study because the wind data were taken from the site towers as measured. However, if the wind data are extrapolated from airport wind data, the use of the average stack height also results in a reduction of wind effects.

It is strongly advised that one should only use the actual house height or the rules given in the ASHRAE standard when the home is really a rectangular box totally above grade.

For the more complex geometries typical of the Northwest, the average stack height should be used in order to avoid a systematic overprediction of the stack effect. The average height so defined is a relatively crude, first-order correction. However, until further theory or field work has resulted in an improved correction, the average stack height is proposed as the height parameter for the simple infiltration models discussed in this paper.

Table 2-1
Comparison of average stack height and full height

	Height (ft)		
	Full	**Avg. Stack**	**Ratio**
Site 1	16.3	13.7	0.85
Site 2	16.3	13.5	0.83
Site 3	16.3	10.5	0.65
Site 4	9.3	8.1	0.87
Site 5	17.7	14.5	0.83
Site 6	16.3	14.5	0.89
Site 7	9.4	8.0	0.85
Average			0.82

3

METHODOLOGY

Only unoccupied homes were tested in Phase II. During the Phase I testing, it was found that occupant behaviors such as opening windows, closing internal doors, and operating fans led to many uncertainties in the testing conditions. Therefore, homes were selected in which the owners were willing to vacate for at least one week.

Air infiltration into the heated space, as well as flows within the living space and between the living space and buffer zones such as the attic and crawl space, was measured using LBL's multitracer measurement system (MTMS). This system operated in the constant injection mode. A description of this system is given by Sherman and Dickerhoff (1989).

The MTMS injects a measured quantity of tracer gas into a zone and measures the concentrations of that gas in each designated zone. When a different tracer gas is injected into each designated zone, flows through and between zones can be calculated from the measured concentrations and injection rates. Tracer gas was injected at two to five points in each zone, each equipped with a continuously operated mixing fan. There were two or three sampling points in each zone. The MTMS made one complete cycle through the zones every three to four and one-half minutes, depending on the site.

The living areas of each home were divided into tracer zones based on the anticipated airflow within the home. At Site 5, which had three clearly distinct levels, each level was measured as a tracer zone. Site 6 had a cathedral ceiling in the living room which would allow mixing of the air between the first and second stories; therefore the entire living space was measured as a single zone. Site 7 was a small manufactured home and its living space was also measured as a single zone. In addition, the attic, crawl space and garage were measured as separate zones where possible.

Air flows through each zone, as well as flows between zones, were calculated from the MTMS injection and concentration measurements using a sophisticated computer program developed at Ecotope.

Natural infiltration is driven by pressure differences across the envelope; hence, pressures across the walls, floor and ceiling are important in helping to understand the causes of infiltration. In each home, at least two pressure differences each across the floor and ceiling were measured. Pressures were also measured across each exterior face at each level of the home; at Site 7, which was only one story but experienced high

wind speeds, pressure differences at two heights were measured on some of the walls. These pressure data were recorded every 30 seconds.

An additional pressure transducer with a scanning valve was used to measure pressure differences sequentially at nine or ten points across the envelope or across interior doors in the home. Although these pressures were measured infrequently--approximately once every six minutes-- they are useful for making estimates of the typical magnitudes of pressures at such points.

Each zone, including the attic, garage, and crawl space, had at least one and as many as three temperature sensors; outside temperature was also measured. Two anemometers with relatively low cut-in speeds measured wind speed and direction at each site. The wind measurements were taken at about 20 feet above grade, which corresponded roughly to the ceiling of a second story. The temperatures and wind speeds were recorded about every three to four minutes. In addition, detailed wind speeds were recorded with the pressure data every 30 seconds.

Hourly temperature and wind speed data were also obtained from three National Weather Service (NWS) stations in the Puget Sound area: Sea-Tac, Olympia, and Yakima. Site weather data were used to model natural infiltration; however, the NWS data from the airport closest to the site were compared with wind and temperature data from the site, using the LBL shielding and terrain classes to extrapolate wind speeds.

Twelve-minute averages of the temperature, pressure and flow data were used for most of the analysis; when necessary, the detailed measurements or the concentration measurements were used to clarify the averaged data. Measured wind-induced pressures on the face of the house were compared with velocity pressures calculated from the site wind speed, and wind pressure coefficients were derived for each face. These calculations are discussed further in Appendix D.

Blower door tests were performed at each site by both LBL and Ecotope technicians to quantify the leakage of the envelope. Ecotope used an orifice-type blower door with a variable-speed fan and a specially developed datalogging system. In keeping with traditional measurements of envelope leakage, the leakage function of each home (with the exception of Site 5) was calculated from data taken at house pressures between 15-60 Pascals. The Ecotope blower door tests, discussed in Section 6, included measurements at house pressures as low as 1 or 2 Pascals.

Using weather data measured at the site and the results from the Ecotope blower door tests, infiltration was predicted using two models: a model developed at Lawrence Berkeley Laboratory (LBL) by Sherman and Grimsrud (1980), and a model developed at the University of Alberta, known as the AIM-2 model (Walker and Wilson, 1990). Equations for both models are included in Appendix F. Each model has two components: a stack effect induced by the indoor-outdoor temperature difference, and a wind effect created by the pressure of the wind on the walls of the home. The two

effects are combined to predict the total infiltration due to natural driving forces, which does not include the effects of mechanical devices such as bath fans or air handlers.

Predictions from both models were compared with the measured infiltration data during periods in which only natural infiltration was occurring. In each case, the wind effect was overpredicted and the magnitude of the wind prediction was reduced prior to combining it with the stack prediction.

In each of the homes, the fan in the forced-air distribution system was controlled by a timer and the status of the fan was recorded by a computer. With the fan forced on, the heating elements in the furnace came on when the thermostat called for heat. During most other times, the fan and heating elements operated under the control of the thermostat. However, it was found that the cycling of the furnace preceding and following the times with the fan running detracted from our ability to produce reliable estimates of the magnitude of the fan effect; at Sites 6 and 7, this problem was remedied by preventing the fan from operating for a period before and after the time when the fan was forced on.

At each site, flows through supply and return registers and exhaust fans were measured with flow hoods. The MTMS was also used to measure the flow through the air handler fan by injecting tracer gas directly into the return and measuring the concentration of that gas both before and after the fan.

Two of the sites had designated exhaust ventilation systems: Site 5 had a neutral-pressure balanced-flow air-to-air heat exchanger, and Site 7 had a designated bath fan. At both of these sites, the exhaust system was controlled with a timer. Site 6 had no designated ventilation system. At each site, several one-time experiments were performed, such as operating the kitchen range hood or one or more fans simultaneously for one or two hours. These experiments were intended to provide additional data on the impacts of mechanical devices on infiltration.

The simple fan model presented in the Phase I report was used with the natural infiltration predictions and measured fan flows and duct leakage; its predictions correlated well with the measured data. In some cases, the measured living-zone infiltration data were used to estimate the added infiltration due to the operation of mechanical systems, and these situations cannot be interpreted as validation of the model.

4

ENVIRONMENTAL CONDITIONS

Temperature Differences

In homes in the Northwest, the primary cause of naturally-induced infiltration is the stack effect, which results from temperature differences between the interior and exterior. In choosing the time of the studies, the intention was to measure each home with a temperature difference to ambient (ΔT) typical of average heating-season values, about 23 F in the Puget Sound area.

Table 4-1 gives a comparison of outdoor temperatures and temperature differences using both the measured site data and NWS station data. Columns 4 through 6 summarize indoor temperatures at the site, concurrent outdoor temperatures at the NWS station, and outdoor temperatures measured at the site. The next two columns list the temperature difference calculated using both NWS and site outdoor temperatures. The last column gives the ratio of the two.

The indoor-to-outdoor temperature differences change by as much as 20% when the NWS station temperature is used instead of the site-measured temperature. This could translate into a difference of approximately 10% in stack-induced infiltration. On average, using NWS outdoor temperatures results in a 4% increase in indoor-to-outdoor temperature difference. It should be noted that in several of the homes, inside temperatures differed by as much as 4 F from one point to another, leading to an even greater uncertainty as discussed in the Phase I report.

Wind

A second driving force inducing natural infiltration results from pressures on the building generated by the wind. If the wind blows directly at one face of a building, these pressures are positive on that face, negative on the opposite face, and generally slightly negative on the two faces parallel to the wind direction.

Table 4-1
Comparison of airport and site temperatures

Site	Period (hrs)	NWS Stn	Temperature (F) Site Indoor	NWS Outdoor	Site Outdoor	ΔT (F) NWS	Site	NWS / Site
1	99	SEA	72.4	50.9	52.8	21.5	19.5	1.10
2	216	OLY	70.1	47.8	51.6	22.2	18.4	1.21
3	240	SEA	69.6	53.1	55.1	16.5	14.5	1.14
4	160	OLY	85.4	50.5	54.7	34.9	30.7	1.14
5	94	SEA	71.2	47.8	47.5	23.3	23.8	0.98
6	161	OLY	68.9	45.7	44.8 [1]	23.2	24.1	0.96
7	139	YAK	69.8	48.4	42.8	21.4	27.0	0.79
		SEA	69.8	46.2	42.8	23.4	27.0	0.87
Avg [2]						23.3	22.6	1.04

1 Estimated from stack pressure measurements due to faulty temperature transducer.
2 Only Yakima data for Site 7 was included in the average.

A major uncertainty in the prediction of wind-induced infiltration is the magnitude of the wind speed at the site. Wind speed data are generally available from National Weather Service (NWS) stations, which are usually located at or near airports. Because of the scarcity of wind measurement stations, it is often necessary to use weather stations at distances of 100 or more miles to estimate a site wind speed.

As noted in the introduction, the Phase II homes were chosen for maximum wind exposure. The site wind speeds for the Phase I homes were generally too low to draw firm conclusions regarding the modeling of infiltration due to wind effect.

Measured wind speeds at the three Phase II and four Phase I homes are summarized in Table 4-2. The table also shows the results of extrapolating airport data to the sites using the LBL wind model. The terrain and shielding classes required by the model, given in columns 4 and 5 of the table, were estimated by Dr. Sherman of LBL. The equations for extrapolating the airport wind speed to site wind speed, along with the terrain and shielding classifications, are contained in Appendix F. The average LBL terrain class was 4.1; the average shielding class was 3.9. These values result in substantially lower predicted site wind speeds than the LBL default values of 3 and 3.

Table 4-2
LBL wind extrapolation compared with measured site wind speed

			Site parameters		Wind speed (mph)			Wind speed ratios		
Site	Period (hrs)	NWS Stn	Terr [1]	Shield [1]	NWS [2]	Est Site [3]	Meas Site	NWS Est	NWS Meas	Est Meas
1	96	SEA	4	5	7.65	1.29	1.53	5.92	5.00	0.85
2	216	OLY	4	3	5.09	2.40	2.06	2.11	2.47	1.17
3	240	SEA	5	4	7.79	1.90	1.60	4.12	4.87	1.18
4	160	OLY	5	5	8.34	1.12	1.10	7.46	7.58	1.02
5	94	SEA	3	5	10.16	2.65	3.52	3.83	2.89	0.75
6	161	OLY	4	4	5.30	1.93	1.91	2.75	2.77	1.01
7	139	YAK	4	1	10.96	6.99	11.77	1.57	0.93	0.60
	139	SEA	4	1	8.63	5.51	11.77	1.57	0.73	0.47
Avg [4]			4.1	3.9				3.97	3.79	0.94

1 Terrain and shielding classes for LBL wind model, estimated by LBL.
2 The airport wind towers are all at 20 feet and assumed to be terrain class 2. The towers at the sites were all at 20 feet with the exception of Site 1, which was at 10 feet.
3 Site wind speed predicted using the LBL model, Equation F.3. Predicted wind is the wind speed at the site tower height, assuming that the site weather tower experiences the same shielding as the home.
4 Only Yakima data for Site 7 was included in the average.

Wind speeds at the nearest hourly National Weather Service (NWS) site are given in the column headed "NWS" for the period of the tracer test. Site 7 was somewhat remote, being about 48 miles from Yakima Airport and 68 miles from Sea-Tac airport, so data from both airports were included. The data from this site is expected to agree better with the Yakima Airport data, because the Cascade mountain range stands between the site and the Seattle Airport. The other sites range from seven to 33 miles from the weather stations used for comparison.

The column labeled "Est Site" gives the extrapolation of the average airport wind speed to the site using the LBL model; the column labeled "Meas Site" lists the wind speeds measured at the sites. The goal of finding windy sites was achieved; the lowest measured average wind speed among the Phase II homes, at Site 6, is comparable to the highest average wind speed among the Phase I homes, at Site 2.

The last three columns in the table show the ratios of the NWS station to the estimated site wind, the NWS station to the measured site wind, and the estimated site wind to the measured site wind.

Site 7 experienced unusually high wind speeds, averaging almost 12 mph for a one-week period. This average wind speed is higher than that measured at either of the airport locations, even though the home is partially sheltered by nearby forest. The abnormal windiness of this location is further indicated by the presence of a large Darius rotor wind generator about 1-1/2 miles from the site.

As shown in the table, wind speeds at the Olympia airport are generally lower than those at the Seattle airport. In fact, the 30-year average wind speeds are 73% those of Seattle. Yakima 30-year averages are 78% those of Seattle, although the Yakima wind speeds were higher during the testing period.

Excluding Site 7, the divisors necessary to reduce the airport wind speed to the estimated site wind speed range from about 2.1 to 7.5. Again excluding Site 7, the LBL-estimated site winds are within ±25% of the measured values. On average, the LBL-estimated site wind speeds are within 6% of the measured values, and airport wind speeds need to be reduced by a factor of 3.8 to reach the measured site wind speed.

5

WIND EFFECTS

The purpose of selecting homes with wind exposure for the Phase II testing was to obtain data which would allow us to address some of the assumptions made in predicting wind-induced infiltration. In previous studies, overprediction of actual infiltration by the LBL model was found to be correlated with the magnitude of the wind prediction (Palmiter and Brown, 1989).

For the Phase I homes, the LBL wind predictions were again found to be too large, even when used with wind speeds measured at the site. However, most of the Phase I homes experienced relatively low wind speeds, and they did not provide sufficient data to draw conclusions about the relationship between wind speed and induced pressures and flows.

Pressures

Wind creates pressures (relative to the outdoor static pressure) on the external surfaces of buildings. If the wind blows directly on one face of the building, it produces positive pressures on that face and negative pressures on the other three walls. If the wind blows onto a corner of the building, it typically produces positive pressures on two walls and negative pressures on the other two walls. If the building has a flat or low-pitched roof, the pressure on the roof is also negative.

The external wind pressures combine additively with the pressures created by the stack effect to create air flows through the building elements. The internal pressure (relative to the outdoor static pressure) comes to an equilibrium value which is essentially a weighted average of the combined stack and wind external pressures; the weights are determined by the leakage distribution (the leakiness of the envelope as a function of location, i.e. floor vs. ceiling). At equilibrium, the air flow in equals the air flow out. In the typical case, with wind directly on one surface, the building is depressurized (relative to outdoor static pressure) because there are three negative surfaces and only one positive surface.

In the case of ventilated attics and crawl spaces, the situation is more complex. In the original simulations used in the derivation of the LBL wind model, it was assumed that the wind pressure coefficients for the floor and ceiling were equal to zero. Because wind typically depressurizes the interior, the LBL assumption leads to the prediction of large flows inward from the attic and crawl space at high wind speeds.

As noted in the Phase I report, it is the authors' opinion that this assumption is highly unrealistic. If buffer areas are well-ventilated in all directions, as tends to be the case when they contain crawl space vents or attic soffit vents, it is reasonable to assume that the wind-induced pressure in the buffer zones is a weighted average of that on the walls. Thus, the attic and crawl space are depressurized in approximately the same fashion as the house interior. As a result, the wind-induced pressure differences, and the corresponding air flows, across the floor and ceiling are very small.

The small delta-pressure assumption has been asserted in the ASHRAE Handbook of Fundamentals (ASHRAE 1989b, p. 21.5) and also in the derivation of the AIM-2 model (Walker and Wilson, 1990). However, it should be noted that the AIM-2 wind model was based on a single wind direction directly on one face, while the LBL wind model was based on averaging the infiltration results for a given wind speed over 12 equally-spaced directions around the compass. Direction is an important factor in determining the pressures and the flows.

Direct simulations by the authors of a home with a leakage exponent of 0.5 (see Chapter 6), averaged over a number of wind directions and floor plan aspect ratios, indicated that the weighted-average assumption produces a wind effect about 28% less than the LBL model. It was also found that the modified pressure coefficient assumption could be fit to the same functional form as the LBL model, the result being that the exponent of the (1-R) term in Equation F-2 should be changed from 1/3 to 0.8. For R=0.5, the effect is to multiply the LBL wind effect prediction by 0.724. This modified LBL model is described in Appendix F.

In two of the homes studied under Phase I, the wind speeds were too low to make assertions about flows from the attic and crawl space. However, the delta pressures across the floor and ceiling remained relatively constant with increasing wind. The largest effects occurred at Site 2, both because it was the most windy and because it had asymmetric leakage in the crawl space. At this site, winds from the east were found to have no effect on ceiling delta pressure; winds from the west did have an effect, but the sign was opposite to that predicted by the LBL assumption.

The generally high wind speeds at the Phase II sites allow a more thorough examination of wind effects on pressure and infiltration. Pressure differences were measured across each wall; if the wall was two stories high, measurements were made at both levels. At least two measurements of differential pressure were made across the floor to the crawl space and across the ceiling to the attic. In addition, a pressure tube was run on the ground some distance from the house to measure the internal pressure of the house relative to outdoor static pressure. All of the differential pressure measurements are summarized in Appendix D, which also describes the regression technique used to estimate the individual effects of wind, stack and equipment operation.

It is conventional to express wind-induced pressures in terms of pressure coefficients (C_p) which relate the pressure at some point on the envelope to the free-stream wind velocity pressure. The velocity pressure is calculated as

$$P_v = \frac{1}{2}\rho v^2 \qquad \text{(eq. 1)}$$

where P_v = velocity pressure (Pa)
ρ = density of outdoor air (kg/m^3)
v = wind velocity (m/s)

The pressure coefficient for a particular measurement point is the pressure at that point divided by the velocity pressure.

Typical wind pressure coefficients are summarized in Table 5-1 for the three sites for the walls, floor and ceiling. The internal pressure coefficient is also included in the table. The wall, floor and ceiling pressure coefficients have the sense of outside pressure minus outside static pressure; the internal pressure is given as inside pressure minus outside static pressure. The outside static pressure is assumed to be zero. The last three columns of the table give the delta pressure coefficients across each surface. It should be noted that it is actually the delta pressures which were measured, and the ordinary pressure coefficients are derived by adding (with the sign convention in the table) the house pressure coefficient.

It is clear that the wind-induced differential pressurization across the floor and ceiling due to wind is much smaller than the effect on the walls. At Sites 5 and 6, wind produces almost no additional pressure or flow across the floor and ceilings. The sign of the small pressure coefficient is, however, in agreement with the LBL assumption.

At Site 7, wind depressurizes the crawl space more than the house, resulting in air flow from the house down to the crawl space; this phenomenon is contrary to the LBL assumption that air is forced into the house. The pressure induced across the floor is still a factor of 20 smaller than that induced across the walls. The situation with the attic at Site 7 is very complex and discussed in more detail below and in Appendix C.

The pressures relate well to the wind velocities; the prediction of the pressures from the wind seems reasonable. All three homes are slightly depressurized by the wind. The positive pressure coefficients in the table indicate the primary wind direction at the site.

At Site 5, the winds blew from the water which lay directly to the west. The table shows that the only positive pressure coefficient is on the west face. The detailed results for this site in Appendix A indicate that, on the windward face, the pressure coefficients are slightly larger on the first floor. The south and east pressure coefficients are negative. The north side of the house was quite close to another building and may have experienced very little wind.

Table 5-1
Summary of wind pressure coefficients at three sites

	Pressure Coeff			Delta Pressure Coeff		
Location	Site 5	Site 6	Site 7	Site 5	Site 6	Site 7
Attic	-0.10	-0.04	-0.06	0.00	0.02	-0.02
Crawl	-0.08	-0.06	-0.14	0.02	0.02	-0.06
North	-0.08	-0.62	0.30	0.01	-0.54	0.38
South	-0.32	0.31	-0.45	-0.23	0.38	-0.37
East	-0.33	-0.59	-0.32	-0.24	-0.52	-0.24
West	0.38	0.42	0.40	0.48	0.50	0.48
House	-0.09	-0.07	-0.08	--	--	--

At Site 6, the winds generally came from the southwest. Wind directions at this site were more variable than at the two other sites, so the velocity pressure was multiplied by a sinusoidal function before performing regressions. As expected for a building with the wind directed at a corner, pressure coefficients for two faces are positive and two are negative. The pressure coefficients on the first and second floor were about the same, despite the presence of a six-foot-high fence around the building.

Site 7 had strong winds from the northwest. Again, two faces have positive pressure coefficients and two have negative coefficients. Although this home was only one story, pressures were measured at two different heights on the east and west walls due to the large wind effects; however, the coefficients at different heights on the same wall differ very little.

The effect of wind on wall, floor and ceiling pressures is shown graphically in Figure 5-1 for each of the three sites. Each pressure is plotted versus the predicted velocity pressure. The slope of each line is the wind pressure coefficient. At each site, the pressure on the windward face increases linearly with velocity pressure. Pressures on the opposite face decrease linearly, but the pressure coefficient has a smaller magnitude than that on the windward face, with the exception of Site 6. The depressurization of the attic and crawl space at Site 7, and the negligible effect on these buffer zones at the other sites, is evident from the graphs.

As stated previously, Site 7 was the windiest location; velocity pressures at this site reached more than 50 Pa. This home was unusual in that the pressures induced by the wind in the attic varied greatly among different measurement points. Because the section of attic above the cathedral ceiling in the center of the home was completely filled with blown-in insulation, the wind was unable to blow through the attic; hence, the attic was strongly pressurized on the windward side and strongly depressurized on the leeward side. This situation is illustrated in the lower-right graph of Figure 5-1. The

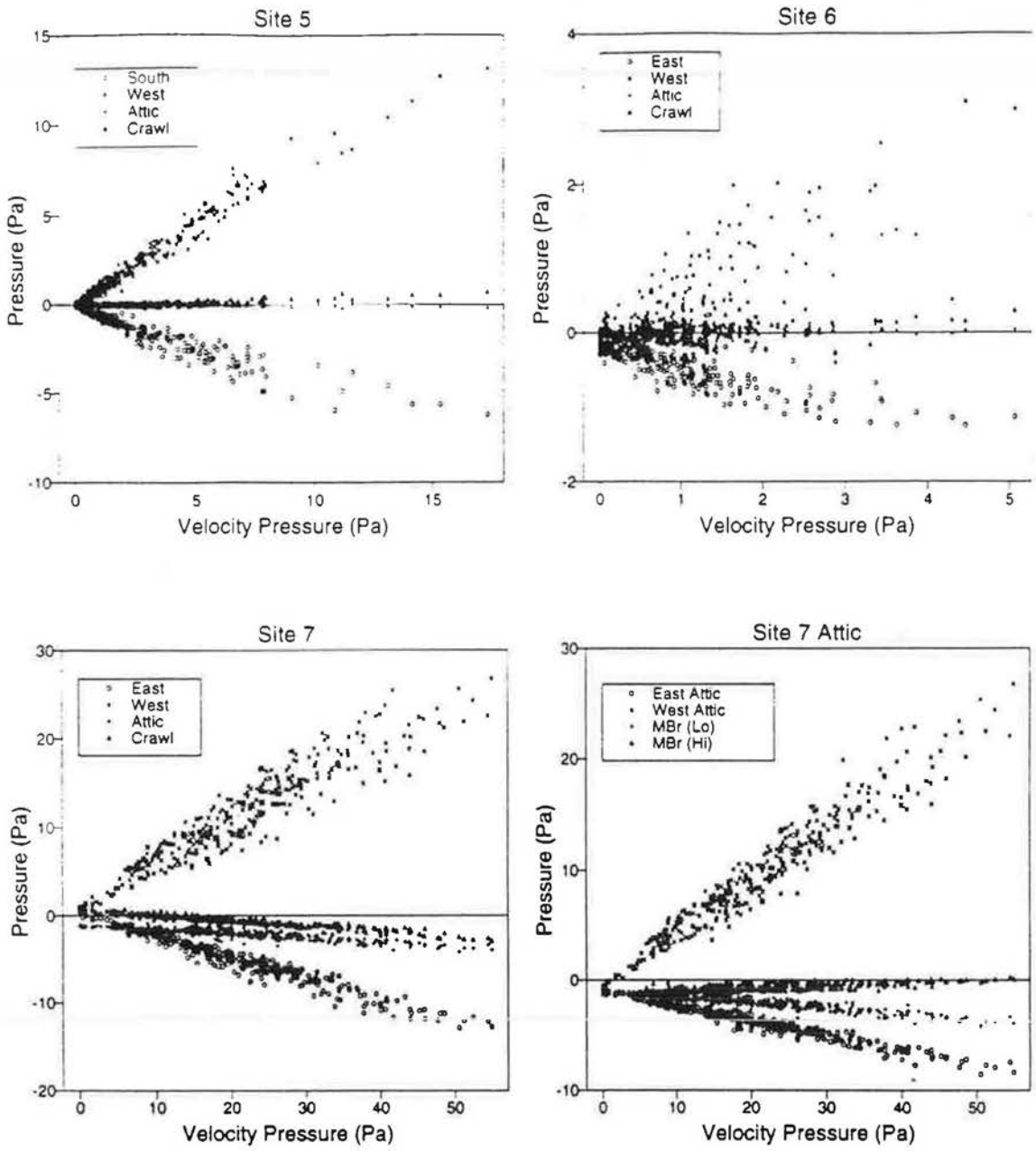

Figure 5-1
Effect of wind on wall, floor and ceiling pressures at three sites

two pressures in the center were measured above the cathedral ceiling in the master bedroom; one of these pressures was used in the graph comparing wall pressures at Site 7.

Infiltration Prediction

Table 5-2 summarizes the predicted infiltration effects due to wind at the seven sites tested during Phase I and Phase II. The first column gives the average wind speed at each site; the average at Site 7 was over three times higher than that at the next windiest home, Site 5. The modeled wind effect is the predicted infiltration which would occur if no other driving forces, including the stack effect, were in operation. The infiltration increase is the change in infiltration above the stack effect which occurs due to the action of the wind; the stack and wind predictions were combined and the stack prediction was subtracted from the combination. For most of the homes it was necessary to adjust the predicted infiltration due to wind effects downward in order to match the tracer data with stack effects removed.

In all cases, standard assumptions about leakage parameters (R=0.5, X=0, defined in Appendix F) were used in the infiltration models. R=0.5 indicates that half the total leakage is present in the floor and ceiling; X=0 means that the leakage is equally distributed between the floor and ceiling. In some cases, the parameter R may have been considerably larger than the default value. For example, ductwork leaks in the crawl space or leaks into the attic through recessed lights can be large, and may not be equivalent to leakage through walls.

Even though both Sites 5 and 6 experience significant wind speeds, the wind-induced infiltration is still a very small fraction of the total. At Site 7, the infiltration is very wind-dominated because of the extremely high wind speeds. This is the only house of the seven in which the wind is actually the major cause of infiltration; in fact, it is difficult to distinguish the effects of stack and mechanical equipment.

The right-hand column of Figure 5-3 shows the tracer-measured infiltration, with stack effect removed, versus wind speed. At Site 5 the wind effect is clearly discernible, while at Site 6 the wind effect is to a large extent lost in the noise. At Site 7 there is a very strong relationship confirming that wind is the dominant effect. It is interesting to compare these living-zone infiltrations with those of the crawl spaces (left-hand column of Figure 5-3), and attics (Figure 5-2).

From the plots of tracer-measured infiltration in the attics and crawl spaces versus wind speed it is clear that wind is the dominant effect. The greater degree of scatter at Site 6 relative to Sites 5 and 7 is largely due to the fact that the wind blew from essentially one direction at Sites 5 and 7, while it constantly shifted direction at Site 6. As expected, the relationship between infiltration and wind speed is the strongest and most linear at Site 7.

Table 5-2
Adjusted wind-induced infiltration for seven sites [1]

Site #	Wind Speed	Modeled Wind Effect [2]		Infiltration Increase [3]		
	(mph)	cfm	ACH	cfm	ACH	% of Natural Infiltration
1	1.53	18.4	0.09	4.6	0.02	7.8
2	2.06	54.7	0.19	18.1	0.06	13.9
3	1.61	35.2	0.15	13.7	0.06	15.9
4	1.10	4.1	0.03	0.7	0.00	3.6
5	3.52	51.6	0.11	12.3	0.03	7.9
6	1.91	17.7	0.07	0.7	0.00	1.1
7	11.77	99.3	0.61	70.0	0.43	65.2

1 Modeled results for wind and/or stack adjusted as appropriate to match tracer-measured infiltration.
2 Wind-induced infiltration predicted if no other driving forces, including stack effect, were in operation.
3 The increase in infiltration due to wind was obtained by subtracting the modeled stack effect from the combined total.

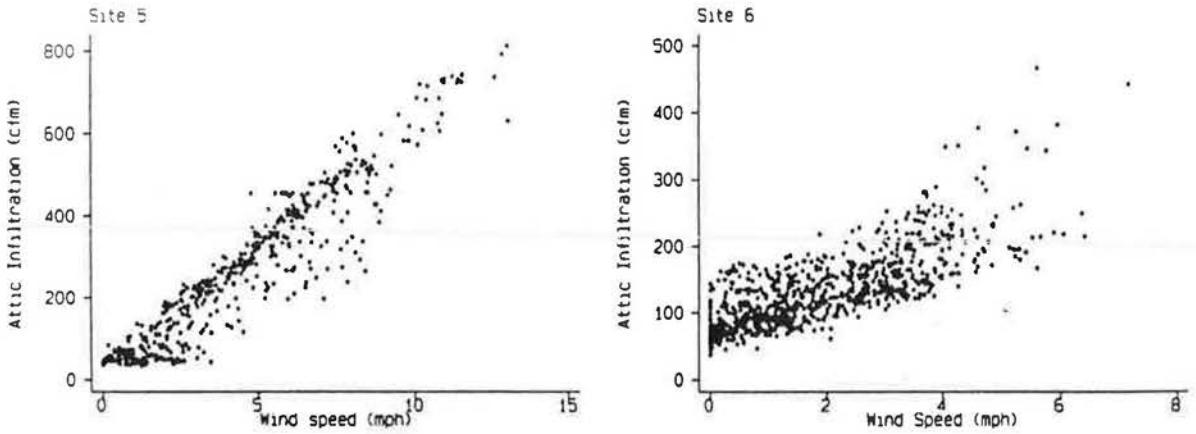

Figure 5-2
Effect of wind speed on attic infiltration at Sites 5 and 6

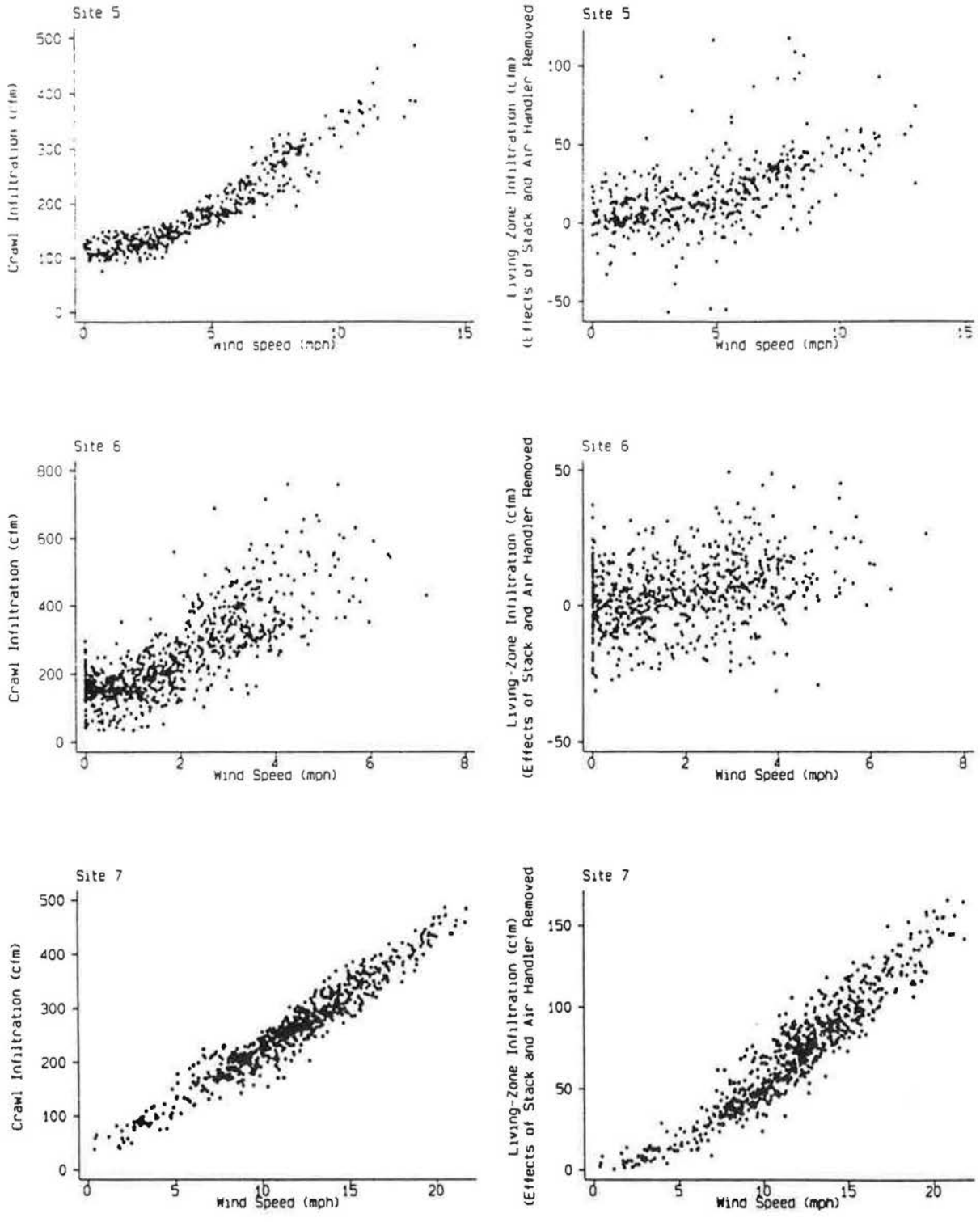

Figure 5-3
Effect of wind speed on crawl (shown on left) and living-zone (shown on right) infiltration at Sites 5-7

An examination of the floor and ceiling pressures measured at the four sites in Phase I showed that they were relatively unaffected by wind relative to pressures across the walls. By using pressures measured to the attic or crawl space, under conditions of nearly equal indoor and outdoor temperatures, it was expected that reliable low-pressure leakage measurements would be obtained. A power law derived from such measurements, used with the AIM-2 model, should give good predictions.

In order to record the measured pressures across the envelope and the flows through the blower door, a system was developed which incorporated two pressure transducers, a datalogger, and an IBM-compatible PC. A program written in BASIC retrieved output from the datalogger and converted it to pressure and flow data which could be viewed as the measurements were taken. Approximately twenty data points were taken at each pressure station, resulting in a total of about 600 data points between house pressures of 1 and 60 Pa.

The blower door used to perform the tests was a standard blower door with three annular low-flow plates. With all the plates installed, the blower door had the ability to produce flows as low as 135 cfm. In the tightest houses, this small flow corresponds to a house pressure of 3 Pa; in the leakier homes, the flow results in a house pressure of less than 1 Pa.

The low-pressure testing was done between August and October of 1991. It was hoped that the summer conditions of low indoor-outdoor temperature difference and low wind speed would produce better conditions for testing. Although ideal conditions were achieved at one site (Site 1) on a windless day, even small amounts of wind interfered greatly with the testing at other sites. House pressures as low as 3 Pa were measured at all of the sites; at four of the homes, measurements were taken down to house pressures of 1 Pa.

With the exception of one site, the nominal house leakage function was determined by a regression on points between house pressures of about 15 and 60 Pa, the range of a traditional blower door test. The leakage function at Site 5 was derived from data at house pressures between 9 and 42 Pa. These leakage functions were used to produce the LBL and AIM-2 infiltration predictions. Regressions were also performed using points between 1 and 10 Pa, where available. In some cases, the data at lower pressures were noisy because of wind or other effects; for these homes, the low-pressure regression was restricted to data which excluded the noise.

Results of Low-Pressure Testing

Table 6-1 shows results from both high-pressure and low-pressure regressions from the blower door data for each site, for the test done with the registers open (house as found). At high pressures, the exponent n is around 0.65; at low pressures, it takes values around 0.70, with a corresponding drop in the flow coefficient C. The low

Table 6-1
Blower door results from high-pressure and low-pressure tests

Site #	1	2	3	4	5	6	7
Standard Test							
C (cfm)	102	227	231	64	274	240	83
n	0.67	0.66	0.66	0.64	0.64	0.61	0.67
ELA (in^2)	74	160	163	44	190	159	60
ACH50	6.84	10.11	12.80	5.00	7.16	10.55	7.02
Low-Pressure Test							
C (cfm)	92	214	198	60	234	188	74
n	0.72	0.69	0.73	0.68	0.71	0.72	0.72
ELA (in^2)	70	157	154	46	177	144	57
ACH50	7.35	10.71	14.53	5.40	7.82	12.51	7.62
Range (Pa)	1.3 - 9.0	3.4 - 10.0	1.0 - 9.5	3.0 - 9.7	1.0 - 10.0	1.0 - 10.0	2.8 - 10.0
Ratio (High-Pressure/Low-Pressure)							
ELA	1.06	1.02	1.06	0.96	1.07	1.10	1.05
ACH50	0.93	0.94	0.88	0.93	0.91	0.84	0.92

pressure regressions over a range of roughly 3 to 10 Pa resulted in an increase of around 9% in the flow predicted at 50 Pa and a decrease of around 5% in the ELA and predicted flow at 4 Pa.

Graphs of the measured flow versus house pressure are given in Appendix E. Sites 1 and 5, especially Site 1, were tested under the best conditions. The results from each site show small departures from the power law at low pressures; the extrapolation tends to overpredict flow and the apparent exponent increases at lower pressures, eventually looking laminar.

To the extent that these measurements are representative, they suggest that the Ethridge description of cracks with both a laminar and an inertial loss is more appropriate than the power law. In the houses with the best data, however, the departure from the power law is not large.

In spite of trying to obtain optimum conditions, these effects could also be caused by bias due to pre-existing stack or wind pressures, or by systematic error when using the smallest orifice on the blower door. Similar low-pressure tests should be done on a large number of homes before drawing firm conclusions about the low pressure relationship.

Comparison of Blower Door Retests

Table 6-2 compares blower door results for the Phase I homes. The first set of values is from the LBL blower door tests performed during Phase I and was used in the model predictions for the Phase I report. The second set of results is from the return visits during the Phase II work. Both are calculated from regressions at typical blower-door house pressures (usually 15-60 Pa).

Site 1 was tested under ideal conditions; the ELA for this home decreased 15% from its previous value. Previously, the LBL stack model overpredicted the measured infiltration by about 10%. The LBL model predictions using the new ELA would therefore be in much closer agreement with the measured data, and might even underpredict the true value.

The leakage parameters at Site 2 changed very little from the previous year. At this site, the LBL model provided a better fit to the measured data than did the AIM-2 model; this conclusion would be unchanged by the new blower door results.

At Site 3, the ELA of the home increased by 17% over the previously used value. During the original blower door and tracer tests of this home, a supply duct was disconnected from the plenum, resulting in a large amount of duct leakage. The homeowner repaired the ductwork following the Phase I testing; prior to the second blower door test, the pipe was disconnected in order to replicate the testing conditions. The original condition may not have been reproduced precisely; however, it is unlikely that this difference would have produced such a large change in the ELA.

Table 6-2
Blower door test results for Phase I homes

	1990 Test				1991 Test				% Change	
Site #	C	n	ELA	ACH50	C	n	ELA	ACH50	ELA	ACH50
1	127.4	0.629	86.8	7.2	102.5	0.639	73.6	6.8	-15	-6
2	238.1	0.66	168.8	10.7	226.7	0.657	160.0	10.1	-5	-6
3	187.5	0.696	139.9	12.0	231.2	0.658	163.4	12.8	17	7
4	64.0	0.643	44.4	5.0	Not retested					

At this home, it was determined that the LBL model corresponded to the data more closely than did the AIM-2 model. New predictions by the LBL model would substantially overpredict the measured infiltration; the AIM-2 model would underpredict the measured data slightly. Given the uncertainty in the condition of the house, this change cannot be interpreted as a validation of either model.

7

INFILTRATION COMPARISONS

Measured Natural Infiltration

Table 7-1 gives the "measured" natural infiltration for each of the seven homes. These values result from adjusting one of the models, either LBL or AIM-2, by a multiplier so that the predicted infiltration closely matched the tracer measured data during periods of no fan operation. In some cases, a separate reduction of the measured site wind speed was necessary to match the trend of the predicted infiltration versus wind speed with that of the tracer-measured data.

Table 7-1
Natural infiltration characteristics of seven homes

	Site 1	Site 2	Site 3	Site 4	Site 5	Site 6	Site 7
Stack Effect (ACH)	0.264	0.383	0.305	0.139	0.261	0.373	0.230
Wind Effect (ACH)	0.022	0.062	0.058	0.005	0.026	0.004	0.431
Natural Infil (ACH)	0.286	0.445	0.363	0.144	0.287	0.377	0.661

Because the stack effect was dominant for all homes except Site 7, it is convenient to calculate the wind effect as the additional infiltration, over and above that which would have been produced by the stack effect only. In other words, the wind effect in Table 7-1 is simply the result of subtracting the stack effect from the total natural infiltration. It should be noted that, in reality, the stack and wind combine in a highly nonlinear fashion, and the separation given here is merely an accounting fiction. Excluding Site 7, the additional infiltration due to wind is generally quite small.

LBL and AIM Models

The leakage function derived from the high-pressure blower door measurements was used in the AIM-2 model; an ELA was calculated using the same leakage function for use in the LBL model. Default values for the leakage ratios of X=0 and R=0.5 were used in both models.

Table 7-2
Comparison of infiltration predicted by the LBL and AIM-2 models [1] (cfm)

	LBL Model			AIM-2 Model			LBL/AIM Ratio		
Site	Stack	Wind	Full	Stack	Wind	Full	Stack	Wind	Full
1	51.3	17.6	55.6	39.1	9.0	40.2	1.31	1.97	1.38
2	106.4	51.9	123.6	82.2	30.3	90.0	1.29	1.71	1.37
3	78.5	41.1	95.2	60.3	23.1	68.1	1.30	1.78	1.34
4 [2]	31.0	8.0	33.1	24.8	4.4	25.4	1.25	1.81	1.30
5	149.4	105.0	191.0	123.9	73.7	149.0	1.21	1.42	1.28
6 [3]	131.7	45.3	144.2	117.1	29.7	121.4	1.12	1.53	1.19
7	37.4	110.4	117.8	27.8	105.8	108.1	1.35	1.04	1.09
Average							1.26	1.61	1.28

1 Unadjusted predictions of LBL and AIM-2 models.
2 Predictions for period with bedroom door open and makeup vent not sealed.
3 Predictions for period prior to duct repair.

Table 7-2 summarizes the unadjusted infiltration predictions from each model, using the weather data measured at each site. For the wind speed, it was assumed that the home was exposed to the same shielding as the tower, and no shielding or terrain multipliers were used. It should be noted that the wind-induced infiltration is that actually predicted by the wind portion of the model, while the infiltration attributed to the wind effect in the appendices is the difference between the full and the stack predictions.

The difference between the model predictions is systematic. For the stack effect, the LBL model predictions average 26% greater with a range from 12 to 35% greater; for the wind effect, the LBL model averages 61% greater with a range from 4 to 97% greater. The LBL full model predictions average 28% greater with a range from 9 to 38% greater than those of the AIM-2 model.

Table 7-3 compares the unadjusted model predictions with the "measured" natural infiltration. The "measured" natural infiltration is given in the first two columns of Table 7-3 in terms of both air-changes per hour (ACH) and in terms of cfm. The modified LBL model differs from the standard LBL model only in the wind effect equation (see Appendix F). The agreement of the three unadjusted model predictions of natural infiltration with the "measured" natural infiltration is characterized by the ratio of the predicted value to the measured value.

Table 7-3
Comparison of measured and modeled natural infiltration

	Measured [1]		LBL Model [2]		Modified LBL [2]		AIM-2 Model [2]	
Site	Flow (ACH)	Flow (cfm)	Flow (cfm)	Ratio to Measured	Flow (cfm)	Ratio to Measured	Flow (cfm)	Ratio to Measured
1	0.286	58.9	55.6	0.944	53.6	0.910	40.2	0.683
2	0.445	130.4	123.6	0.948	116.2	0.891	90.0	0.690
3	0.363	86.1	95.2	1.106	88.4	1.027	68.1	0.791
4 [3]	0.144	25.4	33.1	1.303	32.2	1.268	25.4	1.000
5	0.287	136.2	191.0	1.402	173.3	1.272	149.0	1.094
6 [4]	0.377	117.5	144.2	1.227	138.6	1.180	121.4	1.033
7	0.661	107.4	117.8	1.097	89.5	0.833	108.1	1.007
Avg Error [5]				15.9%		15.2%		15.9%

1 Adjusted for best fit to tracer data.
2 Unadjusted predictions.
3 Predictions for period with bedroom door open and makeup vent not sealed.
4 Predictions for period prior to duct repair.
5 Mean absolute percentage error.

The bottom line of Table 7-3 gives the mean absolute percentage error of each of the three models. The LBL and AIM-2 models each had a mean prediction error of 15.9% with the LBL model tending to overpredict and the AIM-2 model tending to underpredict the measured value. The modified LBL model had a slightly better mean absolute percentage error of 15.2% and less tendency toward systematic over or under prediction.

Figure 7-1 gives a visual comparison of the measured and modeled natural infiltration. The center line is the one-to-one line, indicating perfect agreement. The upper and lower lines are spaced 20% above and 20% below the one-one line. The x and y scales of the graph are logarithmic because the errors tend to be percentage errors (that is, the absolute errors are larger for homes with larger infiltration rates).

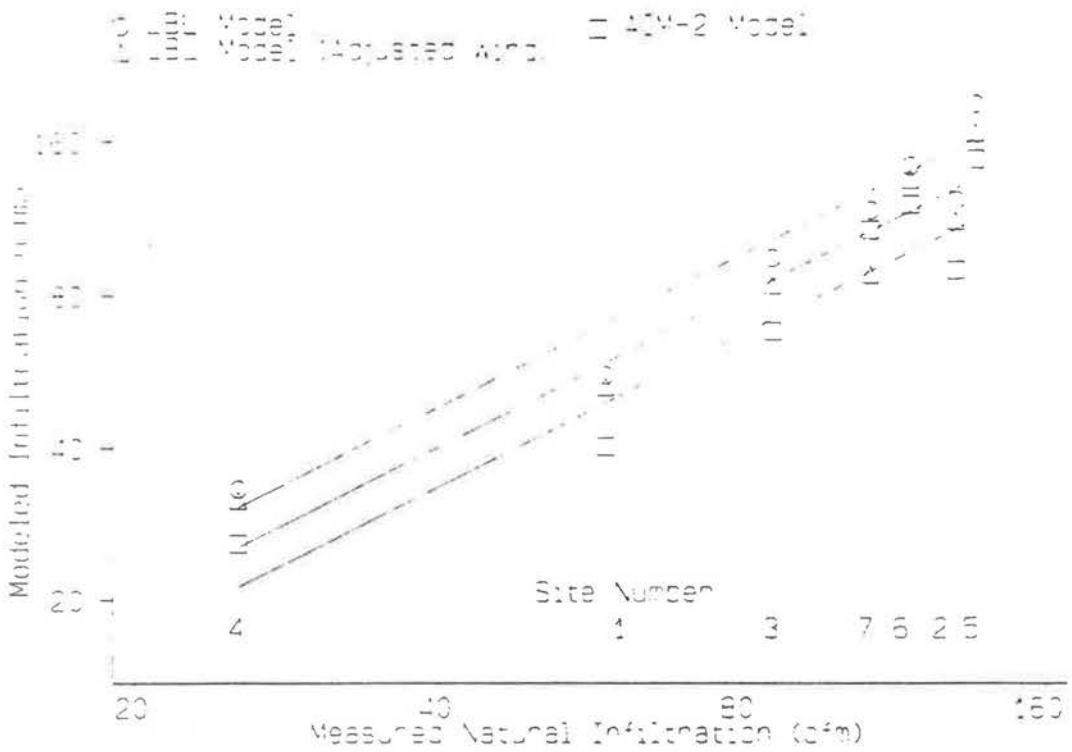

Figure 7-1
Comparison of measured and modeled infiltration

The middle line is the one-one line, indicating perfect agreement with the measured data. The upper and lower lines are 20% above and below the measured values. Note that both the x and y scales are logarithmic.

8

ASSESSMENT OF TIME-AVERAGING BIAS

The perfluorocarbon tracer (PFT) technique is a simple inexpensive tracer test method which has been extensively employed in large infiltration studies such as NORIS and RCDP. The infiltration is inferred from time averaged concentration measurements. This technique is described in detail by Dietz (1986).

Because concentration is inversely proportional to the flow rate, the use of time-averaged tracer concentrations, rather than instantaneously-measured concentrations, can lead to a bias in the estimate of the actual flow. This reciprocal averaging bias was noted by Dietz (1986). The bias has been assessed at about 5% for homes in the Pacific Northwest by Palmiter and Brown (1989), although estimates as high as 27% have been given by Sherman (1989).

The convenience and low cost of the PFT technique, combined with its widespread application in the Northwest and elsewhere, make it important to resolve the issue of the degree of bias under heating season conditions. Simultaneous use of the PFT technique and the MTMS system, as in the present study, provides an excellent method for assessing the potential bias of time-averaged concentration methods, as well as calibration accuracy.

Flows calculated from instantaneous concentrations are those actually occurring at the instant of measurement; these ventilation rates govern heat loss or gain. The time-averaged concentrations yield an effective ventilation rate, which is relevant to indoor air quality. The effective ventilation rate is always lower than the actual ventilation rate.

This is illustrated by the following example. Suppose a home has a constant 0.5 ACH for 168 hours (one week). For unit source strength, the tracer concentration for each hour is then 1/0.5, the average concentration for the week is 2, and the reciprocal of the average concentration is also 0.5 ACH. Now suppose the ventilation rate is 0.2 ACH for 161 hours, and for each day in the week, windows are opened for an hour, resulting in 7.4 ACH during that hour. The average tracer concentration in this case will be

$$\frac{1}{168}\left(161\cdot\frac{1}{0.2}+7\cdot\frac{1}{7.4}\right)=4.80.$$

The actual ACH for the measurement period is still

$$\frac{1}{168}(161 \cdot 0.2 + 7 \cdot 7.4) = 0.5,$$

but the PFT results will indicate an effective ACH of only

$$\frac{1}{4.80} = 0.21.$$

The heat loss will be that for 0.5 ACH, but pollutant concentrations will be the same as for a continuous ventilation rate of only 0.21 ACH.

Relatively constant natural driving forces, such as the stack effect, result in consistent flows; if most of the infiltration is induced by these effects, the time-averaging bias will be small. Variable effects such as wind produce bursts in the natural infiltration rate, leading to larger biases. In the Pacific Northwest, ventilation rates are generally dominated by stack infiltration; this explains the generally low bias.

Table 8-1 gives calculations of the bias in these seven homes. The second and third columns give averages of the actual flow and the time-averaged (steady-state) methods; in the next two columns, these flows are given as air changes. These flows are the total flow through the zones. The steady-to-average ratio in the sixth column is the time-averaging bias. The last two columns are measures of the variability in the flow: the standard deviation as a percentage of the mean, and the ratio of the maximum to the minimum flow.

For these homes, bias for living-zone flows averaged 5% and did not exceed 10%. The bias is noticeable at Sites 3, 6 and 7 (7%, 10% and 8% respectively). Flows at Site 7 were very wind-dominated, and the large bias is to be expected. Site 6 had very little wind-induced infiltration; however, faulty ductwork at this home resulted in a dramatic change in the ventilation rate during the 30% of the time when the furnace fan operated. Given this large change in the ventilation rate, the magnitude of the time-averaging bias is not surprising. Although not as extreme as at Site 6, duct leakage at Site 3 was also large and induced infiltration attributed to the air handler was high.

The bias for flows through attics and crawl spaces can be large, reaching as much as 30%. This is particularly noticeable in wind-dominated buffer zones such as the attic at Site 5 and the crawl space at Site 2.

Table 8-1
Evaluation of bias due to time-averaging of concentrations as used in the PFT technique

	Flow (cfm)		Air changes				
Site	Avg [1]	Steady [2]	Avg [1]	Steady [2]	Steady/Avg Ratio	% Std. Deviation [3]	Max/ Min [4]
Living-Zone Infiltration							
1	82	81	0.40	0.39	0.98	40	6.32
2 [5]	149	144	0.51	0.49	0.97	23	3.87
3	115	107	0.49	0.45	0.93	34	10.81
4	38	37	0.24	0.23	0.97	52	14.72
5	177	172	0.37	0.36	0.97	35	6.33
6	175	158	0.71	0.64	0.90	53	6.84
7	114	105	0.70	0.65	0.92	30	5.46
Average					0.95		
Flow through Attic							
2 [5]	282	231	3.69	3.02	0.82	47	6.43
3	143	134	7.62	7.14	0.94	27	3.40
5	361	282	9.46	7.39	0.78	48	6.76
6	232	222	6.82	6.52	0.96	22	4.07
Average					0.88		
Flow through Crawl							
1	287	256	4.48	4.00	0.89	37	5.27
2 [5]	289	202	6.45	4.51	0.70	76	10.79
3	73	68	2.51	2.34	0.93	29	3.71
4	188	155	2.73	2.26	0.82	44	6.61
5	206	185	1.04	0.93	0.90	39	7.15
6	287	247	8.21	7.06	0.86	41	6.12
7	277	237	6.82	5.84	0.86	34	8.76
Average					0.85		

The values in this table were summarized over all of the available data, including partial days, and over all test conditions, resulting in slightly different air change rates than those presented in other tables.

1 Flows are calculated on a 15-minute basis (for sites 1 through 4) or a 12-minute basis (for Sites 5 through 7) using the measured data and averaged over the measurement period to obtain the average flow.

2 Apparent steady-state flows are calculated using the time-averaged injections and concentrations for the entire measurement period, replicating the methodology of the time-averaged PFT technique. The injections and concentrations used are the LBL tracers.

3 The SD % is the standard deviation of the 12-minute flows expressed as a percentage of the average flow.

4 Max/Min is the ratio of the maximum flow during the measurement period to the minimum flow (both obtained from the 12-minute averages).

5 From 5-zone analysis; figures only available from the first four days.

9

MECHANICAL SYSTEMS

Modeling

The interaction of mechanical ventilation and natural infiltration is quite complicated. The additional ventilation provided by supply and exhaust fans can be estimated using a simple fan model initially proposed during Phase I (Palmiter and Bond, 1991a). The model was extended to predict the infiltration effects of forced-air systems in which both supply and return duct leakage exist. A comprehensive discussion of the interaction of fans with stack effect is given by Palmiter and Bond (1991b).

It is useful to separate ventilation systems into balanced flow systems (neutral pressure) and unbalanced flow systems, which are further subdivided into supply-fan (positive pressure) and exhaust-fan (negative pressure) systems. A balanced-flow system has two fans, one pumping air into the building and one pumping the same amount of air out. The pressure within the building remains unchanged, so there is no interaction between the mechanical system and natural infiltration. The inward flow through the balanced system is simply added to the natural infiltration. Unbalanced systems change the internal pressure, which alters the infiltration and exfiltration through the envelope. This fan model accounts for this interaction and predicts the infiltration resulting from balanced or unbalanced flows induced by mechanical ventilation systems.

Equations for the model are given in Table 9-1. In these equations, Q_{nat} is the natural infiltration rate; Q_{add} is the infiltration added by the mechanical system. The interaction of natural and mechanical infiltration results from changes in house pressure due to unbalanced flows. Q_{max} and Q_{min} are total inward or outward flows through mechanical devices across a system boundary that contains the building envelope, heating system and ductwork. For example, the total outward flow would include flow out of an exhaust fan and leakage out of the heating system supply ducts. Q_{max} is the larger of the total inward flow or total outward flow, and Q_{min} is the smaller of these. If there is only a single exhaust fan and no duct leakage, Q_{max} is the fan flow and Q_{min} is 0. For a balanced ventilation system or balanced duct leakage, Q_{max} and Q_{min} are equal.

The unbalanced flow to the house is given by the difference between Q_{min} and Q_{max}. A change in the equations for added flow occurs when the unbalanced flow is greater than twice the natural infiltration rate. This transition corresponds to the point where the neutral level rises above the ceiling or drops below the floor; that is, all of the flow

through the walls, floor and ceiling is in one direction. The additional term in the equations for duct leakage results because some of the air which leaks into the return exits through supply leaks.

Table 9-1
Equations for fan and duct leakage model

Cause	Condition	Added flow
Ventilation fans	$Q_{max} - Q_{min} < 2Q_{nat}$	$Q_{add} = \frac{1}{2}(Q_{max} + Q_{min})$
	$Q_{max} - Q_{min} \geq 2Q_{nat}$	$Q_{add} = Q_{max} - Q_{nat}$
Duct leakage	$Q_{max} - Q_{min} < 2Q_{nat}$	$Q_{add} = \frac{1}{2}(Q_{max} + Q_{min}) - \frac{Qd_{max}}{Q_{fan}} Qd_{mun}$
	$Q_{max} - Q_{min} \geq 2Q_{nat}$	$Q_{add} = Q_{max} - Q_{nat} - \frac{Qd_{max}}{Q_{fan}} Qd_{mun}$

Definitions		
	Q_{add}	Infiltration added by mechanical system
	Q_{fan}	Flow through air handler fan
	Q_{max}	Larger of (1) total outward flow through exhaust fans plus supply leakage or (2) total inward flow through supply fans plus return leakage.
	Q_{min}	Smaller of (1) total outward flow through exhaust fans plus supply leakage or (2) total inward flow through supply fans plus return leakage.
	Q_{nat}	Natural infiltration
	Qd_{max}	Larger of supply and return leakage
	Qd_{min}	Smaller of supply and return leakage

Table 9-2 gives two equations for the furnace efficiency loss due to duct leakage, one in terms of the actual flows and one in terms of the leakage fractions. The efficiency loss results from heated air leaking out of the supply ducts as well as from the increase in infiltration. This loss is that which occurs solely due to air leakage, assuming that ducts are perfectly insulated; the equations do not include the effects of conduction losses.

The manner in which our model combines mechanical flows with natural infiltration in the case where unbalanced flows are less than twice the natural flow (the building is not fully pressurized or depressurized) is illustrated for several cases in Figure 9-1. F_s and F_r are the leakages in the supply and return ductwork, respectively, expressed as fractions of the total flow through the air handler.

Table 9-2
Equations for efficiency loss due to duct leakage

$$\varepsilon_L = \frac{Q_{add}}{Q_{fan}} \frac{\Delta T_h}{\Delta T_f} + \frac{Qd_s}{Q_{fan}} = F_{add} \frac{\Delta T_h}{\Delta T_f} + F_s$$

F_{add}	Added infiltration as a fraction of air handler flow
F_s	Supply duct leakage as a fraction of air handler flow
Q_{add}	Infiltration added by mechanical system
Q_{fan}	Flow through air handler fan
Qd_s	Supply duct leakage
ε_L	Efficiency loss
ΔT_h	House-to-ambient temperature difference
ΔT_f	Furnace-to-ambient temperature difference

The left column of pictures shows the effect of duct leakage; the right column of pictures are identical except for the addition of a 50-cfm exhaust fan. The upper left picture shows the base case of stack-driven natural infiltration of 100 cfm and exfiltration of 100 cfm.

The picture on the middle left illustrates a situation with dominant return leakage. The flow through the air handler is 1000 cfm, with 100 cfm of return leakage and 50 cfm of supply leakage. In this case, Q_{min} is 50 cfm and Q_{max} is 100 cfm. For this case and those which follow, Qd_{min} is 50 cfm and Qd_{max} is 100 cfm, resulting in an unbalanced flow of 50 cfm to the home.

Because the supply flow exceeds the return flow, the home is partially pressurized, reducing the flow inward through the floor by 25 cfm and increasing the flow outward through the ceiling by 25 cfm. There are inward flows of 75 cfm through the floor and 100 cfm on the return side of the fan, but 5% of the fresh air entering the return is lost through supply leaks, resulting in only 95 cfm of added infiltration. The total flow is 170 cfm, thus yielding an added flow of 70 cfm over natural infiltration.

The lower picture shows the situation with dominant supply leakage of the same magnitudes as the return leakage case. Q_{min} and Q_{max} are 50 and 100 cfm, respectively. In this case, the home is partially depressurized, resulting in reduced flow through the ceiling and increased flow through the floor. The added flow is 70 cfm, as before. If the magnitudes are the same, excess return leakage or excess supply leakage lead to the same added infiltration.

Turning to the cases with the exhaust fan, the upper right picture shows the case of an exhaust fan with a flow of 50 cfm. Here, Q_{min} is 0 and Q_{max} is 50 cfm. The flow through

the ceiling then decreases by 25 cfm, or half of the fan flow, while the flow through the floor increases by 25 cfm. The total infiltration rate is thus increased by 25 cfm.

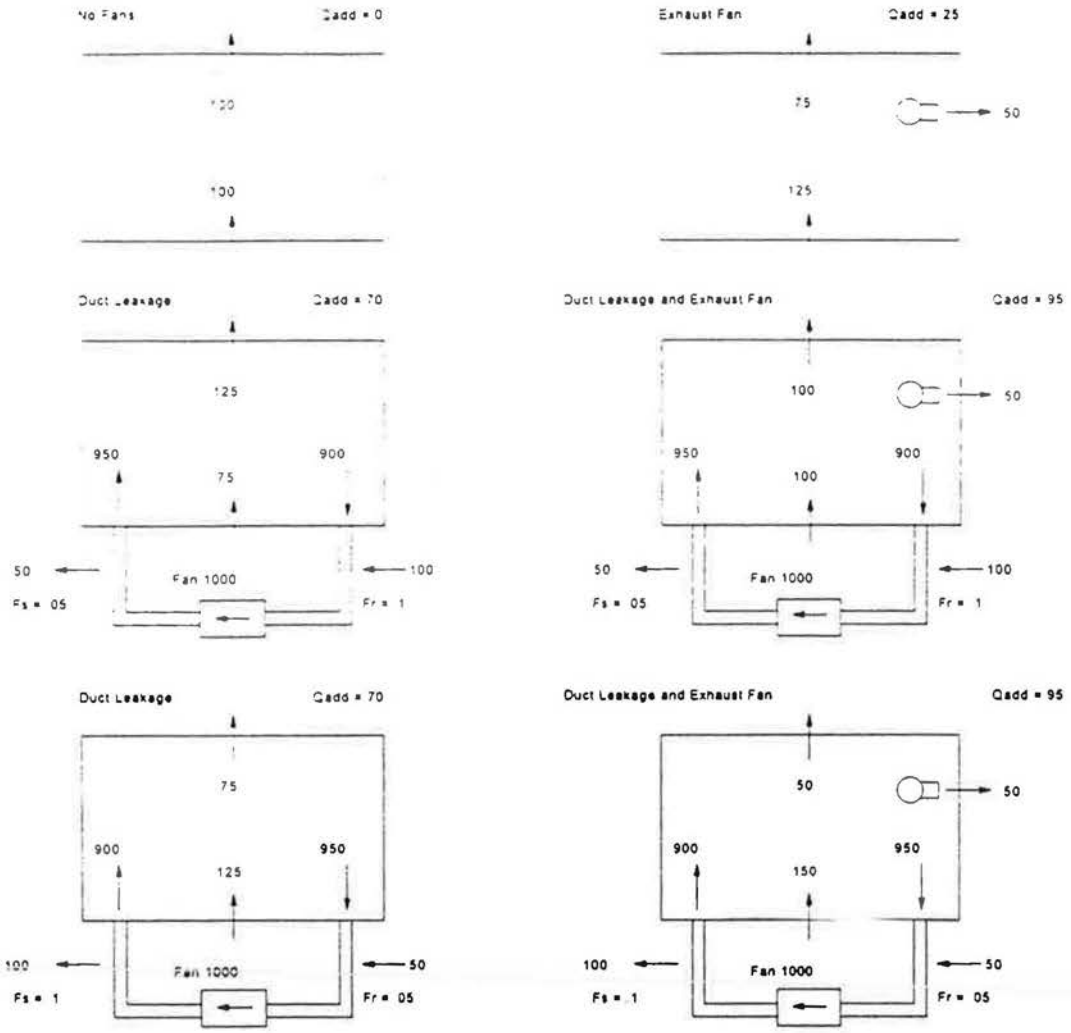

Figure 9-1
Examples of combined flows

Q_{add} is the added flow due to exhaust fans or duct leakage; F_s and F_r are the supply and return leak fractions. The vertical arrows in the center are infiltration and exfiltration through the envelope due to the combination of stack effect and mechanical ventilation.

The middle picture on the right shows the excess return leakage case combined with the exhaust fan. The 50 cfm of extra supply flow is just balanced by the 50 cfm flowing through the fan, so the home remains at neutral pressure. Q_{min} and Q_{max} are both 100 cfm. The natural infiltration remains at the base value, but an added 95 cfm comes through the return system.

The lower right picture shows the exhaust fan combined with the excess supply leakage case. In this case, the exhaust fan combines with the excess return flow of 50 cfm to produce 100 cfm of outward flow, which depressurizes the home more strongly than either system alone. In this case, Q_{min} is 50 cfm and Q_{max} is 200 cfm. The total infiltration now includes 150 cfm entering through the floor and 45 cfm entering through the ductwork; the total added infiltration is 95 cfm.

It is interesting to note that the effect of combining an exhaust fan with duct leakage is symmetric with respect to whether the duct leakage is predominantly on the return side or the supply side; the added flow does not depend on which side the leakage occurs. However, in one case the building remains at neutral pressure, while in the other case it is strongly depressurized.

Field Results

Of the seven homes tested, Site 2 was complicated by occupant effects (frequent window openings), Site 3 experienced very low indoor-outdoor temperature differences and had very high duct leakage, and Site 7 was located on an extremely windy site. The remaining four homes are more representative of the typical magnitudes of the effect of mechanical systems relative to natural infiltration rates under typical winter conditions.

The measured infiltration and predicted living-zone infiltration rates at these four sites are illustrated in Figures 9-2 through 9-5. In each figure, the upper graph shows the natural infiltration prediction as a bold line, compared with the measured infiltration. In the lower graph in each figure, the bold line represents the prediction of total infiltration, calculated by using the fan model to combine measured fan flows with the natural prediction. Results from each site are discussed individually below.

Site 1 had no forced-air heating system; its ventilation system was a multiport exhaust system with a measured flow rate of about 75 cfm. During the tracer test, the exhaust system was operated on a timer, twice each day for a period of four hours. There were six other exhaust fans, which the occupants used extensively. Times recorded in occupant logs and fan flows measured with flow hoods were used to produce a total fan flow for the model.

Even with the extensive fan use, the overall infiltration rate is still dominated by the stack effect, which accounts for 66% of the total infiltration. The multiport exhaust provides 15% of the total infiltration, and other fans account for 12%. If the multiport exhaust ran continuously, the ventilation rate in this home under these conditions would average 95 cfm or 0.46 ACH.

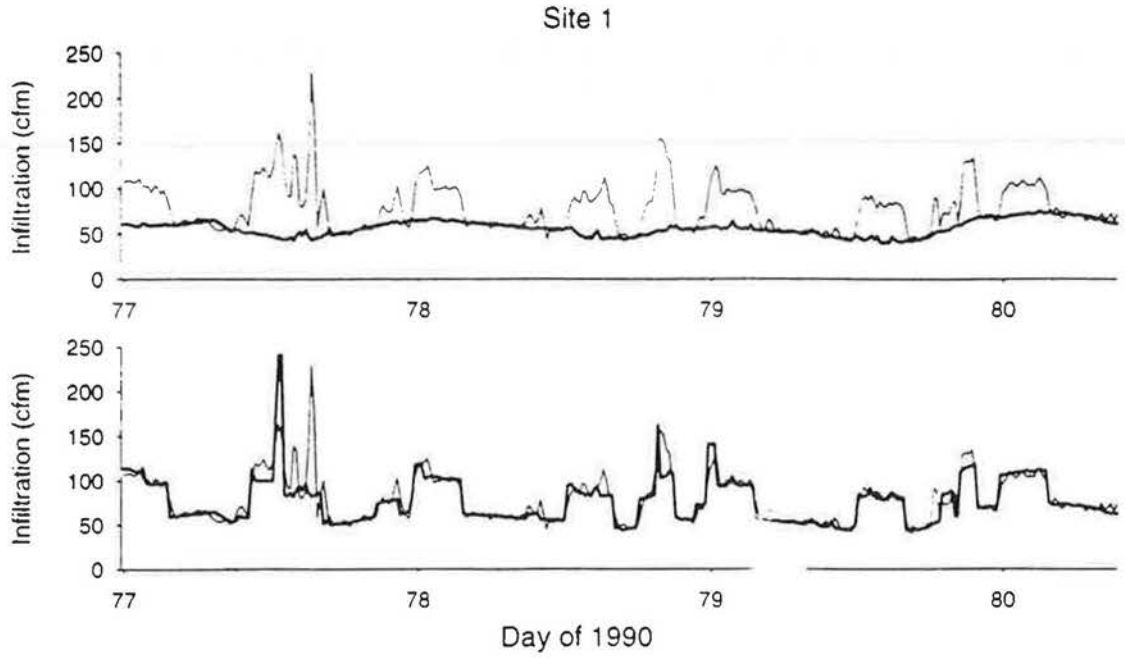

Figure 9-2
Measured and modeled infiltration at Site 1

The bold line in the upper graph is the adjusted natural infiltration prediction; in the lower graph it is the adjusted infiltration combined with the fan model.

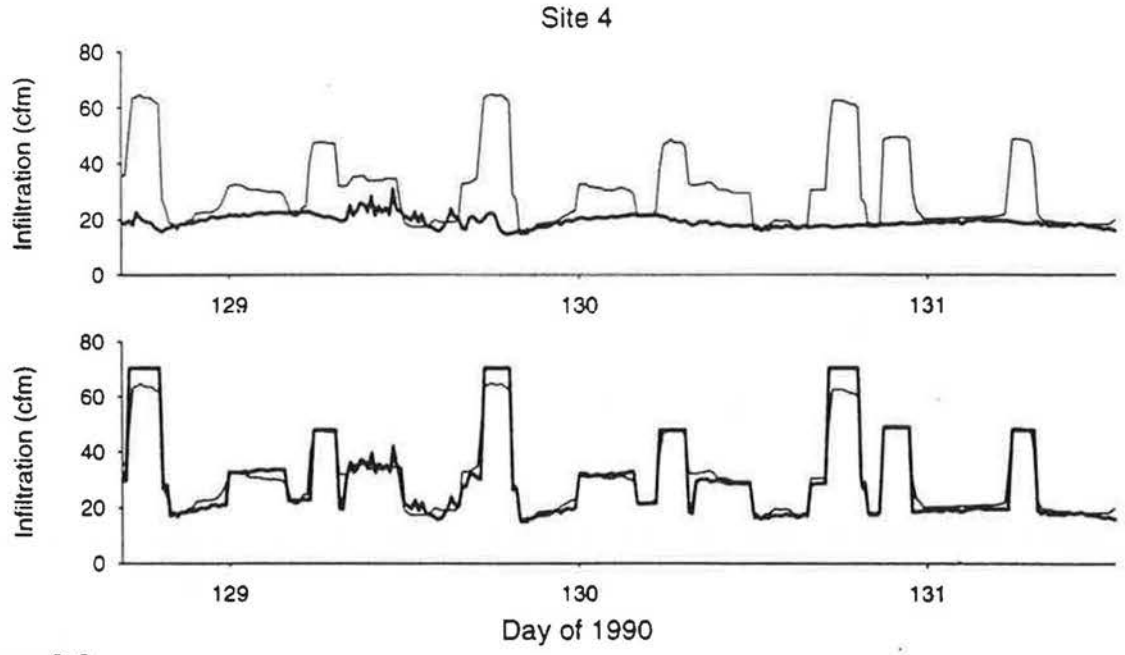

Figure 9-3
Measured and modeled infiltration at Site 4

The bold line in the upper graph is the adjusted natural infiltration prediction; in the lower graph it is the adjusted infiltration combined with the fan model.

The two spikes in the measured data on day 77 are due to door openings, which show clearly in the temperature and pressure data. The other discrepancies were attributed to errors in the occupant log and uncertainties about flows through some of the fans. Considering these uncertainties and the simplifications required for development of the model, the agreement is quite satisfactory.

Site 4, a manufactured home, had a central air handler in the home with supply ducts in the crawl space and a single return grille located just above the air handler, so there was no return duct system. The make-up air system to the air handler was sealed for the period discussed here.

At this site, the air handler fan was operated with a timer, four hours on and four hours off. The bath fan, which was the designated ventilation system for the home, was operated by a timer twice a day for periods of two hours; once in the early morning when the air handler was off, and once in the afternoon when the air handler was running. The range hood was also operated manually once at the end of Day 130.

Because all the supply ducts ran through the crawl space, the flow from the house to the crawl during periods when the air handler was on was used to estimate the supply leakage at about 22 cfm. The flow through the bath fan was measured at about 48 cfm.

In the infiltration graphs, the low wide pulses are caused by the operation of the air handler, and the higher narrow pulses show the effects of the bath fan. Although the bath fan, range hood, and air handler are predicted well on an individual basis, the infiltration when the air handler and bath fan operate simultaneously is overpredicted by the fan model. This suggests that the pressures created by the fan flow and supply leakage cause an interaction effect and that the total outward flow is lower than the sum of the two flows acting separately.

In this home, the flow through the bath fan ventilation system is more than twice the natural infiltration, so the total flow through the home is the bath fan flow when this fan operates. If this ventilation system were operated continuously, the 48 cfm would result in an air-change rate of only 0.30, lower than the minimum ventilation rate of 0.35 specified by ASHRAE.

In these homes, there is typically only a single return per floor; practice in the 1940s dictated returns in all rooms with supplies. As a result, rooms with supplies only, typically bedrooms, can be strongly pressurized when the air handler is running and the door is closed. Pressures across the master bedroom door in these homes ranged from one to eight Pascals.

Site 5 was a large home on a bluff near the open waters of Puget Sound, which experienced a fair amount of wind due to its location. The low peaks in the natural infiltration graph (the upper plot in Figure 9-4) in the evenings of Days 90, 91 and 92 are due to periods of elevated wind speed.

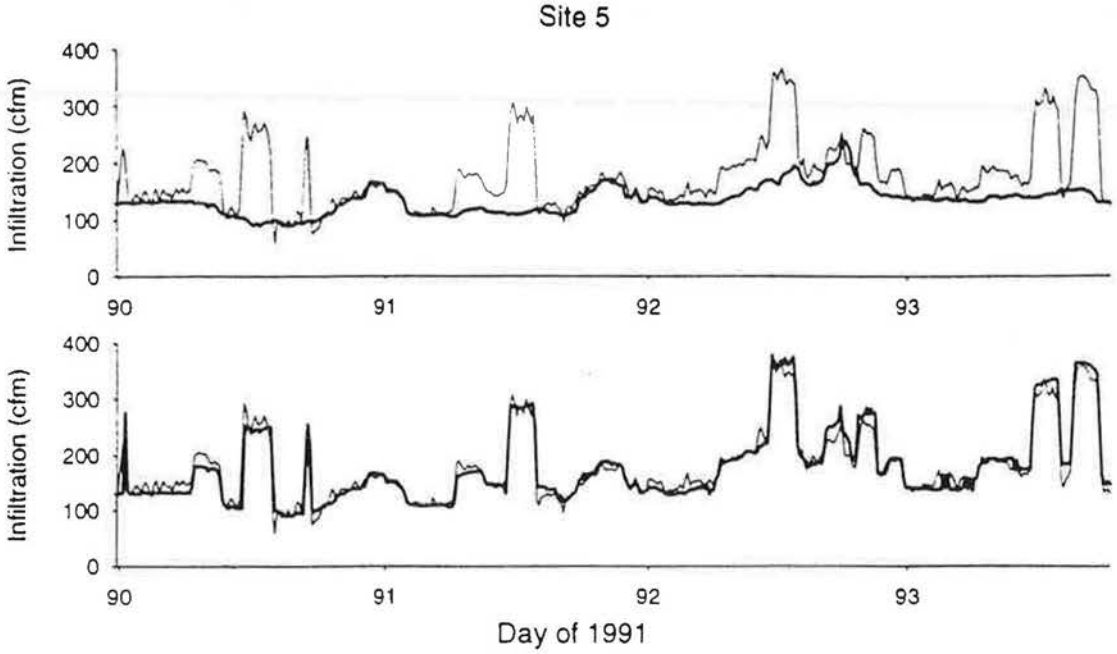

Figure 9-4
Measured and modeled infiltration at Site 5

The bold line in the upper graph is the adjusted natural infiltration prediction; in the lower graph it is the adjusted infiltration combined with the fan model.

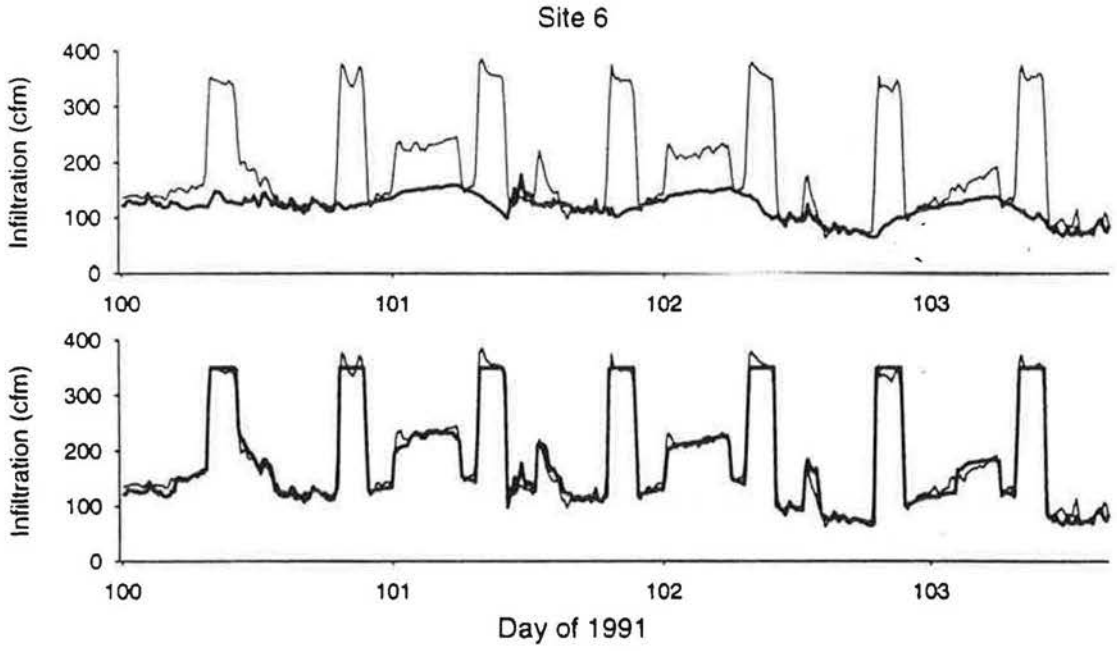

Figure 9-5
Measured and modeled infiltration at Site 6

The bold line in the upper graph is the adjusted natural infiltration prediction; in the lower graph it is the adjusted infiltration combined with the fan model.

This home had an electric heat pump and an air-to-air heat exchanger (AAHX); the air handler fan was operated from 6:30 to 9:00 each morning. The heat pump was also allowed to provide heat when required, resulting in its cycling most of the time. The added infiltration during times when the heat pump is cycling is calculated by multiplying the fractional on-time by the added infiltration predicted by the duct model.

The large pulses occurring just after noon each day are the air-to-air heat exchanger, which was timer-controlled to run for two hours each afternoon. The heat exchanger was also operated for two brief periods on Day 90. The second large pulse during the afternoon of Day 93 was caused by the simultaneous operation of the air-to-air heat exchanger and the heat pump.

Three subsidiary peaks are visible after the heat exchanger cycle on Day 92. The first and third peaks are due to our manual operation of the heat pump. The second pulse is caused by operation of the range hood for about 1-1/2 hours.

It is of interest to note that the heat pump had an electronic air cleaner and the occupants typically ran both the heat pump and air-to-air heat exchanger fans continuously, although they usually turned the heat pump fan off at night. In this home, natural infiltration alone produces 136 cfm, or 0.29 ACH. With the continuous operation of the heat exchanger, the house would receive 296 cfm or 0.62 ACH of ventilation.

Site 6 was a six-year-old home with a gas furnace. This home was pressurized by 6 Pa when the fan was operating due to the large return leaks in the duct system. One of the return ducts had been mounted in an incorrect joist space (the space adjacent to the one with the return grille), while the other duct had a large hole which was open to the attic.

The air handler fan was operated on a schedule twice a day, between 7:30 and 10:00 a.m. and 7:00 and 9:30 p.m. On the first day, it was noted that the furnace cycled almost continuously to supply the heating load, so the schedule was altered to force the heat off for 1-1/2 hours before and after the fan cycles. This allowed clean measurements of the impact of the air handler fan and estimation of the natural infiltration rate.

The tall pulses are the experimental operation of the air handler fan and the remainder of the elevation above natural infiltration is due to cycling of the furnace. Because the home is completely pressurized, the total flow through the home when the fan runs is the unbalanced flow through the air handler, or 350 cfm. During periods of cycling, the infiltration is modeled as the unbalanced flow multiplied by the fractional fan on-time plus the natural infiltration times the fractional off-time.

Continuous operation of the air handler fan in this home would produce a constant flow of 350 cfm, or 1.41 ACH, of ventilation.

Ventilation Systems

To verify the simple fan model for ventilation systems, actual and predicted changes in infiltration due to these systems at each site for which data were available were compared. Except for the balanced-flow air-to-air heat exchanger at Site 5, these systems were all exhaust ventilation systems. Table 9-3 summarizes fan flows for each system evaluated; these were measured with either a flow hood or tracer gas.

The measured change in infiltration was the difference between infiltration with the fan off and with the fan running during periods when there were no other mechanical devices operating. For the range hood at Site 5 and the bath fans at Site 6, these measurements were taken from a single experiment; the remainder of the ventilation systems were operated on timers throughout the tracer test, and the measured change in infiltration is an average value.

As shown in the table, the ratios of measured to predicted infiltration range from 0.83 to 1.30, with a mean of 1.01 and a median of 1.00. The largest discrepancy occurs with the three simultaneously running bathroom fans at Site 6.

Table 9-3
Assessment of simple fan model

	Measured Fan Flow [1] (cfm)	Change in Infiltration (cfm)		
		Measured	Predicted	Ratio
Site 1 - Multiport exhaust	75	37.0	37.5	0.987
Site 3 - Bathroom (1st floor)	27	13.5	13.5	1.000
Site 4 - Bathroom (Hall)	50	25.8	25.0	1.032
Site 4 - Range hood	67	30.7	33.5	0.916
Site 5 - AAHX	154	160.0	154.0	1.039
Site 5 - Range hood	205	85.0	102.5	0.829
Site 6 - Bath fans (3)	94	61.0	47.0	1.298
Average		413.0	425.0	1.014

1 Fan flows were measured with flow hoods, except for the range hood at Site 5, which was measured with tracer gases.

Forced-Air Distribution Systems

As illustrated in Figures 9-2 through 9-5, forced air distribution systems can have a large effect on living-zone infiltration rates. Effects of these systems occur when the air handler fan is off as well as when it is running.

Table 9-4 lists results from blower door tests with the heating registers unsealed. Blower door tests were also performed with the registers sealed; the difference between these two measurements is an estimate of the leakage in the ductwork. These leakage estimates are also given in Table 9-4 as a percentage of the total leakage of the home. For these homes, duct leakage ranges from 5% to 33% of the total leakage of the home, to a first approximation. This means that the natural infiltration rate is correspondingly increased during the times when the fan is not running.

The infiltration effects when the air handler is running are difficult to predict because of varying pressures and differing leakage areas throughout the duct system, and are best measured using tracer gas methods. For example, a small hole under high pressure may leak as much as a larger hole under less pressure. In addition, many of the actual leaks in a duct system may be to or from the house rather than the crawl space or the attic.

The fan-on infiltration effects of duct leakage for these sites are summarized in Table 9-5. The first row shows the flow through the air handler fan. The second section characterizes the percentage leakage with the air handler running; total leakage ranges from 3% to 64% of the flow through the air handler. It is clear that the leakage at Site 6 is disastrously large.

It is important to distinguish supply leaks from return leaks, because of the differing temperatures. Under heating conditions, a return leak simply introduces additional infiltration into the home, while a supply leak not only creates additional infiltration but results in the loss of air which has already been heated. Assuming that, under design conditions, the temperature difference across the furnace is approximately the same as that from the house to outdoors, the equations in Table 9-2 can be used to calculate the efficiency loss. These losses are given in the last row of Table 9-5; for these homes, they range from 3% to 47%, with a median of 9%.

Because, for the most part, the air handler fans were run on timers as scheduled experiments in these homes, the total amount of added infiltration as realized in the measured data is not necessarily representative of actual operating conditions. In addition, due to differences in weather conditions, the homes were tested with varying indoor-outdoor temperature differences.

In typical winter weather, it was estimated that a furnace or heat pump operates on a 33% duty cycle for 18 hours each day. During the other six hours, the system is off. This results in an overall runtime of six hours per day.

In order to calculate the overall infiltration impact of the ductwork, the natural infiltration in each of the homes was adjusted to correspond to a temperature difference of 25 F and assumed a runtime of six hours per day for the heating system.

Table 9-4
Blower door test results for seven homes

	Site 1	Site 2	Site 3	Site 4	Site 5	Site 6	Site 7
Effective leakage area (in^2)	86.8	159.9	163.4	44.3	189.7	158.6	59.6
Flow at 50 Pa (ACH)	7.24	10.10	12.79	5.01	7.16	10.55	7.03
Flow at 50 Pa (cfm)	1492	2962	3033	792	3400	2616	1141
Duct Leakage as Percent of Total							
Flow at 50 Pa (%)	--	8.9	18.9	4.8	4.8	32.8	19.3
ELA (%)	--	7.8	21.1	4.8	6.7	39.3	21.5

Table 9-5
Tracer-based estimates of duct leakage

	Site 2	Site 3	Site 4	Site 5	Site 6	Site 7
Air handler flow (cfm)	1100	727	700	1500	955	680
Duct Leakage with Air Handler Running (Percent of Fan Flow)						
Supply leak (%)	2.8	11.5	3.2	2.9	19.4	7.0
Return leak (%)	2.8	7.8	0	3.9	45.0	4.5
Total leak (%)	5.6	19.3	3.2	6.8	64.4	11.6
Estimated Impact on Furnace Efficiency at Design Conditions						
Efficiency loss (%)	5.5	20.2	4.8	3.3	47.4	12.4

The results of these calculations are given in Table 9-6. The first line shows the natural infiltration assuming measured wind and a temperature difference of 25 F. The second section summarizes the added infiltration with the fan on, the fan off, and the total. The last section gives the total infiltration and the infiltration added by the heating system as a percentage of the total. These percentages range from 13% to 60%.

In general, the findings concerning added infiltration due to duct leakage, both with the fan off and with the fan on, are consistent with other findings in the literature (Cummings and Tooley, 1989; Cummings et. al., 1990; Lambert and Robison, 1989; Modera, 1989; Modera et. al., 1991; Parker, 1989).

Table 9-6
Overall infiltration impact of ductwork (Air handler running 6 hours/day)

	Site 2	Site 3	Site 4	Site 5	Site 6	Site 7
Base natural infil. (cfm, sealed)	127.4	82.2	20.4	127.4	78.9	86.1
Q added, fan on (cfm)	11.0	20.0	3.2	14.1	67.3	14.4
Q added, fan off (cfm)	9.4	14.4	.8	4.8	28.9	15.4
Total added (cfm)	20.4	34.4	4.0	18.9	96.2	29.8
Total infiltration (cfm)	147.8	116.6	24.4	146.3	175.2	115.9
Added as % of total	13.8%	29.5%	16.3%	12.9%	59.9%	25.7%

Effects of Closing Bedroom Doors

As is common in Northwest homes, the tested homes had supply grilles in each bedroom and in the common areas, and central returns. When a bedroom door is closed while the air handler is running, the net flow to that room is unbalanced, causing a pressurization of the bedroom and a depressurization of the remainder of the home. Table 9-7 summarizes pressures across the bedroom doors at the six homes with central heating systems. Supply flows to these bedrooms are also listed in the table.

Because these pressures are large compared with the magnitudes of typical naturally-induced pressures, the infiltration effects of closing bedroom doors can be large. A separate test on Site 4 was performed with the master bedroom door closed. The pressure across the door was 6 Pa, resulting in a 4.5 Pa pressurization of the bedroom relative to ambient and a depressurization of 1.5 Pa of the rest of the home. The measured infiltration was more than doubled with the door closed. It should be noted that this effect is worsened if duct leakage is low.

Pressures at Site 6 were smaller than typical for other sites due to unusual conditions of this home. The lack of induced pressure across the master bedroom door at Site 6 is highly unusual and may have been caused by leakage into a vertical firred-out return chase, which was strongly depressurized, located in the master bedroom. Pressures induced across the doors of the study and bedroom 1 were smaller than typical due to low supply flow to these rooms.

Table 9-7
Pressures across bedroom doors with air handler running

	Door Location	Supply Flow (cfm)	ΔP (Pa)
Site 2	Master bedroom	92	4.5
	Guest bedroom	102	4.3
	Office (2nd floor, partly closed)	44	2.4
	Bathroom (2nd floor)	46	2.9
	Bathroom (1st floor)	67	4.0
Site 3	Master bedroom	97	2.3
	Master bathroom	39	1.4
	Bedroom 1	65	1.6
	Bedroom 2	58	1.6
Site 4 [1]	Master bedroom	178	4.5
	Master bathroom	98	4.0
	Guest bedroom	17	2.8
	Bathroom	45	1.9
	Sewing room	40	2.8
Site 5 [2]	Master Bedroom	120	2.4
	Study	84	2.6
	Bedroom 2	73	1.8
	Bedroom 3	82	1.2
Site 6	Master Bedroom	99	0.0
	Study	65	0.5
	Bedroom 1	32	1.1
Site 7	Master Bedroom	138	1.0
	Den	95	3.4
	Bedroom 1	99	3.7
	Bathroom	56	1.9

Door pressures were tested with all other interior doors open.

1 These measurements were done with the Blend-Air fan on the roof operating. These pressure differences across each door were reduced relative to those measured during the tracer test, when the Blend-Air fan was disabled.
2 Pressures were measured with heat pump operating and AAHX vents in each room open.

10

FINDINGS AND CONCLUSIONS

Suggested Improvements to LBL Model

The analysis to date supports several suggestions for improving the LBL model and the calculation of required inputs.

Throughout this project we have used an average stack height for the height parameter in both the LBL and AIM-2 model. This average stack height was also used for the NORIS homes. For these 134 homes, the reduction in height was about 32% relative to the height between the lowest leak and the highest leak. The reduction in predicted infiltration is about 16%. For the seven homes tested for this project, the average reduction in height was about 18%, resulting in a 9% reduction in predicted infiltration.

The wind-effect portion of the LBL model produces more accurate results when modified to account more realistically for wind-generated pressures across the floor and ceiling in the case of ventilated attics and crawl spaces. Analysis of the data strongly suggests that the original assumptions made in the LBL model are not justified. The Ecotope-modified LBL wind model typically predicts infiltration rates 28% lower than the original model. The predictions of the modified model agree well with the wind portion of the AIM model which uses the same external pressure coefficient assumptions as the Ecotope modification.

For homes in the Pacific Northwest, the terrain and shielding coefficients should each be set to a value of 4, whereas original LBL defaults were each set at 3. In this study, the extrapolation of airport wind speed to the site was within 6% of the site-measured wind speed, on average.

It should be noted that even when the measured site wind speed is used it was still necessary to reduce the wind speed for best agreement with the tracer-measured infiltration. This may be because the fraction of leakage in the walls is less than our default assumption of one-half.

Comparison of LBL and AIM-2 Models

The LBL and AIM-2 models differ systematically in their predictions of natural infiltration; the LBL model predictions were 26% greater for the stack effect, 61%

greater for the wind effect, and 28% greater for the total natural infiltration. Most of the difference between the two models is due to the consistent use of the blower door C and n in the AIM-2 model.

The wind-effect infiltration predicted by the modified LBL model is about 28% less than that of the standard LBL model and about 16% greater than that of the AIM-2 wind model.

Comparison of Measured and Modeled Infiltration

For these seven homes, both the LBL model and the AIM model had mean absolute prediction errors of 16%, and the modified LBL model had a mean absolute prediction error of 15%.

Effects of Ventilation Systems

Air-to-air heat exchangers typically have two fans; a supply fan pumping outdoor air into a building and an exhaust fan pumping indoor air out. If the supply and exhaust flows are balanced, there is no interaction with natural infiltration. The added infiltration is simply the supply flow through the ventilation system.

If supply and exhaust flows are not balanced, the ventilation system pressurizes or depressurizes the home. Under these conditions, the induced flows interact in a complex fashion with natural infiltration. We have proposed a simplified model of this interaction which agrees reasonably well with the measured data in these homes.

For typical natural infiltration rates seen in energy-efficient all-electric homes, and a typically sized exhaust fan system (50 cfm), it is necessary to operate the system continuously in order to meet ASHRAE Standard 62 for minimum ventilation rates, which requires an air-change rate of 0.35 ACH (ASHRAE, 1989a). Intermittent operation of one to two hours in the morning and evening will produce almost no measurable increase in ventilation.

Effects of Forced-Air Distribution Systems

Forced air distribution systems and associated duct leakage can have large effects on pressures and whole-house infiltration rates. Assuming a standard runtime of 6 hours/day, the median infiltration due to duct leakage was 21% of the total. Infiltration rates are increased both when the fan is off and when it is on.

In these homes, the median increase in natural infiltration due to duct leakage was 14%, which compares with other recent studies indicating a 16 to 20% increase (Palmiter and Brown, 1989; Palmiter et. al., 1991).

The increased infiltration when the fan is on tends to be much larger than the increase in natural infiltration, because the pressures produced by the air handler are much greater than natural pressures.

The measured data also show a large impact on infiltration due to closing one or more doors to bedrooms with supplies but no returns. Typical pressures measured across the bedroom doors were 4 Pascals.

The extension of the fan model to unbalanced flows due to duct leakage agrees reasonably well with the measured data.

Although a return leak and a supply leak of the same magnitude have the same effect on infiltration, supply leaks have much greater impacts on furnace efficiency than do return leaks.

Measured Natural Infiltration

The measured natural infiltration under winter conditions ranged from 0.14 to 0.66 air changes per hour, with an average of 0.37 ACH for the seven homes. Excluding Site 7 with its unusually windy location, the average was 0.32 ACH. Natural infiltration in three of the seven homes would fail to meet the 0.35 ACH minimum ventilation rate required by ASHRAE Standard 62, thus indicating the need for mechanical ventilation. With the exception of Site 7, natural infiltration in these homes is stack-dominated and the additional infiltration due to wind is small.

Time-Averaging Bias

The average bias due to the time-averaging as used in the PFT technique is 5% for living-zone infiltration, 12% for attic infiltration and 15% for crawl space infiltration. The measured data confirm the simulation results, which show that buildings in which the infiltration is totally wind-dominated can have substantial bias; the highest measured was 30% for the crawl space at Site 2. The bias which occurs under stack-dominated conditions is small.

Infiltration Rates in Attics and Crawl Spaces

All of these homes had well-ventilated crawl spaces, and, except for the two manufactured homes, they had ventilated attics. Crawl space infiltration rates averaged 4.6 ACH and attic infiltration rates averaged 6.9 ACH, compared with an average for the living space of 0.37 ACH. The infiltration into attics and crawl spaces is very wind-dominated.

Blower Door Tests

We performed precision blower door tests covering a range of pressures between 1-2 Pa and 60-70 Pa on six of the seven sites. At all sites, except for Site 4, the measured flows at low pressure were less than those obtained by extrapolating using the power law fit obtained from the data taken between 15 and 60 Pa. The exponents estimated from the low-pressure data (roughly 1-10 Pa) were higher in all cases, an average of 0.71 compared with the 0.65 for the conventional pressures.

These results are consistent with the Ethridge model of the pressure-flow relationship. However, in spite of trying to obtain optimum conditions, such effects could also be caused by bias due to pre-existing stack or wind pressures, or by systematic error when using the smallest orifice on the blower door. Similar low-pressure tests should be done on a large number of homes before drawing firm conclusions about the low-pressure relationship.

11

REFERENCES

ASHRAE. 1989a. *ASHRAE Standard* 62-1989, "Ventilation for Acceptable Indoor Air Quality." Atlanta: American Society of Heating, Refrigerating, and Air-Conditioning Engineers, Inc., Atlanta.

ASHRAE. 1989b. *1989 ASHRAE Handbook: Fundamentals.* American Society of Heating, Refrigerating and Air Conditioning Engineers, Inc., Atlanta.

Baker, P.H., S. Sharples, I.C. Ward. 1987. "Air Flow Through Cracks." *Building and Environment*, Vol. 22, No. 4, 1987.

Cummings, J.B.; J.J. Tooley; and N. Moyer. 1990. "Impacts of Duct Leakage on Infiltration Rates, Space Conditioning Energy Use, and Peak Electrical Demand in Florida Homes." Proceedings of the ACEEE 1990 Summer Study on Energy Efficiency in Buildings.

Cummings, J.B.; and J.J. Tooley. 1989. "Infiltration and Pressure Differences Induced by Forced Air Systems in Florida Residences." *ASHRAE Transactions*, June 1989.

Lambert, L.A.; and D.H. Robison. 1989. "Effects of Ducted Forced-Air Heating on Residential Air Leakage and Heating Energy Use." *ASHRAE Transactions 1989*. 95:2.

Liddament, M.W. 1986. "Air Infiltration Calculation Techniques– An Applications Guide." Air Infiltration and Ventilation Centre. Bracknell, Berkshire, Great Britain.

Modera, M.P. 1989. "Residential Duct System Leakage: Magnitude, Impacts and Potential for Reduction." *ASHRAE Transactions 1989*.

Modera, M.; D. Dickerhoff; R. Jansky; and B. Smith. 1991. *Improving the Energy Efficiency of Residential Air Distribution Systems in California.* Lawrence Berkeley Laboratory Report LBL-30886. Berkeley, CA.

Palmiter, L.; and I.A. Brown. 1989. "Northwest Residential Infiltration Survey: Analysis and Results." Prepared for the Washington State Energy Office under Contract No. 88-04-21.

Palmiter, L.; I. Brown; and T. Bond. 1991. "Measured Infiltration and Ventilation in 472 All-Electric Homes." *ASHRAE Transactions 1991.* Atlanta: American Society of Heating, Refrigerating, and Air-Conditioning Engineers, Inc.

Palmiter, L.; and T. Bond. 1991a. *Measured and Modeled Infiltration: A Detailed Case Study of Four Electrically Heated Homes.* Electric Power Research Institute Report CU-7327, May 1991.

Palmiter, L.; and T. Bond. 1991b. "Interaction of Mechanical Systems and Natural Infiltration." Presented at the AIVC Conference on Air Movement and Ventilation Control Within Buildings, Ottawa, Canada, September 1991.

Parker, D.S. 1989. "Evidence of Increased Levels of Space Heat Consumption and Air Leakage Associated with Forced Air Heating Systems in Houses in the Pacific Northwest." *ASHRAE Transactions*, June 1989.

Sherman, M.H. 1989. "Analysis of Errors Associated with Passive Ventilation Measurement Techniques." *Building and Environment* **24**, 131-139.

Sherman, M.H.; and D.J. Dickerhoff. 1989. "A Multigas Tracer System for Multizone Air Flow Measurement." Proceedings of the ASHRAE/DOE/BTECC/CIBSE Thermal Performance of the Exterior Envelopes of Buildings Conference, December 1989.

Sherman, M.H.; and D.T. Grimsrud. 1980. "Measurement of Infiltration Using Fan Pressurization and Weather Data." Lawrence Berkeley Laboratory Report LBL-10852. Berkeley, CA.

Walker, I.S.; and D.J. Wilson. 1990. "The Alberta Air Infiltration Model." Technical Report 71. University of Alberta, Department of Mechanical Engineering.

APPENDIX A. DETAILED RESULTS - SITE 5

Site Characteristics

Site 5 was a three-level house located on a steep bluff near the open waters of Puget Sound in Tacoma, Washington. It was built in 1988 and certified under the local utility's "Super Good Cents" program.

Basic characteristics of the home are listed in Table A-1. The home was fairly large, with a floor area of 3,500 square feet. Both the floor area and volume are about 80% larger than those of typical Northwest energy-efficient homes.

The average stack height of the home, which was used in the infiltration models, was 19% lower than the actual height of the home, measured from the lowest floor to the highest ceiling. This reduction occurred because the levels of the home are staggered, as discussed below, so that a portion of the structure has only one story.

Table A-1 also gives several leakage parameters of the home, which are derived from a blower door depressurization test over a range of house pressures from 9 to 42 Pa (unlike the other homes, which were tested between 15 and 60 Pa). The effective leakage area (ELA) is the area which would result in the flow predicted from the leakage function at a pressure of 4 Pascals. This home has a relatively large ELA because of its large size. However, the home is typical of recently built, energy-efficient homes in normalized measures of leakage such as the specific leakage area (SLA) and the air changes at 50 Pa.

During the depressurization test, a large amount of leakage from the recessed lights (28 upstairs and 21 downstairs) and from the equipment room was detected. There was also air leakage around several of the operable windows.

The three levels of the home were staggered; the arrangement of these levels is most easily visualized by looking at the elevation drawing in Figure A-1. A schematic floor plan of the home is shown in Figure A-2. The lowest level of the home contained four bedrooms. The upper level, directly above, included the living room, family room and kitchen. These levels were on the west side of the home. The middle level, directly

below the garage, was approximately four feet above the first level; it consisted of a recreation room, laundry room and storage room. This level was located on the east side of the home against the bluff, so it had very little exposure to the wind.

The lower and middle levels were built over crawl spaces, which were connected by a narrow passageway. Because the home was built on a slope, the height of the crawl space ranged from about two feet to about ten feet. Figure A-3 shows a schematic drawing of the crawl space, including the ductwork.

The home also had two attics: one above the upper level and one above the garage. The two attics had no connection and are also depicted in Figure A-3.

Test Conditions

Each level of the home was treated as a separate zone fc :e purposes of the tracer test. The crawl space and attic were also measured as zones.

During the tracer test, both the heat pump fan and the AAHX were controlled by computer. The heat pump fan ran from 6:30 a.m. to 9:00 a.m. The heat pump also ran whenever the thermostat called for heat, so that it cycled during most of the morning. The heat exchanger ran from 11:30 a.m. to 1:30 p.m.

Several experiments were performed on April 2 and 3 (Days 92 and 93) to study the effects of the heat pump, the heat exchanger and the kitchen range hood. The results of these experiments are discussed later in this chapter.

Weather Conditions

Site 5 was selected for its wind exposure; the prevailing winds came from Puget Sound to the west. Because of the home's position on a bluff, the west face of the home was exposed to the wind. However, the north and south sides were quite sheltered because of the proximity of neighboring houses. The east side, facing the bluff, received very little wind.

Table A-2 summarizes environmental conditions during the test; these are graphically represented in Figure A-4. The average indoor-outdoor temperature difference during the tracer test was about 24 F, comparable with typical heating season conditions in the Puget Sound region. The site was quite close to the Seattle-Tacoma airport, and the measured outdoor temperatures are about the same as those at the airport.

Wind speeds were measured with two towers, one above the northwest corner of the house at about roof level, and one at the southeast corner of the home 20 feet above the ground. The wind speeds averaged about 4 mph and reached as much as 12 mph, much greater than those at any of the sites in Phase I. As expected, the west measurement was

higher, by about 30%. Infiltration predictions made with the wind speed measured on the east side of the home were found to correlate better with the measured data.

Equipment

The home was heated and cooled by a single Trane heat pump located in an equipment room in the lower level. The heating supply ducts for the lower and middle levels ran through the crawl space; for the upper level, the ducts ran through the space between the two floors. There was air leakage through holes and joints in the supply plenum.

The air handler system included a Honeywell electronic air cleaner located above the return plenum. The homeowners typically ran the fan continuously during the day to clean the air, but turned it off at night because of the noise. The air handler fan was controlled separately during the tracer test.

There were two return grilles in the house. The grille in the lower level was in the hallway near the furnace room, and the return air ran through a joist space to the air handler. The return in the upper level was ducted through the attic to the second-story wall above the furnace room, and a passage through the wall was intended to serve as the remainder of the return duct. This passage terminated in the space between the first and second stories.

With the air handler running, the equipment room was depressurized by about 8 Pa, indicating large return leaks in the room. The return plenum next to the ceiling was found to be completely open on top, although the ceiling wallboard disguised the fact. Thus, return air was drawn not only through the joist space to the lower level and the wall cavity to the upper level, but also from the entire space between the two floors.

Table A-3 lists measured flows through the supply and return registers in each level. The supply flow was greater than the return flow in each zone, resulting in an apparent imbalance of about 770 cfm. However, the home was not pressurized by the operation of the heat pump, suggesting that the actual imbalance was small. We believe that air returned from the house to the heat pump through many passages in the walls of the home due to the problems with the return ducting.

Super Good Cents specifications require a ventilation system with exhaust and intake provisions; as in many homes in Tacoma, this requirement was met with an air-to-air heat exchanger (AAHX). The homeowners usually ran the AAHX continuously, although this unit was operated on a timer during the tracer test.

The AAHX in this house was unusual because the exhaust air was drawn from several points in the home, including the bedrooms, and there was a single supply in the heat pump return register in the lower level. This resulted in a direct supply of fresh air to the central air handler when both the AAHX and the heat pump were operating. The system may have been designed to provide balanced flow to the individual rooms. The

AAHX had no damper between the supply side and the outdoors, so the heat pump was able to draw fresh air in through the return whenever it ran.

AAHX return ducts from the lower and middle levels ran through the crawl spaces; returns from the upper level were located in the ceiling and ducted through the upper attic. Both intake and exhaust ducts ran through the lower crawl space to the west face of the house. The exhaust duct had become disconnected from its connection through the floor of the house, and exhaust air entered the crawl space when the system ran.

Infiltration

Figure A-5 shows the measured living-zone infiltration rate along with infiltration predicted by the AIM-2 model. This model was selected because it agrees more closely with the measured data than the LBL model during periods with no fan operation and low wind speeds. The upper graph shows the prediction of the AIM-2 stack model; the middle graph shows the AIM-2 full model. The full model, using the site wind speed, greatly overpredicted the infiltration, and it was necessary to multiply the wind prediction by 0.7 before combining the stack and wind models.

The bold line in the lower graph is the infiltration predicted by the fan model, using measured flows through the AAHX, heat pump and range hood and the AIM-2 full model.

The large pulse in measured infiltration in the middle of each day is caused by the air-to-air heat exchanger. The smaller humps in the morning are due to continuous operation of the heat pump fan; the infiltration is elevated prior to this period because the heat pump was cycling.

On April 2 (Day 92), the heat pump was run with the equipment room door open, beginning about 4:30 p.m. and ending about 6:00 p.m. Because return air was drawn from this room and it was strongly depressurized by the operation of the heat pump, opening the door was expected to reduce pressure effects in both this room and the remainder of the home. Unfortunately, this experiment coincides with an increase in wind-driven infiltration.

On the same day, the range hood was also run for 1-1/2 hours beginning at about 7:30 p.m. This event shows clearly in the measured infiltration, which is in reasonable agreement with the fan model predictions.

Our final experiment on this day involved sealing off the heat exchanger supply connection to the heat pump return duct so the heat pump would not draw air directly from outdoors. The heat pump was run under this condition from about 10:00 p.m. to 11:30 p.m. and then the seal was removed. Although the duct leakage values used in the model were not altered for this experiment, the measured and predicted infiltration

agree well, suggesting that the operation of the heat pump did not change greatly due to the blockage and that the heat pump drew very little air from the outdoors.

On April 3 (Day 93), the last day of the test, the heat pump and AAHX simultaneously were run for 2-1/2 hours, beginning around 2:45 p.m. This occurrence appears as the last pulse in measured infiltration in the graph.

Table A-4 gives summaries of the infiltration over the period of the tracer test. Despite the windiness of the site, the infiltration was still dominated by the stack effect; 70% of the total infiltration, and 90% of the natural infiltration, can be ascribed to stack-effect driving forces. Wind contributed another 7%.

Next to the stack effect, the operation of the AAHX had the greatest effect, adding 22 cfm to the overall infiltration although it ran only 3.4 hours per day. This system provided 13% of the total infiltration; heat pump operation added 17 cfm, or 9%. It should be noted that the combination of natural infiltration and continuous operation of the AAHX would have produced an average infiltration rate of 0.62 ACH, so that the system as normally operated results in greatly overventilating the home.

The second and third block of Table A-4 gives the breakdowns of infiltration and exfiltration with all fans off, with the heat pump running and with the AAHX running. The total infiltration differs from the value in the previous block because the times of our experiments have been excluded from these summaries.

When no fans are running, most of the air comes from the crawl space and goes to the attic. A large portion also comes from and goes to the outdoors. With the heat pump operating, there is additional infiltration from the attic, which must be caused by a return leak.

Infiltration and exfiltration values with the AAHX running are summarized over the first period of its operation only, because the heat pump was cycling during all other periods of AAHX operation. During this period, the natural infiltration was lower than the average over the tracer test, so the difference between the fans-off and the AAHX-running infiltration cannot be taken as a measure of the infiltration induced by the AAHX.

The fourth block of the table contains our best estimate of the flows through each fan and the infiltration induced by each device. These estimates, combined with the fractional ontimes, were used to predict the average infiltration effect of each fan.

The last block in Table A-4 gives the measured flows through the crawl space and attic. The crawl space had less than 1 ACH, due in part to its large volume and the fact that its location on the bluff (see Fig. A-1) prevented the wind from blowing through. The attic had a very high air-change rate of over 9 ACH because of the winds.

Table A-1
Physical characteristics of Site 5

Site Characteristics		
House type	Two-story multilevel, attached garage	
Number of bedrooms/Number occupied	4 / 1	
Foundation type	Vented crawl space	
Year built/Location	1988 / Tacoma, Washington	
Distance from Sea-Tac Airport	16 mi	26 km
Distance from Olympia Airport	29 mi	47 km
Elevation	200 ft	92 m
Dimensions		
Living zone floor area	3503 ft^2	325.5 m^2
Living zone volume	28510 ft^3	807.3 m^3
Average stack height	14.5 ft	4.4 m
Actual height [1]	17.7 ft	5.4 m
Mechanical Equipment		
Number of exhaust fans	6, excluding AAHX	
Ventilation system	Air-to-air heat exchanger	
Heating system	Trane heat pump with electronic air cleaner	
Leakage Characteristics		
Wind parameters	Terrain=3, Shielding=5	
Assumed leakage ratios	R=.5, X=0	
Leakage function	Q (cfm) = 273.7 $\Delta P^{0.644}$ (ΔP in Pa)	
Effective leakage area @ 4 ; LA)	189.7 in^2	1224 cm^2
Specific leakage area (SLA)	3.76	
Flow at 50 Pa	3400 cfm	5777 m^3/hr
ACH at 50 Pa	7.16	
Rule of thumb ACH50/20	0.358	
Testing Conditions		
First full day of test	Day 90 of 1991 (3/31/91)	
Last full day of test	Day 92 of 1991 (4/2/91)	

1 Does not include stairway to garage

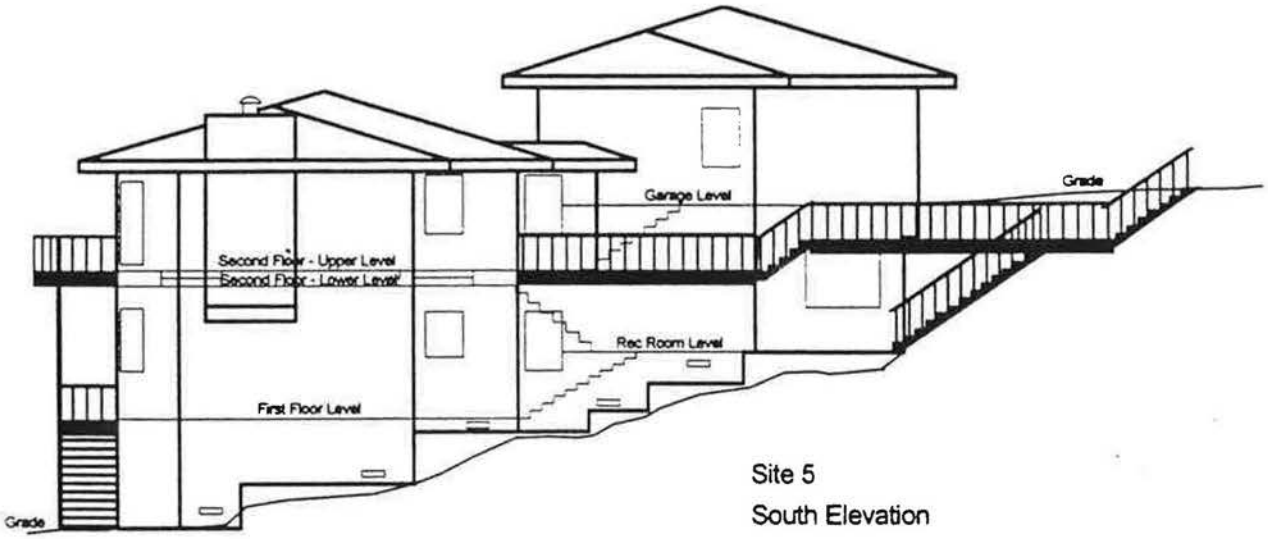

Figure A-1
Elevation view of Site 5

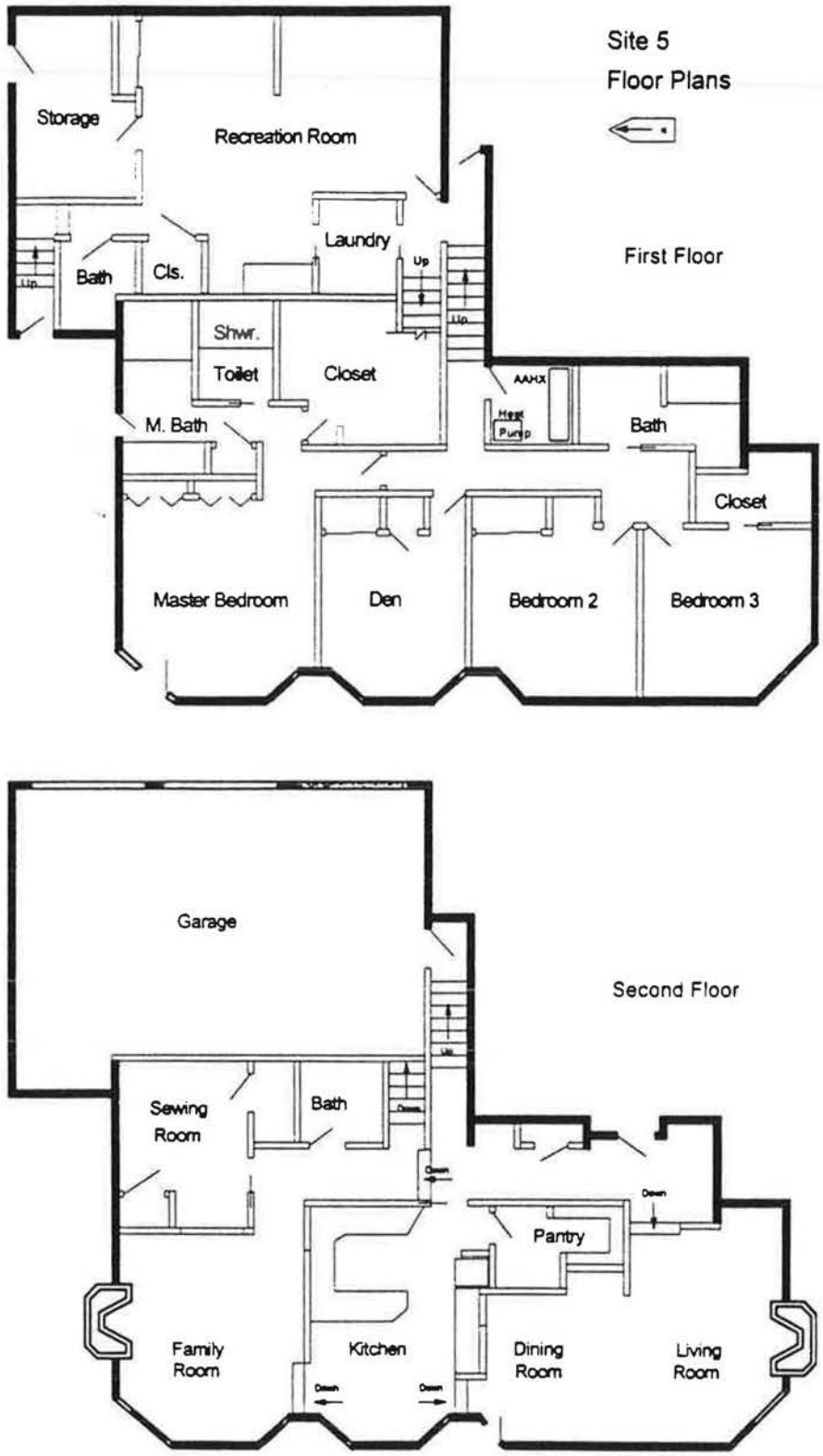

Figure A-2
Schematic floor plan of Site 5

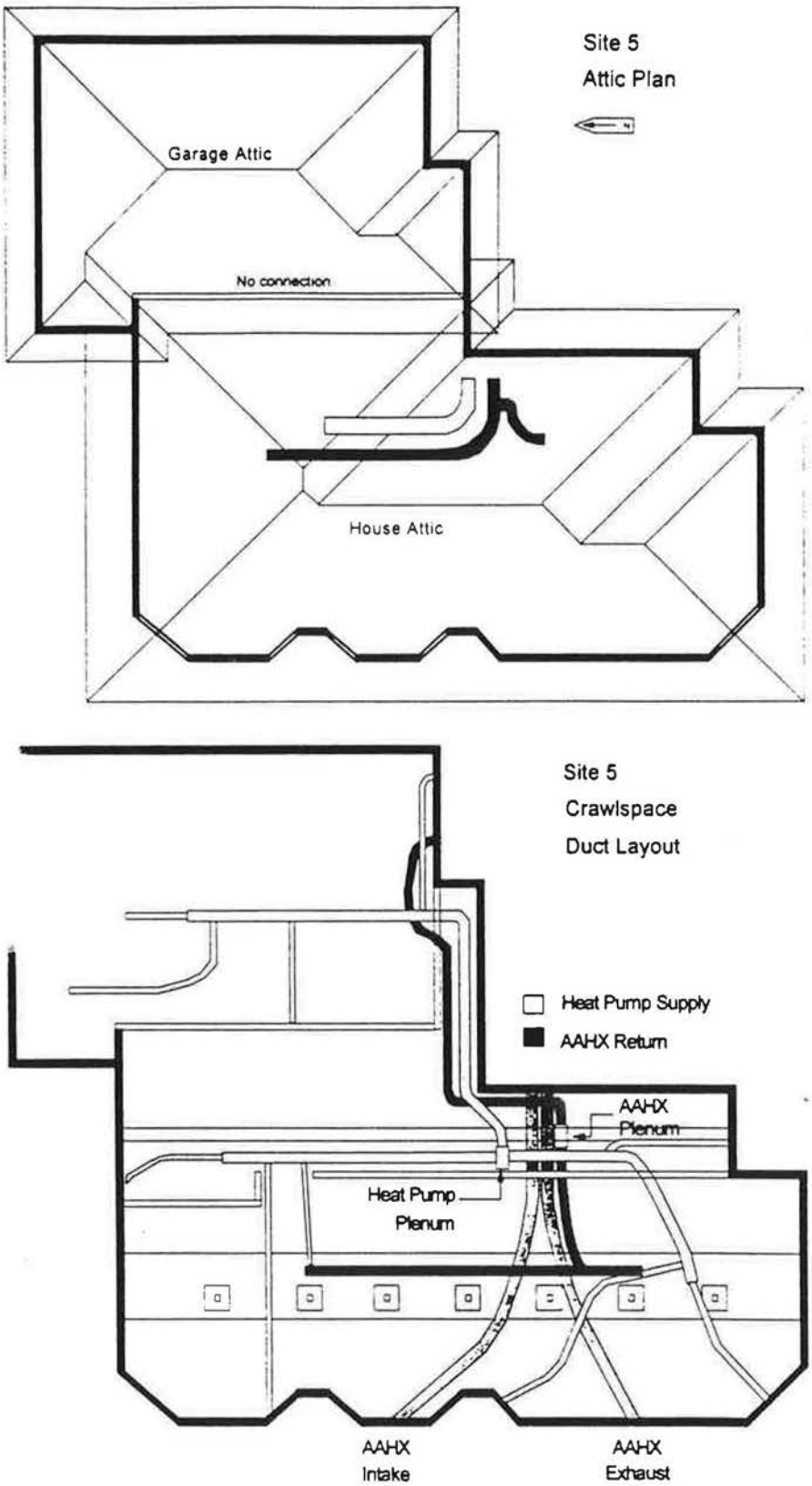

Figure A-3
Schematic drawing of attic and crawl space at Site 5

Table A-2
Environmental conditions at Site 5

Indoors			Outdoors		
Temperatures	**F**	**C**	**Temperatures**	**F**	**C**
1st floor	68.9	20.5	Site 1	47.4	8.6
Rec room	73.0	22.8	NWS (Sea-Tac) [2]	47.8	8.8
2nd floor [1]	71.1	21.8	NWS (Olympia)	46.4	8.0
ΔT	23.7	13.2	**Wind Speeds**	**mph**	**m/s**
Attic	56.5	13.6	Site tower #1	4.55	2.04
Crawl	52.9	11.6	Site tower #2 [1]	3.52	1.57
			NWS (Sea-Tac) [2]	10.16	4.54
			NWS (Olympia)	7.92	3.54

1 Used in models.
2 Weather station closest to site.

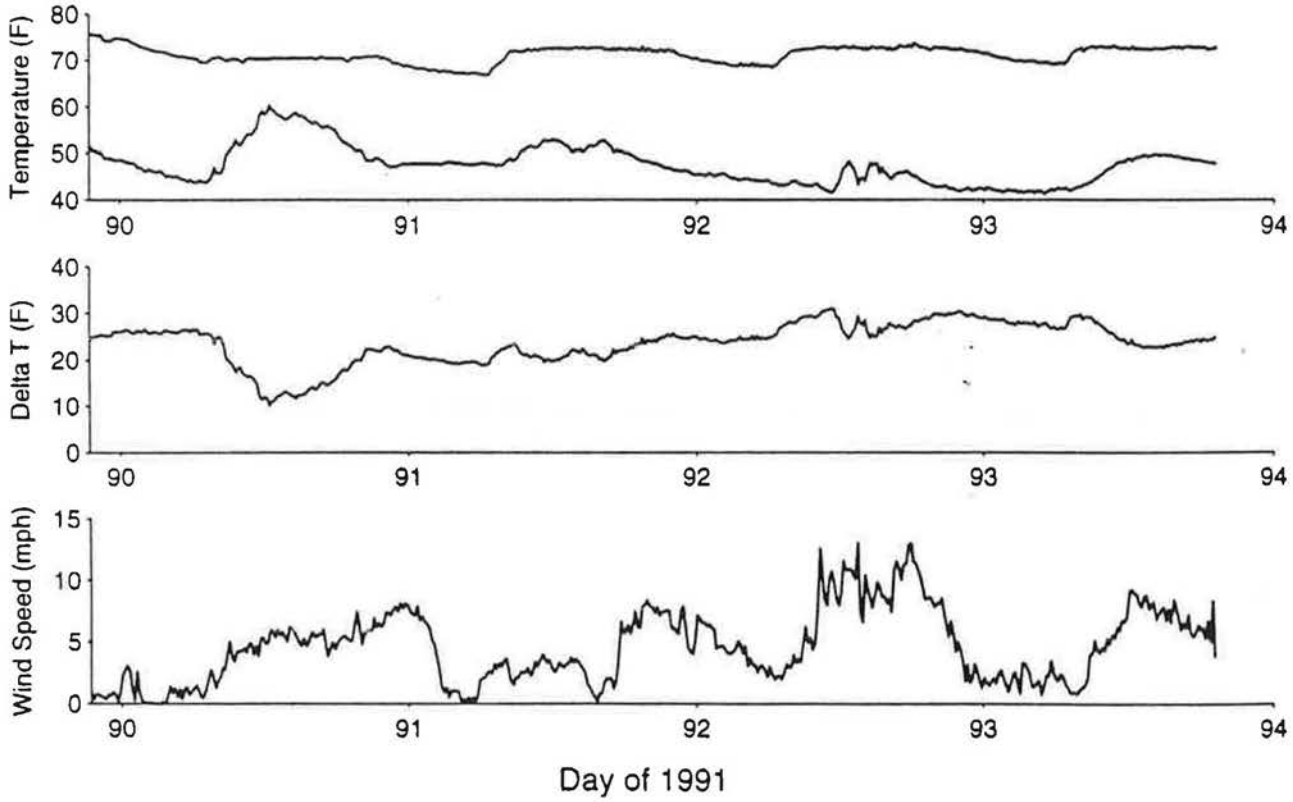

Figure A-4
Environmental conditions at Site 5

Table A-3
Air handler flows at Site 5 (cfm)

Level	Supply	Return	Imbalance
Lower	465	341	124
Middle	298	--	298
Upper	597	250	347
Total	1360	591	769

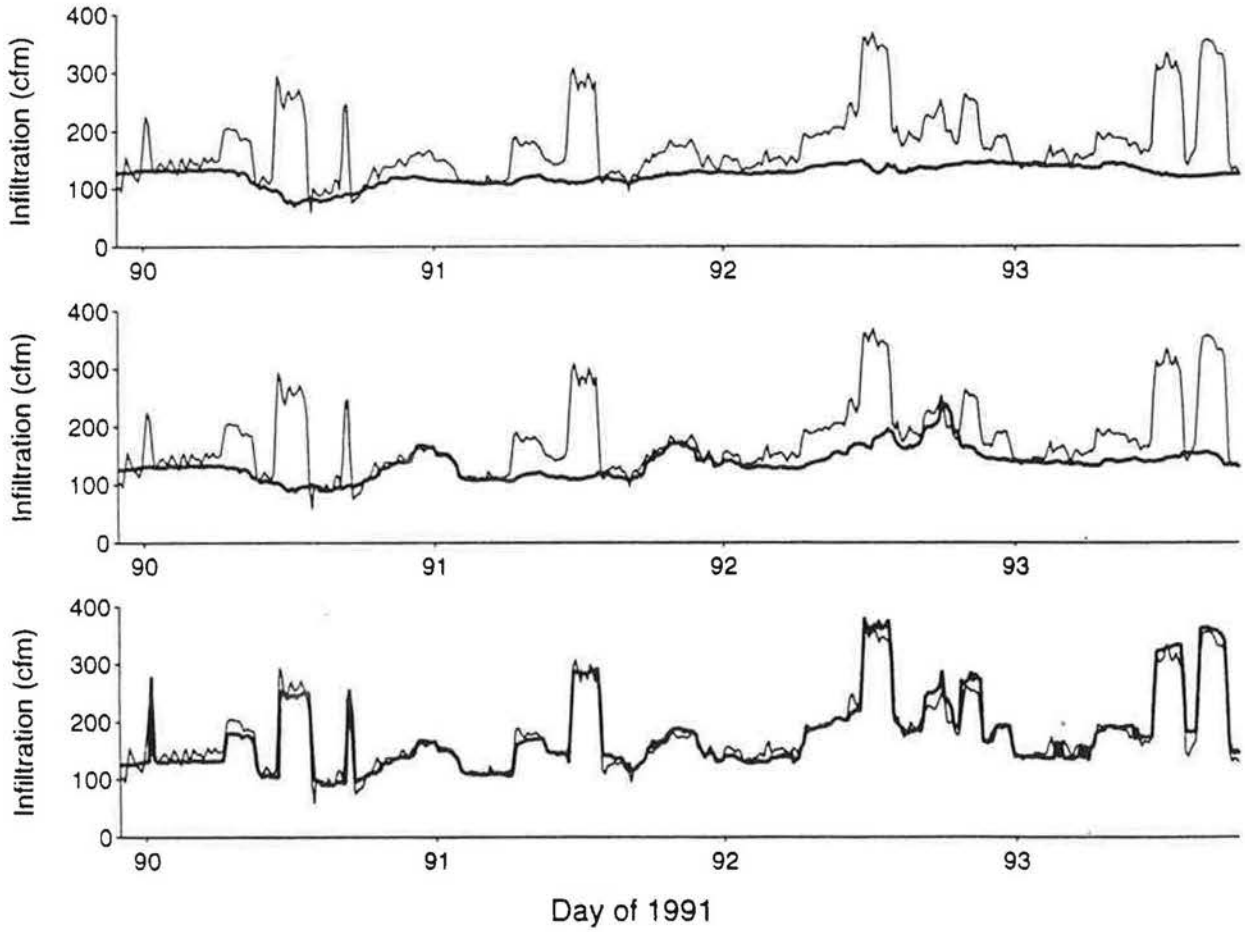

Figure A-5
Measured and predicted infiltration at Site 5

The bold line in each graph is the predicted infiltration; AIM-2 model predictions were used for the natural infiltration. The upper graph shows stack effect only; the middle graph shows the full AIM-2 model; the lower graph shows the prediction including the fan model. For the full model, the wind prediction was reduced by 30% prior to combining the stack and wind predictions.

Table A-4
Summary of infiltration at Site 5

Average Infiltration Effect [1]	cfm	ACH	%	Cum %
Stack	123.9	0.261	70	70
Wind [2]	12.3	0.026	7	77
Heat pump	17.1	0.036	9	86
Heat exchanger	22.5	0.047	13	99
Other fans	2.0	0.004	1	100
Discrepancy	-1.1	-0.002	0	100
Total	176.7	0.372	100	100

Infiltration	Total		Fans off		HP on		HX on	
Breakdown [3]	cfm	%	cfm	%	cfm	%	cfm	%
Outside	78.7	46	52.8	39	74.0	38	202.7	80
Crawl	77.6	46	77.1	57	85.3	44	44.1	17
Attic	13.4	8	5.8	4	35.1	18	7.3	3
Total	169.7	100	135.7	100	194.4	100	254.1	100

Exfiltration	Total		Fans off		HP on		HX on	
Breakdown [3]	cfm	%	cfm	%	cfm	%	cfm	%
Outside	72.6	43	53.8	40	49.1	25	201.1	79
Crawl	15.1	9	2.4	2	43.2	22	10.7	4
Attic	82.0	48	79.5	58	102.1	53	42.3	17
Total	169.7	100	135.7	100	194.4	100	254.1	100

Fan Effects [4]	Fan Flow	Induced Infiltration		Runtime
	cfm	cfm	ACH	(h/day)
Range hood	205	102	0.215	0.37
Heat pump	1500	50	0.105	8.18
Heat exchanger	160	160	0.337	3.36

	Leakage	Volume	From Ambient		Total Through Zone	
Other Zones	(in^2)	(ft^3)	cfm	ACH	cfm	ACH
Crawl	520	11919	188	0.95	206	1.037
Attic	1358	2290	276	7.23	361	9.46

1 Average effect of components over entire test period.
2 Additional infiltration caused by wind, calculated as the difference between the AIM-2 full and stack models (wind prediction multiplied by 0.7).
3 Summarized over periods when no one-time experiments were being performed.
4 Extra infiltration induced by operation of fans.

APPENDIX B. DETAILED RESULTS - SITE 6

Site Characteristics

Site 6 was located in Olympia, Washington; the home was selected because the site was moderately windy and the home had a gas furnace located in the attached garage. The home was not built under an energy-efficiency program and had no designed ventilation system.

Table B-1 lists physical characteristics of the home. The home is sl ghtly smaller than average Northwest homes. The average stack height is 12% lower than the full height, reflecting the reduction due to the cathedral ceiling. The home was partially two-story, with a cathedral ceiling over the living room and entry. Figure B-1 shows a schematic floor plan of the first and second stories of the home.

Figure B-2 shows a schematic plan of the attic and crawl space, including the accessible ductwork. There was a second attic over the garage which did not connect with the main attic. The garage attic contained both supply and return ducts and directly adjoined the second story.

The envelope characteristics show that the home is quite leaky. Compared with a random sample of 134 Northwest homes not built under energy-efficiency programs, the specific leakage area of 6.50 is 36% larger than average; the air changes at 50 Pa, at 10.54, is 14% larger than average (Palmiter and Brown, 1989).

Test Conditions

Because the home had a cathedral ceiling which would encourage air flow between the upstairs and downstairs, it was not possible to separate the home into distinct zones. Therefore, the home was measured as a single zone. The garage, attic and crawl space were measured as separate zones.

The furnace fan was operated twice daily, from 7:30 a.m. to 10:00 a.m. and from 7:00 p.m. to 9:30 p.m. In order to provide a clean estimate of fan effects, the furnace was

forced off for two hours before and 2-1/2 hours after fan operation. During other periods, the furnace operated whenever the thermostat called for heat.

On day 103, midway through the tracer test, some of the ductwork was repaired. The end cap which had fallen off a supply duct was replaced, and the large hole leading from the attic to the return from the second floor was sealed. Later another opening, approximately 24 square inches in size, from the attic to the return was discovered. The pressure across the envelope caused by the air handler did not change measurably after the repairs.

A short experiment was conducted during the tracer test in which all three bathroom fans were run for two hours on day 105.

Weather Conditions

Indoor and outdoor conditions during the tracer test are summarized in Table B-2 and depicted graphically in Figure B-3. The indoor temperatures are within about 1-1/2 F of each other with the exception of the temperature on the second floor, which was measured at the top of the stairway. The reason for the large discrepancy in this temperature is not understood and it was not used in the models.

Unfortunately, the aspirator containing the thermocouple for the outdoor temperature stalled during the test, causing heating of the thermocouple and faulty readings. The measured stack pressure was used to infer an indoor-outdoor temperature difference and thus an outdoor temperature. The average temperature difference thus inferred was comparable with typical heating-season conditions.

Site 6 was the least windy of the three sites measured during Phase II. The site wind is predominantly convective, with high wind speeds in the afternoon and early evening and zero at night.

Equipment

As mentioned previously, the home had a gas furnace located in the garage. The supply plenum was cast into the concrete, and a large (18" round) duct connected it to the duct system in the crawl space. Large cutouts in the return cabinet resulted in return leaks from the garage.

Most of the supply ducts, including those to two upstairs bedrooms, ran through the crawl space, but the ducts to the master bedroom and the two upstairs bathrooms ran through the space between the floors. An end cap had fallen off the duct leading to an upstairs supply register, and heated air was b ng blov nto the crawl space.

The home had two return grilles, one on each floor. Serious problems were found with the return ductwork. The second-story return was ducted through the attic to a vertical passage through the walls, which can be seen in the southwest corner in the master bedroom in Figure B-1. This passage was open to the attic where it met the duct from the return grille, resulting in a large amount of return air being drawn from the attic. The passage was also open to plumbing penetrations in the space between the floors.

The return for the first floor was supposed to run through a joist space, but the return grille in the family room was located in a different joist space than the return duct to the air handler. Thus, the air handler was attempting to draw air from a closed space, strongly depressurizing it and drawing very little air through the return grille. This situation resulted in a depressurization of the wall cavities and the space between floors.

Prior to the tracer test, the homeowners told us that the heating system was ineffective, and that they heated their home with the wood stove located in a corner of the family room. The return grille on the first floor was positioned to draw warm air from the wood stove so that running the air handler fan would circulate it throughout the home; the homeowners complained that this mechanism did not work either. Given the problems with the ductwork, especially the erroneous installation of the return grille, it is not surprising that they found both methods of heating their home inadequate.

Table B-3 shows measurements of register flow made with a flow hood; the supply and return measurements differ by about 440 cfm. This amount of return air was drawn either from the house through paths other than the grilles, from the attic, or from outdoors. The large return leaks resulted in pressurization of the home by about 6 Pa while the air handler fan was running.

Pressure Differences

The extreme effect of the air handler on house pressures is shown in Figure B-4. In the top graph, the pressure across the floor, measured as outdoor minus indoor pressure, is shown with the air handler signal. With the fan off, the pressure is positive due to the stack effect. The air handler fan causes a change of approximately 6 Pa in the house pressure and the home is pressurized relative to ambient.

The lower graph in Figure B-4 shows the dimensionless neutral level, which is the fraction of house height at which there is zero pressure across the wall. Below this point, air flows into the house from the outdoors; above this point, air flows outward. Under conditions of natural infiltration only, the neutral level is about 0.6, located about 20" above the second floor.

When the home is pressurized due to the excessive return leaks in the ductwork, the neutral level drops below zero, indicating that there is no neutral-pressure point between the floor and the ceiling and that flow through the envelope occurs in one

direction only. A large negative value of the neutral level has no physical meaning other than to represent the strong pressurization of the home.

Unbalanced exhaust flows depressurize the home and raise the neutral level. In the lower graph of Figure B-4, late on Day 105, the simultaneous operation of the three bathroom fans can be seen as an increase in the neutral level.

Infiltration

Measured infiltration, along with our predictions, is shown in Figure B-5. The large pulses on each day are caused by the operation of the air handler; the narrow pulse of the same magnitude as the air handler pulses on the afternoon of Day 103 occurs just after the ducts were repaired, when the system was operated briefly. The lower, wider pulses during the mornings are furnace cycles. The small infiltration pulse just prior to the air handler pulse in the evening of Day 105 is caused by our simultaneous operation of the three bath fans.

Tables B-4 and B-5 summarize infiltration results before and after ductwork repairs. The AIM-2 model was used to predict the wind and stack infiltration because it provided a better fit to the measured data. The results of the blower door test with the system in the unrepaired state were used in the infiltration model; however, the stack model overpredicted the baseline infiltration after the ducts were repaired. Blower door tests done by LBL indicate that the leakage area was reduced by 11%. The predictions were multiplied by 0.9 for the period after the repairs to account for the reduction in leakage area.

The AIM-2 full model overpredicted the peaks caused by wind. This overprediction was slight because the magnitude of the predicted wind effect was small; however, multiplying the wind prediction by 0.6 prior to combination of the stack and wind models produced a better fit.

The first block of the tables lists the average contribution of each factor to the total infiltration. As expected, wind contributes very little to the infiltration in this house, and stack infiltration is dominant. The noticeable drop in stack-induced infiltration after the duct repairs is due partly to lower temperature differences and partly to the reduction in leakage area. The natural infiltration rate of the home is large compared to other homes in the Northwest due to the relative leakiness of the envelope.

The air handler triples the infiltration rate through the home; it causes over 35% of the total infiltration, although it runs only 6 to 7 hours per day. Both prior to and after the duct repairs, the air handler adds about 0.95 ACH or 236 cfm to the infiltration rate. The home's leakiness and the substantial effects of the air handler result in the home being severely overventilated.

The second and third blocks of the tables list the flow to and from the living zone from each exterior zone. With the air handler off, most of the flow through the house passes in from the crawl space and out to the attic, in accordance with the stack effect.

Prior to the main tracer test, a short tracer test was performed which included the garage attic as a zone. This data indicates the presence of both supply and return leaks in the garage attic. During the main tracer test, the attic above the garage was not tagged as a zone, so any airflows to or from this attic would be interpreted as airflow to or from outside.

When the air handler runs, the home is pressurized relative to all the other zones and the outdoors, so no flow can enter through the envelope. Under these conditions, all the infiltration must be caused by leaks into the air handler return. Most of the infiltration comes from outdoors (39% before repairs and 44% after) and from the attic (37% before repairs and 30% after).

The exfiltration breakdown is more difficult to interpret. The flows to outdoors and to the crawl space include supply leaks; all the flows include exfiltration caused by the pressurization of the home. As expected, most of the air (80% before repairs and 71% after) exits through the ceiling of the home to the attic under stack-only conditions. The reduction of the percentage airflow to the attic may indicate the change in the leakage area of the ceiling relative to the total.

When the air handler runs, only 25% of the exfiltration goes to the attic; this air must leak through the ceiling, because there are no supply ducts in the attic. Air flows to the garage accounted for 9% of the exfiltration with the fan running.

Flow to the crawl space accounts for 29% of the exfiltration prior to the duct repairs and 20% after the repairs. The home is pressurized relative to the crawl space, so this number includes both supply duct leakage and flows through the floor. However, because the pressure difference between the home and the crawl space was approximately the same before and after the repairs, it is reasonable to assume that the decrease of 9%, or about 36 cfm, was due to the replacement of the end cap on the supply duct.

The flow through the air handler and its infiltration effects are summarized in the fourth block of Tables B-4 and B-5. As previously stated, the air which enters the home must all come from return leaks; therefore, the magnitude of the return leaks must be given by the measured infiltration rate. The infiltration added by the fan is the total infiltration minus the predicted natural infiltration.

The last block of the tables summarizes flows and leakage areas through the garage, crawl and attic. The garage had about 1 ACH, comparable to other garages measured under this project. Both the attic and crawl were quite well ventilated, with air-change rates of 7 and 8 ACH respectively.

Table B-1
Physical characteristics of Site 6

Site Characteristics		
House type	Split-level, attached garage	
Number of bedrooms/Number occupied	3 / 1	
Foundation type	Vented crawl space	
Year built/Location	1985 / Olympia, Washington	
Distance from Sea-Tac Airport	29 mi	47 km
Distance from Olympia Airport	7 mi	11 km
Elevation	200 ft	92 m
Dimensions		
Living zone floor area	1695 ft^2	157.5 m^2
Living zone volume	14876 ft^3	421.3 m^3
Average stack height	14.5 ft	4.4 m
Actual height	16.3 ft	5.0 m
Mechanical Equipment		
Number of exhaust fans	3	
Ventilation system	None	
Heating system	Gas furnace in garage Wood stove in family room	
Leakage Characteristics		
Wind parameters	Terrain=4, Shielding=4	
Assumed leakage ratios	R=.5, X=0	
Leakage function	Q (cfm) = 239.6 $\Delta P^{0.611}$ (ΔP in Pa)	
Effective leakage area @ 4 Pa (ELA)	158.6 in^2	1023 cm^2
Specific leakage area (SLA)	6.50	
Flow at 50 Pa	2616 cfm	4444 m^3/hr
ACH at 50 Pa	10.55	
Rule of thumb ACH50/20	0.527	
Testing Conditions		
First full day of test	Day 100 of 1991 (4/10/91)	
Last full day of test	Day 105 of 1991 (4/15/91)	

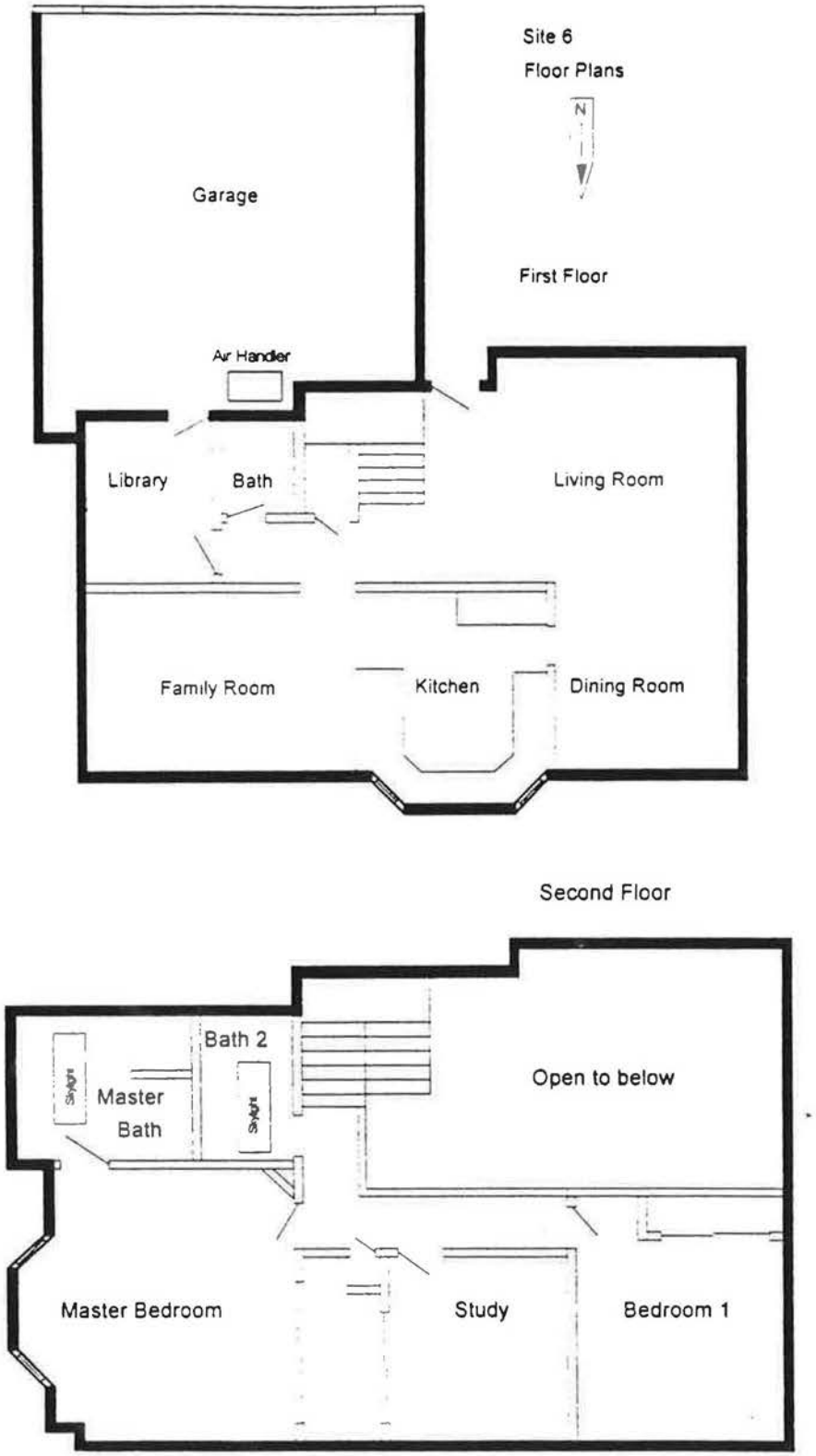

Figure B-1
Schematic floor plan of Site 6

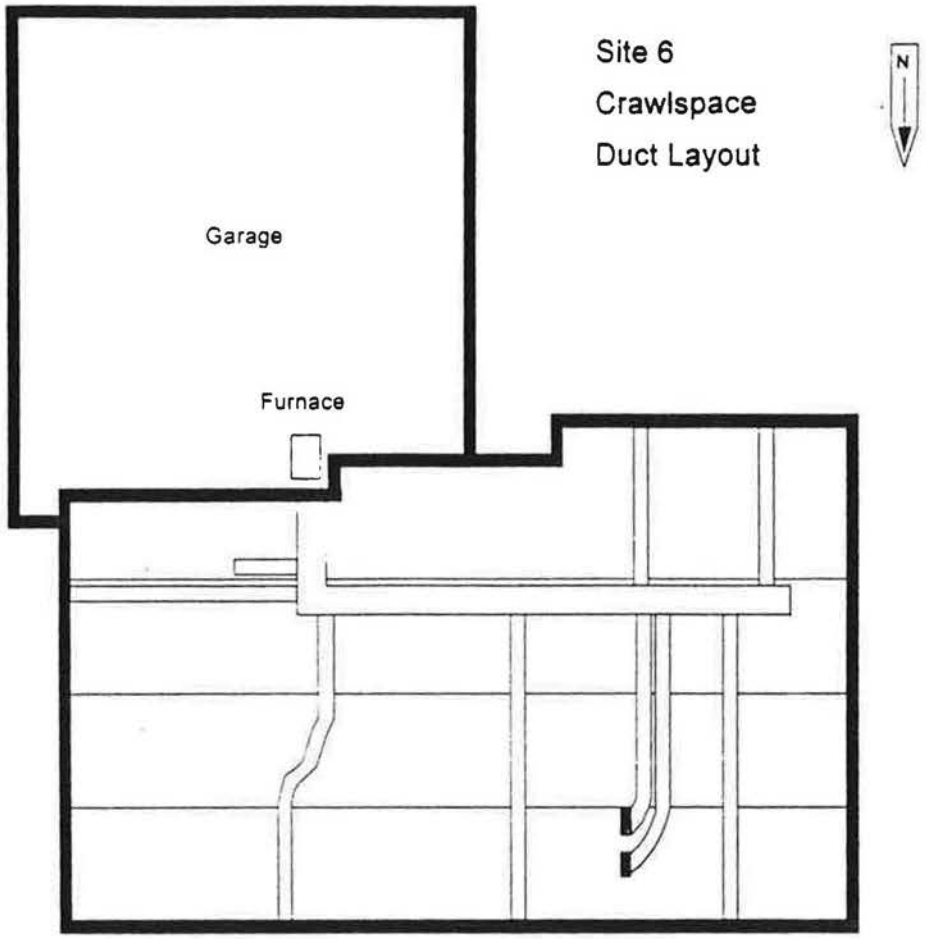

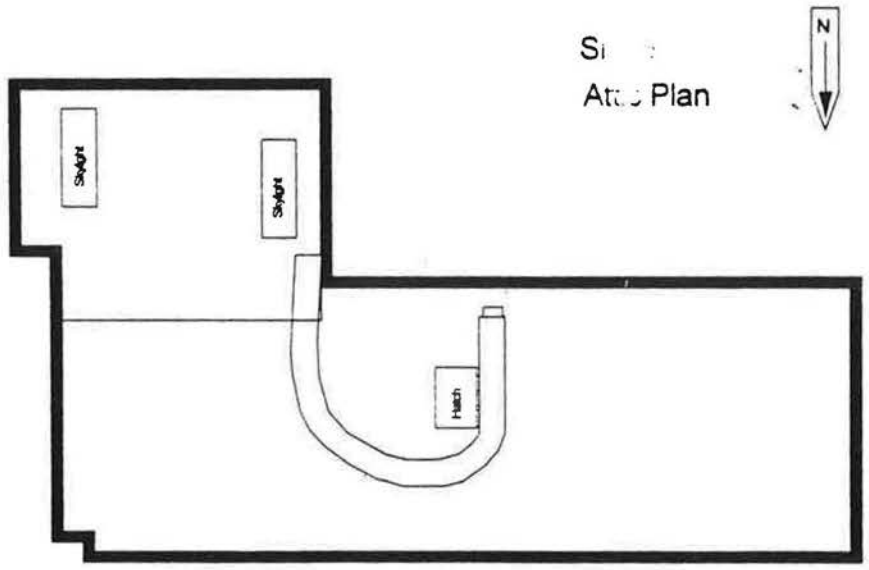

Figure B-2
Schematic drawing of attic and crawl space at Site 6

Table B-2
Environmental conditions at Site 6

Indoors			Outdoors		
Temperatures	**F**	**C**	**Temperatures**	**F**	**C**
1st floor #1 [1]	68.9	20.5	Site [1 3]	44.8	7.1
1st floor #2	67.7	19.8	NWS (Sea-Tac)	48.4	9.1
2nd floor	65.7	18.7	NWS (Olympia) [2]	45.7	7.6
Master Bedroom	67.3	19.6			
ΔT [3]	24.1	13.4	**Wind Speeds**	**mph**	**m/s**
Garage	54.9	12.7	Site tower #1 [1]	1.91	0.85
Attic	57.4	14.1	Site tower #2	2.06	0.92
Crawl	55.0	12.8	NWS (Sea-Tac)	6.71	3.00
			NWS (Olympia) [2]	5.30	2.37

1 Used in models.
2 Weather station closest to site.
3 Calculated from pressure measurements

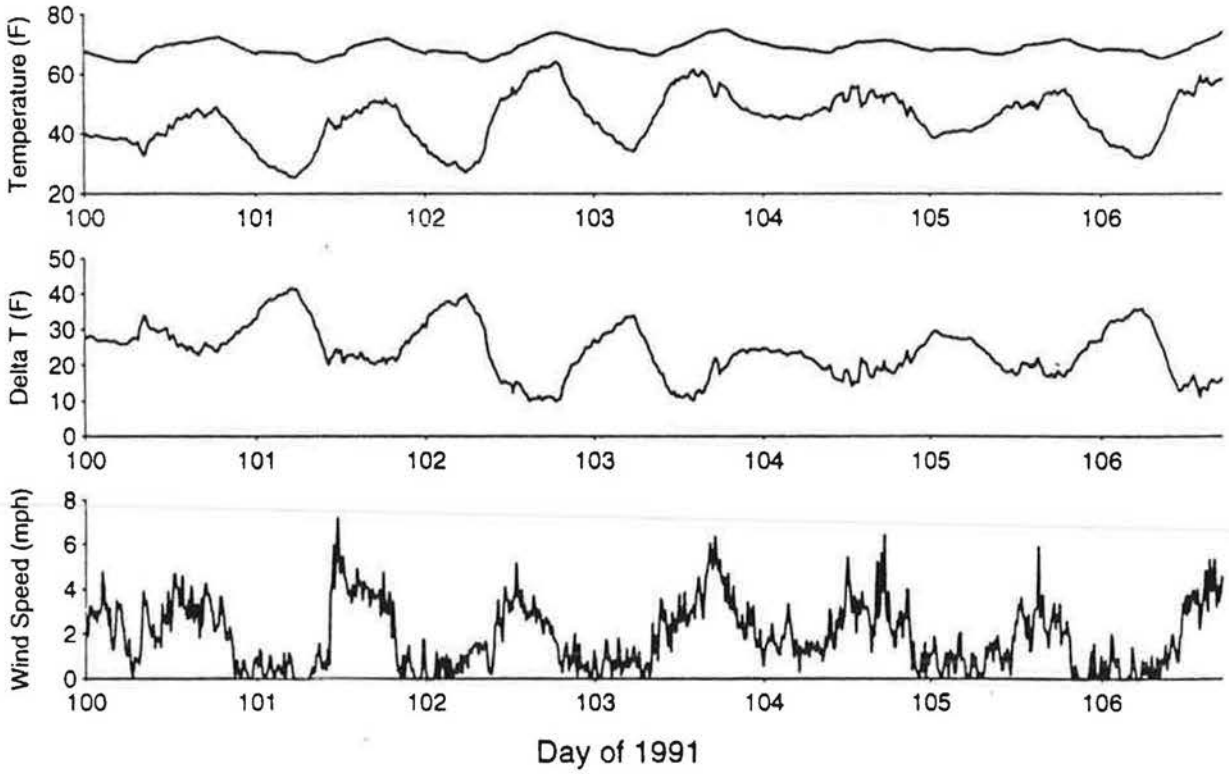

Figure B-3
Environmental conditions at Site 6

Table B-3
Air handler flows at Site 6 (cfm)

Supply flow	1st floor	251
	2nd floor	523
	Total	774
Return flow	1st floor	126
	2nd floor	204
	Total	330
Imbalance	1st floor	125
	2nd floor	319
	Total	444

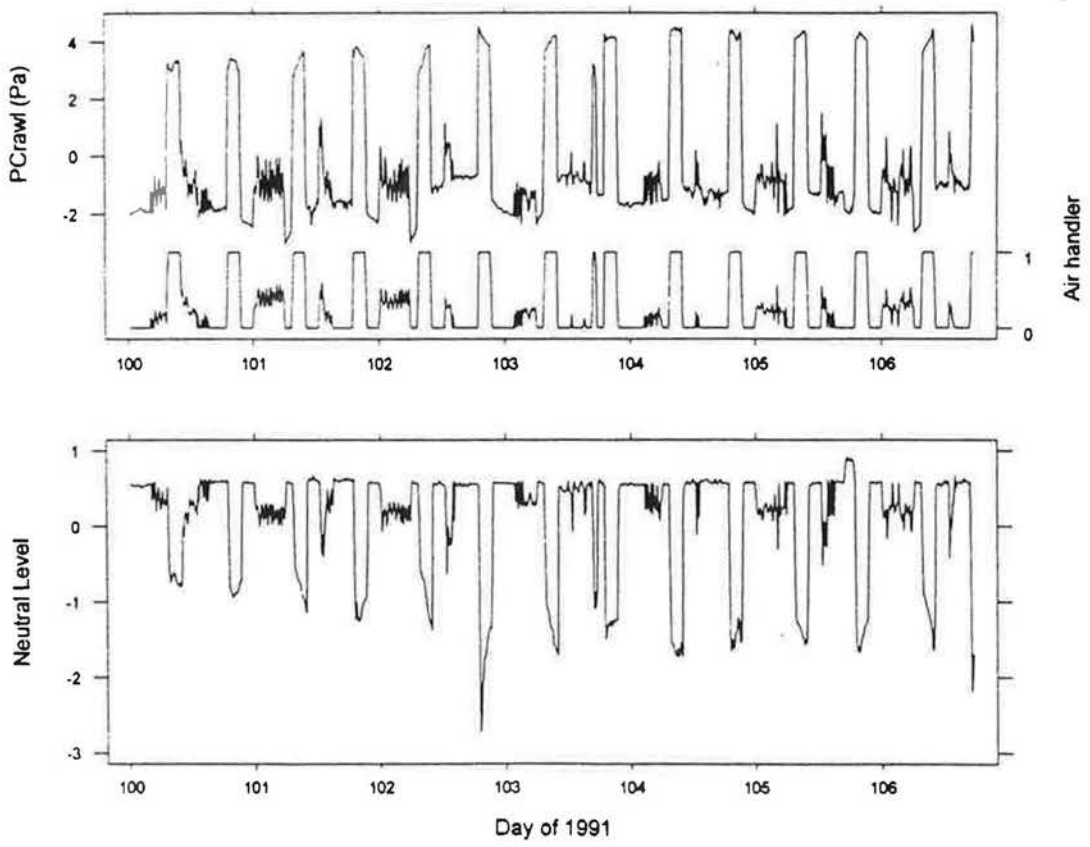

Figure B-4
Effect of air handler on pressures at Site 6

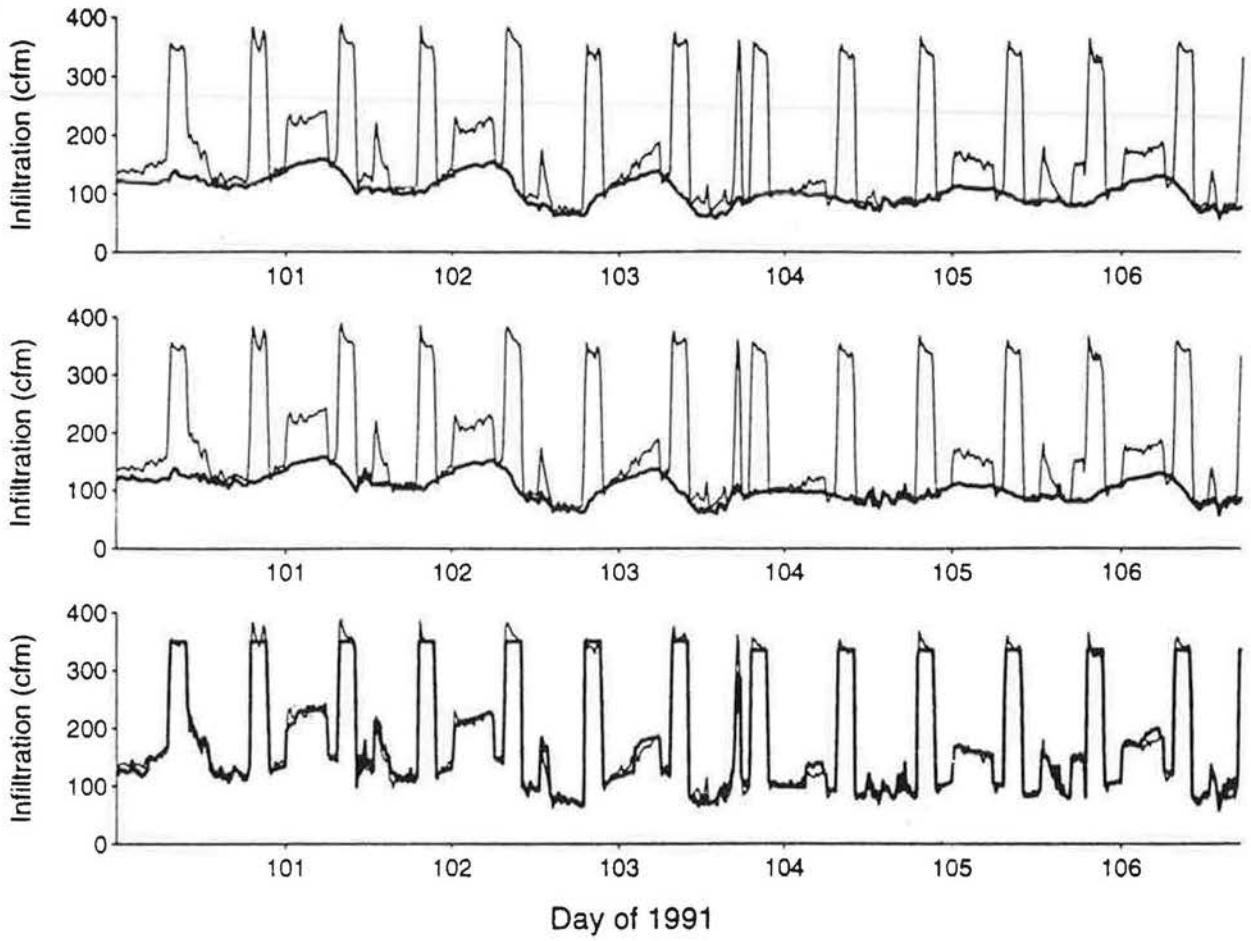

Figure B-5
Measured and predicted infiltration at Site 6

The bold line in each graph is the predicted infiltration; AIM-2 model predictions were used for the natural infiltration. The upper graph shows stack effect only; the middle graph shows the full AIM-2 model; the lower graph shows the prediction including the fan model. For the full model, the wind prediction was reduced by 30% prior to combining the stack and wind predictions.

Table B-4
Summary of infiltration at Site 6 (before repairs)

Average Infiltration Effect [1]	cfm	ACH	%	Cum %
Stack	117.1	0.473	62	62
Wind [2]	0.4	0.002	0	62
Air handler	72.5	0.292	38	100
Discrepancy	0.8	0.003	0	100
Total	190.8	0.770	100	100

	Total		AH off		AH on [4]	
Infiltration Breakdown [3]	cfm	%	cfm	%	cfm	%
Outside	63.3	33	29.0	24	136.6	39
Garage	26.6	14	6.8	6	66.3	19
Crawl	59.3	31	76.6	64	18.6	5
Attic	41.5	22	7.2	6	126.6	37
Total	190.7	100	119.6	100	348.1	100

	Total		AH off		AH on	
Exfiltration Breakdown [3]	cfm	%	cfm	%	cfm	%
Outside	52.4	27	19.3	16	126.1	36
Garage	8.9	5	0.2	0	29.4	9
Crawl	31.7	17	4.2	4	102.5	29
Attic	97.7	51	95.9	80	90.1	26
Total	190.7	100	119.6	100	348.1	100

Fan Effects [5]	Fan Flow	Induced Infiltration		Runtime
	cfm	cfm	ACH	(h/day)
Air Handler	955	237	0.96	7.33

	Leakage	Volume	From Ambient		Total Through Zone	
Other Zones	(in^2)	(ft^3)	cfm	ACH	cfm	ACH
Garage	--	4314	51	0.71	71	0.99
Crawl	924	2098	239	6.84	284	8.12
Attic	506	2042	137	4.03	252	7.40

1 Average effect of components over entire test period.
2 Additional infiltration caused by wind, calculated as the difference between the AIM-2 full model with the wind effect multiplied by 0.6 and the AIM-2 stack model.
3 Summarized over periods when no one-time experiments were being performed.
4 Must be return leak
5 Extra infiltration induced by operation of fans.

Table B-5
Summary of infiltration at Site 6 (after repairs)

Average Infiltration Effect [1]	cfm	ACH	%	Cum %
Stack [2]	92.5	0.373	58	58
Wind [2,3]	1.1	0.004	1	59
Air handler	62.7	0.254	39	98
Bath fans	1.5	0.006	1	99
Discrepancy	1.1	0.004	1	100
Total	158.9	0.641	100	100

	Total		AH off		AH on [5]	
Infiltration Breakdown [4]	cfm	%	cfm	%	cfm	%
Outside	61.3	39	29.4	31	147.9	44
Garage	25.9	17	8.7	9	68.7	21
Crawl	40.0	25	49.2	53	18.1	5
Attic	30.5	19	6.5	7	99.0	30
Total	157.7	100	93.8	100	333.7	100

	Total		AH off		AH on	
Exfiltration Breakdown [4]	cfm	%	cfm	%	cfm	%
Outside	58.0	37	23.4	25	153.3	46
Garage	8.3	5	0.2	0	30.1	9
Crawl	19.4	12	3.6	4	66.7	20
Attic	72.0	46	66.6	71	83.6	25
Total	157.7	100	93.8	100	333.7	100

Fan Effects [6]	Fan Flow	Induced Infiltration		Runtime
	cfm	cfm	ACH	(h/day)
Air Handler	955	236	0.95	6.38
Bath fans (Total flow)	94	62	0.25	0.57

	Leakage	Volume	From Ambient		Total Through Zone	
Other Zones	(in^2)	(ft^3)	cfm	ACH	cfm	ACH
Garage	--	4314	46	0.64	64	0.89
Crawl	924	2098	265	7.58	291	8.32
Attic	506	2042	129	3.79	210	6.17

1 Average effect of components over entire test period.
2 Multiplied by 0.9 to account for reduction in leakage area due to repairs.
3 Additional infiltration caused by wind, calculated as the difference between the AIM-2 full model with the wind effect multiplied by 0.6 and the AIM-2 stack model.
4 Summarized over periods when no one-time experiments were being performed.
5 Must be return leak.
6 Extra infiltration induced by operation of fans.

APPENDIX C. DETAILED RESULTS - SITE 7

Site Characteristics

Site 7 was a three-bedroom manufactured home located in Cle Elum, Washington, east of the Cascade mountain range. During the winter, the areas east of the Cascades tend to be colder and windier than those to the west; this fact, combined with the home's position on a small unsheltered bluff, made this site the windiest by far.

Characteristics of the home are given in Table C-1. The home was built under the local utility's Super Good Cents program in 1990. It is slightly smaller than the average newly-constructed manufactured home, but it is typical in its size and equipment.

Blower door measurements of leakage are also given in Table C-1. Because wind affects the pressures across the envelope during a blower door test, it was difficult to perform an accurate test during the windy conditions experienced at this site; the figures given are our best estimates. The home is slightly leakier than typical energy-efficient manufactured homes in the Northwest in terms of normalized leakage measurements such as the specific leakage area and air changes at 50 Pa (Palmiter et. al., 1992).

Like many manufactured homes, including the home tested during Phase I, Site 7 had a cathedral ceiling in the living area, master bedroom and kitchen. The high ceiling separated the east and west sides of the inaccessible attic, which had two screened soffit vents on each end.

This home had two separate ventilation systems. The first consisted of a bath fan controlled by a 24-hour timer and four Fresh-80 inlet vents on the bedroom and living room walls. The second ventilation system was a Coleman Blend-Air system. This system doubled as an attic pressurization system and a makeup air system; when the furnace ran, a damper between the Blend-Air and the furnace opened and fresh air was supplied to the furnace.

A schematic floor plan of the home and the crawl space, including the ducts, is shown in Figure C-1. The furnace had a single return register just above the unit. The supply ducts ran between the floor and the belly blanket in the crawl space. The ducts were

installed by a common method which involves placing a long duct under the floor along the length of the home, punching a hole through the floor and duct simultaneously, and patching the connections. Because of the inaccessibility of the junctions formed in this way, they are more difficult to seal and these ducts are usually leakier than are those installed by more traditional methods. In this home, when the air handler operated, the belly blanket inflated visibly due to supply leaks from the ducts located inside it.

Test Conditions

Because of the small size of the home, it was treated as a single zone for the tracer test. The crawl space was measured as a separate zone; the attic could not be measured as a tracer zone because it was inaccessible.

The designated bath fan was set to run between 1:00 p.m. and 3:30 p.m. The furnace fan and the Blend-Air ran each day between 1:00 a.m. and 3:30 a.m. The furnace was forced off for 2.5 hours before and 3 hours after fan operation so that the effects of the fan would be clearly visible. The fan was also forced off from 10:30 a.m. to 5:30 p.m. During other periods, the furnace ran when the thermostat called for heat.

During the tracer test, several one-time experiments were conducted, which are discussed below. However, the large infiltration rate and pressures induced by the wind obscured many of the results of our tests.

Two experiments involved the Blend-Air and the damper between the unit and the furnace. In the first, the damper was opened at 10:15 p.m. on day 116 and left it open until 6:00 p.m. the next day. For the second test, the Blend-Air damper was disabled from 11:00 p.m. on day 117 until 2:00 a.m. on day 119. While the damper was disabled, the Blend-Air operated twice, from 5:30 a.m. to 7:30 a.m. on day 118 and from 11:00 p.m. on day 118 to 1:30 a.m. on day 119. The system in this condition pressurized the attic without providing makeup air to the furnace.

The four intake vents were opened between 5:45 p.m. and 8:15 p.m. on day 116. To estimate the effects of the range hood on infiltration, it was operated from 6:00 p.m. to 9:00 p.m. on day 118.

Weather Conditions

Table C-2 and Figure C-2 summarize the environmental conditions during the tracer test. Indoor temperatures were fairly uniform; the attic and crawl temperatures were slightly greater than outdoor temperatures. The indoor-outdoor temperature difference averaged 27 F. It is interesting that, although the site is closer to, and is on the same side of the Cascades as Yakima Airport, temperatures at the site correlate better with those at Sea-Tac Airport than with Yakima Airport.

A comparison of wind speeds shows that the site is not only windier than any of the previously studied sites, but also windier than both airports; wind speeds at the site averaged over 11 mph for the entire tracer test. This creates problems with extrapolation, as noted previously, because airport wind speeds are usually reduced to reach site wind speeds.

The wind blew primarily from the north and west and reached its highest speed in the late afternoon. Generally, there was a good correlation between the wind directions at the site and those at the Yakima airport.

Pressures

In addition to one or two pressures across each wall, several pressures across the ceiling and the floor were measured. Two transducers measured the house-to-crawl-space pressure difference; a third was connected across the floor and measured the pressure between the house and the space inside the belly blanket, where the supply ducts were located.

Because of the constricted attic, pressures across the ceiling in the east and west ends of the attic were measured, as well as pressures in the upper attic above the cathedral ceiling. The pressures in the east and west attics behaved very much like those on the east and west walls; the west attic was strongly pressurized and the east attic was strongly depressurized. The pressures in the upper attic showed very little wind effect.

Infiltration

Graphs of measured and modeled infiltration are shown in Figure C-3; Table C-3 summarizes infiltration characteristics of this home. Unlike all the other sites, the infiltration in this home is dominated by wind. Wind-induced airflow accounts for 70% of the infiltration, twice as much as the stack effect. The windiness of the site resulted in a high overall infiltration rate of 0.70 ACH.

The upper panel of Figure C-3 shows that the predicted stack effect generally lies far below the measured infiltration. Early on day 114, the prediction almost agrees with the measurement; these few hours were the only time with very low measured wind speeds.

The middle panel of the graph shows the full LBL model predictions and the measured infiltration. With the wind speeds measured at the site, the model overpredicted the measured infiltration, so the wind model was reduced by 10% prior to combining the wind and stack models.

The air handler induced about 37 cfm of infiltration when operating, more than twice the air flow added by the furnace at Site 4, the other manufactured home. Because the

furnace operated only 3.4 hours per day, this translated to 5 cfm during the entire period, or only 5 percent of the total infiltration.

Because the wind pressurized the home relative to the crawl space, counteracting the stack effect, infiltration from the crawl space was quite low. Flow from the house into the crawl space was also small, except that supply leaks pumped air into the crawl when the air handler ran. These leaks accounted for 41% of the total exfiltration when the air handler was running.

The third panel shows the predictions obtained when the furnace-induced flows were combined with the natural infiltration using the fan model. The predictions and measurements are in good agreement. The flows induced by other fans, such as the range hood, could not be identified because of the large magnitude and variability of the wind-induced flows.

The effects of wind-induced pressures across the floor are shown in Figure C-4. Flow from the crawl space to the house and from the house to the crawl space are plotted versus the pressure across the floor, which is given as crawl minus house pressure. At low wind speeds, the stack effect dominates the flow and the pressure across the floor is positive, resulting in upward flows from the crawl space. Flow from the house to the crawl space is negligible.

As wind speeds increase, the house becomes pressurized relative to the crawl space, the positive pressure across the floor decreases, and the upward flow drops correspondingly. When the wind effect is large enough, the pressure across the floor is reversed, and air begins to flow from the house into the crawl space in a nearly linear relationship with the pressure across the floor.

Parallel to this line but much higher are flows to the crawl space when the air handler is operating. This line includes flows to the crawl space due to the supply leak. During periods of air handler operation, no flow occurs from the crawl space to the house, although the air handler depressurizes the home and thus should increase the flow through the floor. This indicates that most of the leaks from the crawl to the home are through the ductwork and that the floor is nearly airtight. When the air handler operates, no leakage path exists between the crawl space and the home. Figure C-5 shows the effect of the air handler on the flow through the floor by separating periods with the air handler running from those when it is off.

Table C-1
Physical characteristics of Site 7

Site Characteristics		
House type	1-story manufactured home	
Number of bedrooms/Number occupied	3 / 2	
Foundation type	Vented crawl space	
Year built/Location	1990 Cle Elum, Washington	
Distance from Sea-Tac Airport	68 mi	109 km
Distance from Olympia Airport	48 mi	77 km
Elevation	2300 ft	701 m
Dimensions		
Living zone floor area	1217 ft^2	113.1 m^2
Living zone volume	9746 ft^3	276.0 m^3
Average stack height	8.0 ft	2.4 m
Actual height	9.4 ft	2.9 m
Mechanical Equipment		
Number of exhaust fans	4	
Ventilation system	a) Coleman Blend-Air b) Designated bath fan controlled by timer; four Fresh-80 inlet vents in walls	
Heating system	Electric forced-air furnace in home; return on unit Supply ducts between floor and belly blanket; crossover duct in crawl space	
Leakage Characteristics		
Wind parameters	Terrain=4, Shielding=1	
Assumed leakage ratios	R=.5, X=0	
Leakage function	Q (cfm) = 83.0 $\Delta P^{0.670}$ (ΔP in Pa)	
Effective leakage area @ 4 Pa (ELA)	59.6 in^2	385 cm^2
Specific leakage area (SLA)	3.40	
Flow at 50 Pa	1141 cfm	1939 m^3/hr
ACH at 50 Pa	7.03	
Rule of thumb ACH50/20	0.351	
Testing Conditions		
First full day of test	Day 114 of 1991	(4/24/91)
Last full day of test	Day 118 of 1991	(4/28/91)

Site 7

1st Floor Plan

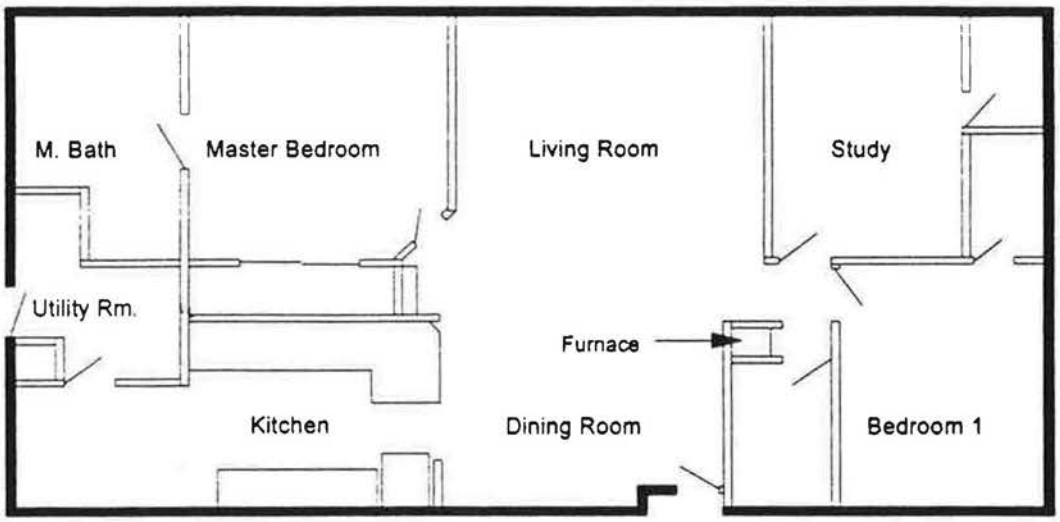

Site 7

Crawlspace Duct Layout

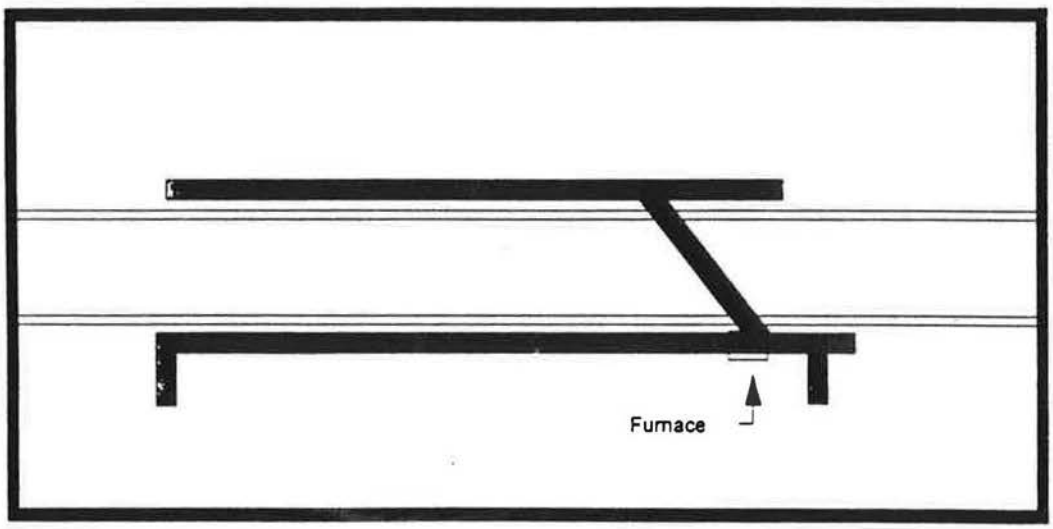

Figure C-1
Schematic floor plan of Site 7

Table C-2
Environmental conditions at Site 7

Indoors			Outdoors		
Temperatures	**F**	**C**	**Temperatures**	**F**	**C**
Living Room [1]	69.8	21.0	Site [1]	42.8	6.0
Master Bedroom	69.4	20.8	NWS (Sea-Tac)	46.2	7.9
			NWS (Yakima) [2]	48.4	9.1
ΔT	27.0	15.0			
			Wind Speeds	**mph**	**m/s**
Attic	46.2	7.9	Site tower #1 [1]	11.77	5.26
Crawl	48.2	9.0	Site tower #2	11.38	5.09
			NWS (Sea-Tac)	8.63	3.86
			NWS (Yakima) [2]	10.96	4.90

1 Used in models.
2 Weather station closest to site.

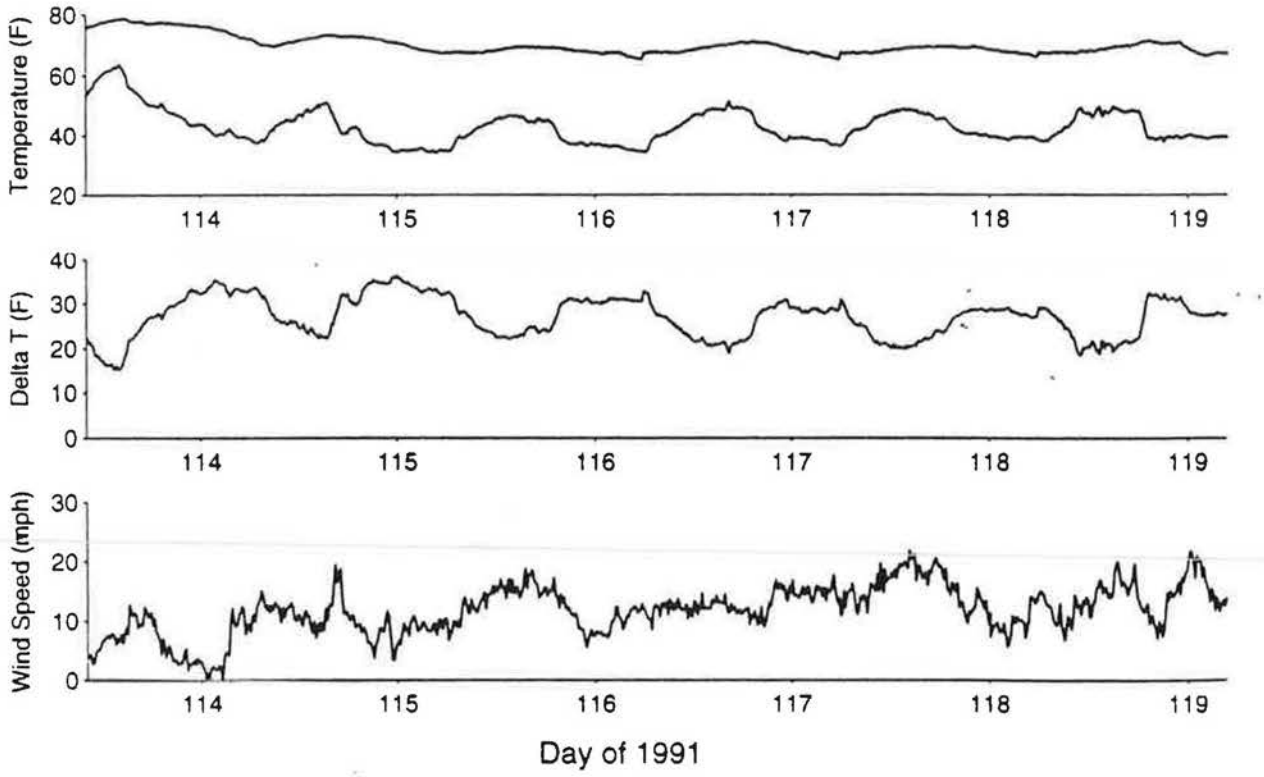

Figure C-2
Environmental conditions at Site 7

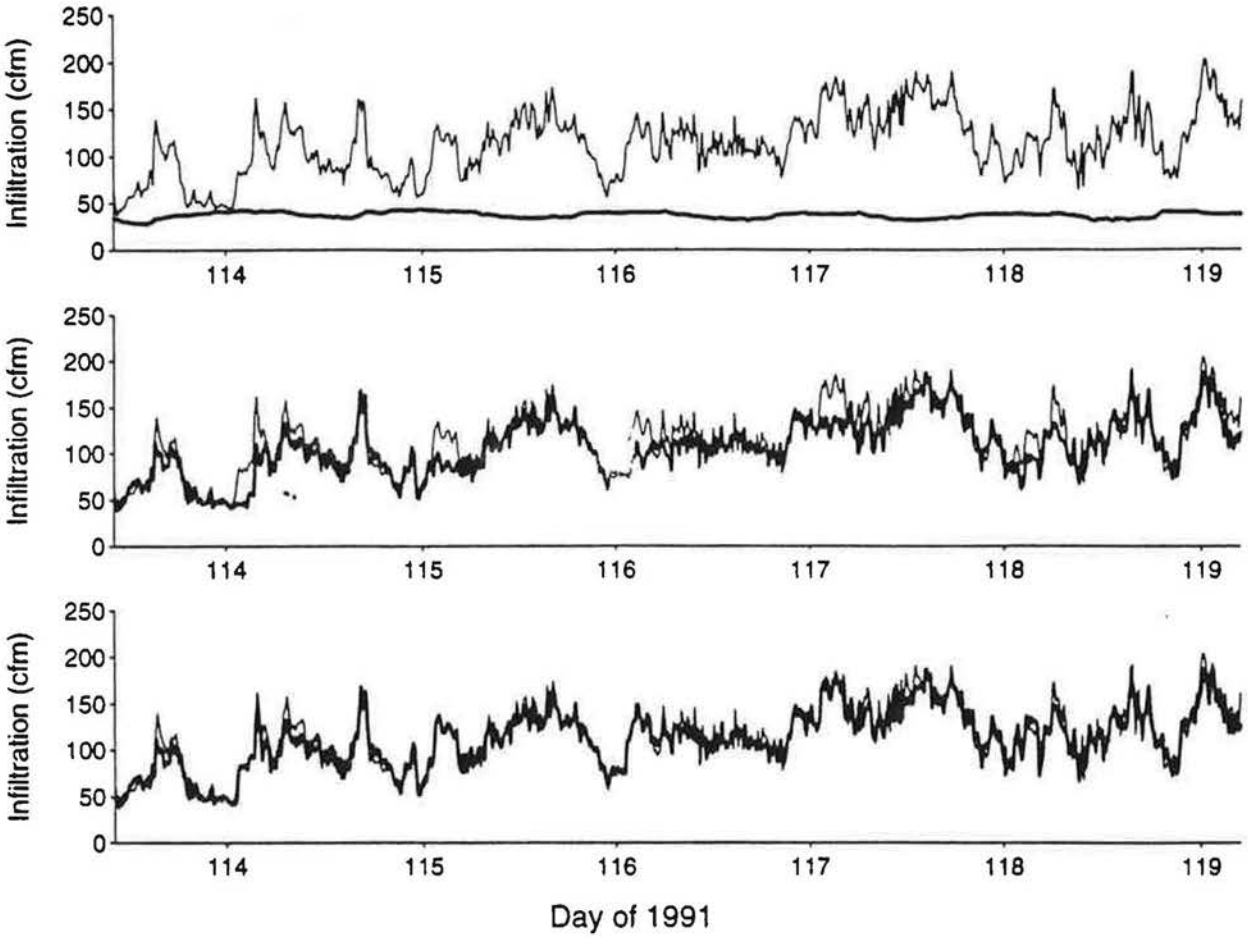

Figure C-3
Measured and predicted infiltration at Site 7

The bold line in each graph is the predicted infiltration; LBL model predictions were used for the natural infiltration. The upper graph shows stack effect only; the middle graph shows the full LBL model with the wind effect reduced by 10% prior to combination. The lower graph shows the prediction including the duct leakage model.

Table C-3
Summary of infiltration at Site 7

Average Infiltration Effect [1]	cfm	ACH	%	Cum %
Stack	37.4	0.230	33	33
Wind [2]	70.0	0.431	61	94
Air handler	5.3	0.033	5	99
Other fans [3]	--	--	--	99
Discrepancy	1.0	0.006	1	100
Total	113.7	0.700	100	

	Total		AH off		AH on	
Infiltration Breakdown [4]	cfm	%	cfm	%	cfm	%
Outside	106.4	95	101.9	94	119.7	97
Crawl	5.7	5	6.4	6	4.1	3
Total	112.1	100	108.3	100	123.8	100

	Total		AH off		AH on	
Exfiltration Breakdown [4]	cfm	%	cfm	%	cfm	%
Outside	97.6	87	100.1	92	73.4	59
Crawl (AH supply leak)	14.5	13	8.2	8	50.4	41
Total	112.1	100	108.3	100	123.8	100

Fan Effects [5]	Fan Flow	Induced Infiltration		Runtime
	cfm [6]	cfm	ACH	(h/day)
Air handler	680	37	0.228	3.41

	Leakage	Volume	From Ambient		Total Through Zone	
Other Zones	(in^2)	(ft^3)	cfm	ACH	cfm	ACH
Crawl	330	2436	263	6.48	277	6.82

1 Average effect of components over entire test period.
2 Additional infiltration caused by wind, calculated as the difference between the LBL full and stack models. The wind effect was multiplied by 0.9 prior to combination with the stack model.
3 Due to extreme variations in wind-induced infiltration, it is not possible to estimate the effects of these fans.
4 Summarized over periods when no one-time experiments were being performed.
5 Extra infiltration induced by operation of fans.
6 Manufacturer's rated flow.

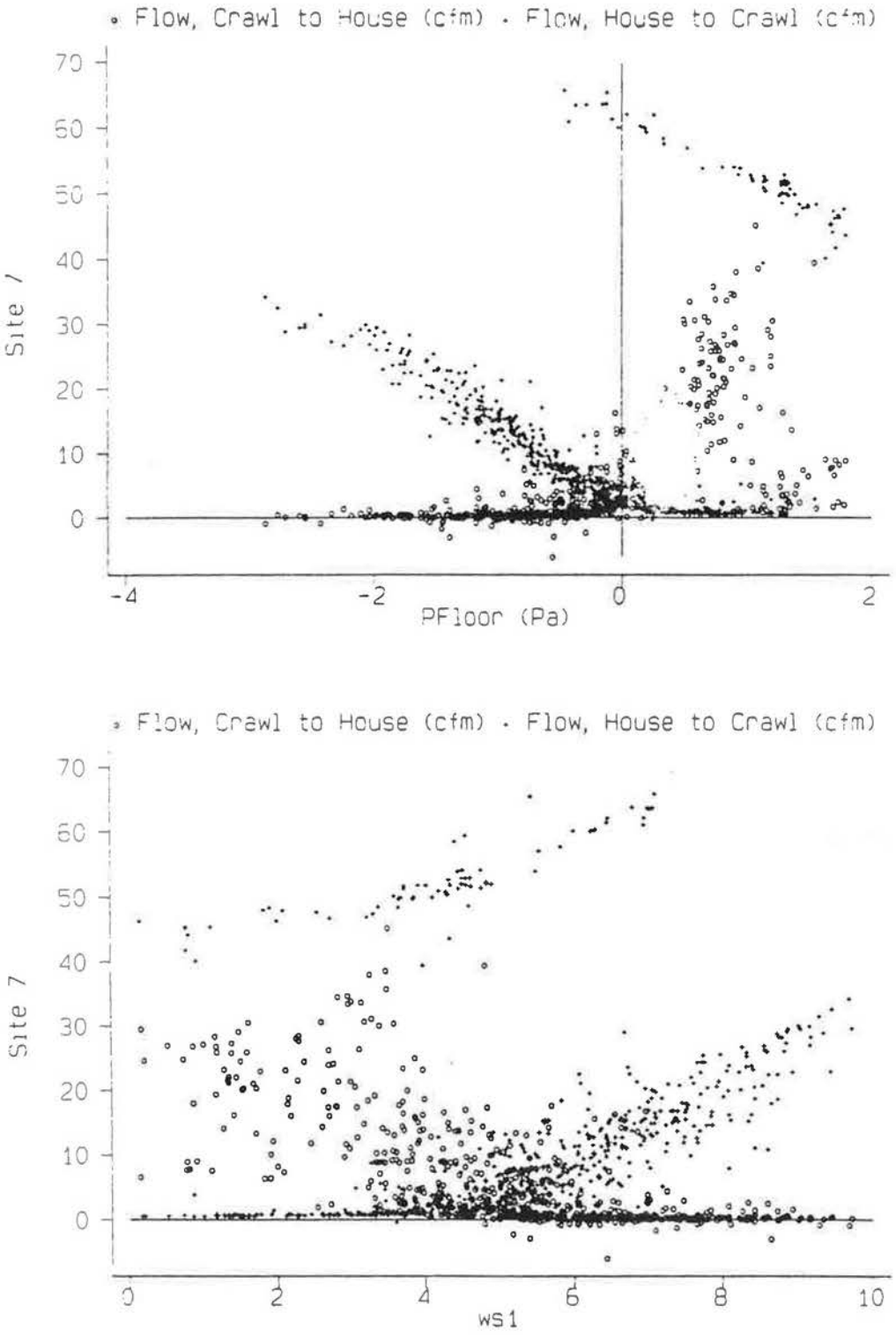

Figure C-4
Effect of crawl pressure and wind speed on flow through floor

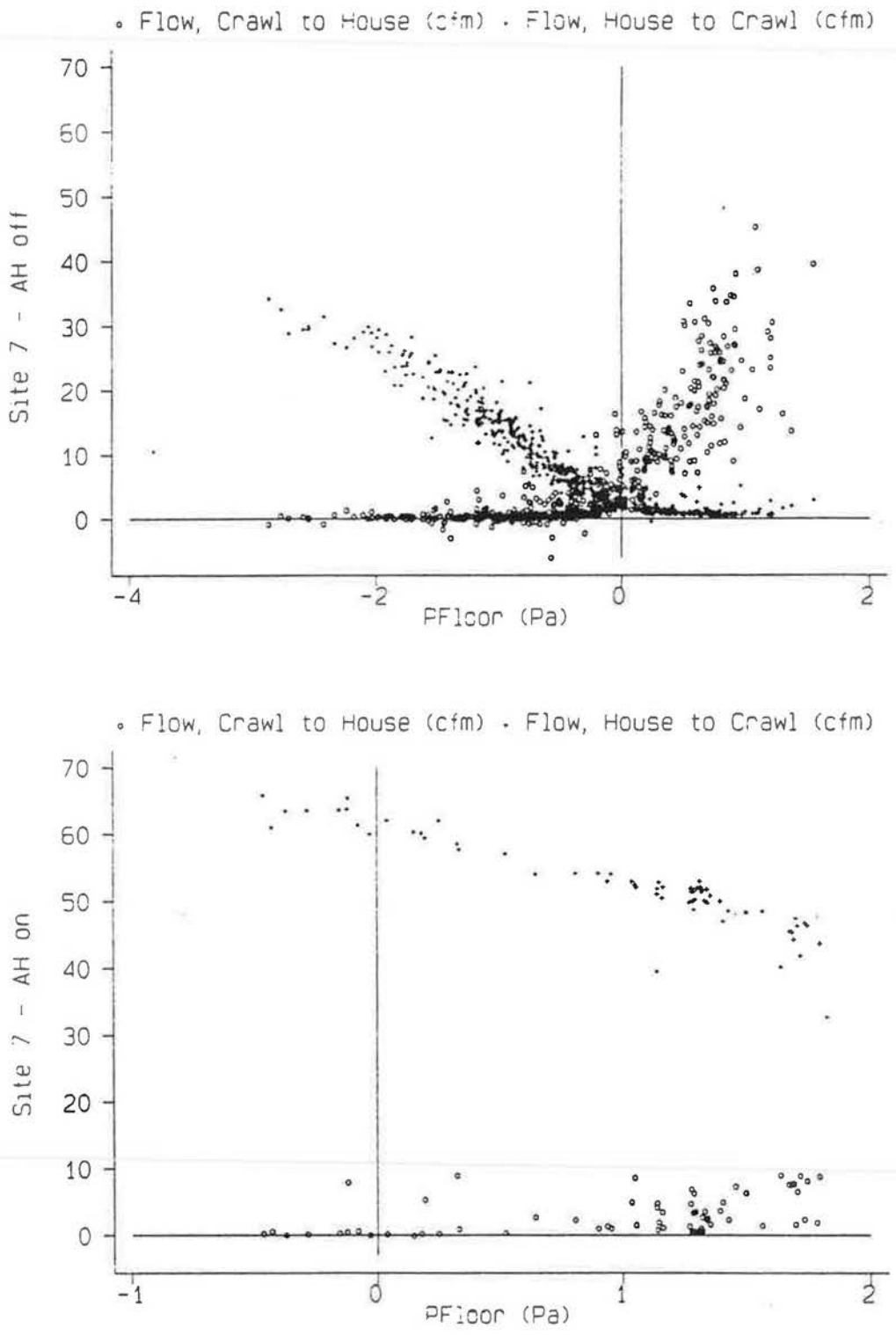

Figure C-5
Effect of air handler on flow through floor

APPENDIX D. PRESSURE COEFFICIENTS

This appendix contains pressure coefficients derived by performing regressions of measured pressures on the variables affecting those pressures. Measured wind speeds were used to calculate velocity pressures (the pressure created by moving air coming to a stop). The ratio between the actual pressure on a surface and the velocity pressure is known as the wind pressure coefficient, C_p.

Other factors which affect the pressure across a surface are the effects of stack and mechanical systems. Theory predicts that the stack pressure should be directly proportional to the indoor-outdoor temperature difference (ΔT). To a first approximation, the additional pressure induced by a mechanical device such as an exhaust fan is a constant if the flow through the fan is constant.

The pressure across a wall, ceiling or floor of an envelope can therefore be expressed as a linear function of the velocity pressure, ΔT and mechanical system operation as follows:

$$P = C_p P_v + C_s \Delta T + C_f Fan$$

where P_v is the velocity pressure, C_s is the temperature coefficient, C_f is the pressure induced by a ventilation fan, and *Fan* is a signal indicating the status of the fan (0=off, 1=on). If more than one mechanical device is present, there is a separate C_f *Fan* term for each. The coefficients in the equation can be estimated by performing regressions of the measured pressures on the indicated variables.

Tables D-1 through D-3 give the results of these regressions for measured pressures at Sites 5 through 7. At Site 5, signals from the heat pump and air-to-air heat exchanger were included in the regression. The table shows that the heat pump generally pressurizes the home, indicating that there are more return leaks than supply leaks. The air-to-air heat exchanger has little or no effect on the pressure inside the home, which is to be expected from a balanced-flow unit.

At Site 6, the furnace signal was divided into two signals, one before and one after the duct repair. This allowed the pressure effects of the air handler to be estimated

separately for each period. The operation of the air handler strongly pressurizes the home, indicating large return leaks. After the duct repair, the pressurization of the home actually increases. Repairs were made to a large return leak in the attic; however, it was later found that only part of the leak had been patched. The slight additional pressurization must be due to the repair of a supply leak, which increased the net imbalance.

Because the wind direction was quite variable at this home, the pressure experienced by each wall varies with the cosine of the wind direction. Therefore, the calculated velocity pressure was multiplied by a cosine function before using it in the regression.

The wind at Site 7 was the primary cause of pressure across the envelope. Although there was stack effect at this home, and the bathroom exhaust fan was operated regularly, the pressure induced by these effects were so small relative to the wind pressures that they could not be distinguished in the data. Therefore, only the velocity pressure and the air handler fan signal was included in the pressure regressions. The table shows that operation of the air handler depressurizes the home; this occurs because of supply leaks to the crawl space.

Table D-1
Results of pressure regressions for Site 5

Pressure Transducer	Average ΔP (Pa)	ΔC_p [1]	ΔT (Pa/ C)	HP Signal (Pa)	AAHX Signal (Pa)	Const (Pa)
Attic (S)	1.24	-0.01	0.092	0.60 [2]	-0.02	0.14
Attic (N)	1.35	0.00	0.096	0.69 [2]	-0.00	0.10
Crawl (High)	-1.48	0.01	-0.135	0.33	0.03	-0.21
Crawl (Low)	-1.91	0.02	-0.144	0.23	-0.00	0.05
West (S, 2nd)	-1.83	0.45	0.020	0.56	0.01	0.63
West (S, 1st)	-2.65	0.50	-0.055	0.34	0.03	0.68
West (N, 2nd)	-1.45	0.39	-0.028	0.45	0.09	0.05
West (N, 1st)	-3.17	0.57	-0.046	0.38	0.08	0.85
North	-0.02	0.01	0.001	-0.04	0.10	-0.01
South (Low)	-0.30	-0.31	-0.142	0.44	-0.21	-0.43
South (High)	-0.17	-0.15	-0.058	0.54	-0.09	0.01
East (Gar door)	1.67	-0.24	0.036	0.71	-0.01	-0.25
House	0.74	-0.09	-0.045	0.37	0.06	-0.62

1 Using wind speed from Tower 1.
2 Air handler depressurizes attic.

Table D-2
Results of pressure regressions for Site 6 (cosine fits used for wall pressures)

Pressure Transducer	Average ΔP (Pa)	ΔC_p [1]	ΔT (Pa/ C)	Fan Sig [2] (Pa)	Fan Sig [3] (Pa)	Const (Pa)
South	0.18	0.38	-0.112	5.64	5.93	-0.05
North (1st)	0.20	-0.49	-0.088	5.62	6.00	-0.17
North (2nd)	1.56	-0.60	0.022	5.57	5.93	-0.28
West (1st)	0.01	0.50	-0.112	5.54	5.90	-0.03
West (2nd)	1.54	0.49	0.012	4.98	5.57	-0.05
East (1st)	0.37	-0.57	-0.100	5.61	5.99	0.01
East (2nd)	1.82	-0.47	0.009	5.61	5.92	-0.00
Attic (High)	2.99	0.02	0.096	5.70	6.00	0.02
Attic (Low)	2.62	0.03	0.086	5.65	5.92	-0.20
Crawl (W)	-0.21	0.04	-0.150	5.33	5.74	0.23
Crawl (E)	-0.44	-0.01	-0.155	5.43	5.93	-0.00
Garage door	0.59	0.26	-0.086	5.52	5.95	0.03
4-wall average	0.23	-0.17	0.084	5.23	5.64	-0.07
House	0.41	-0.07	0.098	5.27	5.57	0.19

1 Using wind speed from Tower 1.
2 Prior to repairs.
3 After repairs.

Table D-3
Results of pressure regressions for Site 7

Pressure Transducer	Average ΔP (Pa)	ΔC_p [1]	AH Signal (Pa)	Const (Pa)
West (Low)	-8.50	0.48	-1.47	0.02
West (High)	-7.37	0.48	-1.44	1.15
East (Low)	4.48	-0.26	-0.90	0.05
East (High)	5.04	-0.23	-0.86	0.98
North	-8.01	0.38	0.01	-1.06
South	5.57	-0.37	-0.03	-0.71
Crawl (Over blanket)	0.19	-0.06	-1.43	-0.57
Crawl (Master bedroom)	0.16	-0.06	-1.00	-0.74
Crawl (Den)	0.97	-0.07	-0.94	-0.14
Attic (MBr, low)	1.72	-0.05	-0.79	1.14
Attic (MBr, high)	0.81	0.02	-0.78	1.30
Attic (West)	-7.27	0.47	-2.13 [2]	1.21
Attic (East)	3.34	-0.13	-0.81	1.15
4-wall average	1.81	0.08	0.45	0.43
House	2.33	0.08	0.47	0.71

1 Using wind speed from tower 1.
2 Blend-Air unit pressurizes the attic when air handler is on.

APPENDIX E. BLOWER DOOR RESULTS

This appendix presents results from blower door tests, including low-pressure tests, performed during Phase II. Sites 1 through 3 and Sites 5 through 7 were tested between August and October of 1991. The test on Site 4 had been completed during Phase I.

Each graph shows flow through the blower door fan versus pressure across the building envelope on a log-log scale. Each circle represents one data point, which is an average of six instantaneous measurements. The data points are clustered into pressure stations; typically, twenty points were recorded at each station.

The solid line in each graph is the flow prediction from the leakage function derived from high-pressure data (typically 16 to 60 Pa). The vertical lines indicate the range of data from which the high-pressure leakage function was derived.

Sites 1 and 5, especially Site 1, were tested under the best conditions. The results from each site show small departures from the power law at low pressures; the extrapolation tends to overpredict flow and the apparent exponent increases at lower pressures, eventually looking laminar. To the extent that these measurements are representative, they suggest that the Ethridge description of cracks with both a laminar and an inertial loss is more appropriate than the power law. In the houses with the best data, however, the departure from the power law is not large.

In spite of trying to obtain optimum conditions, these effects could also be caused by bias due to pre-existing stack or wind pressures, or by systematic error when using the smallest orifice on the blower door. Similar low-pressure tests should be done on a large number of homes before drawing firm conclusions about the low pressure relationship.

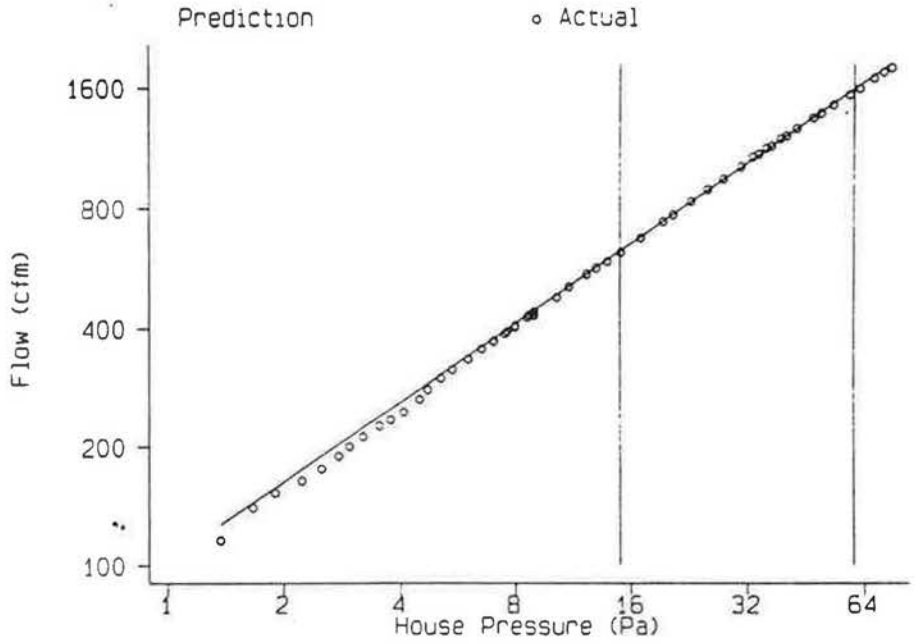

Figure E-1
Results from blower door test at Site 1, using pressure across the floor as envelope pressure

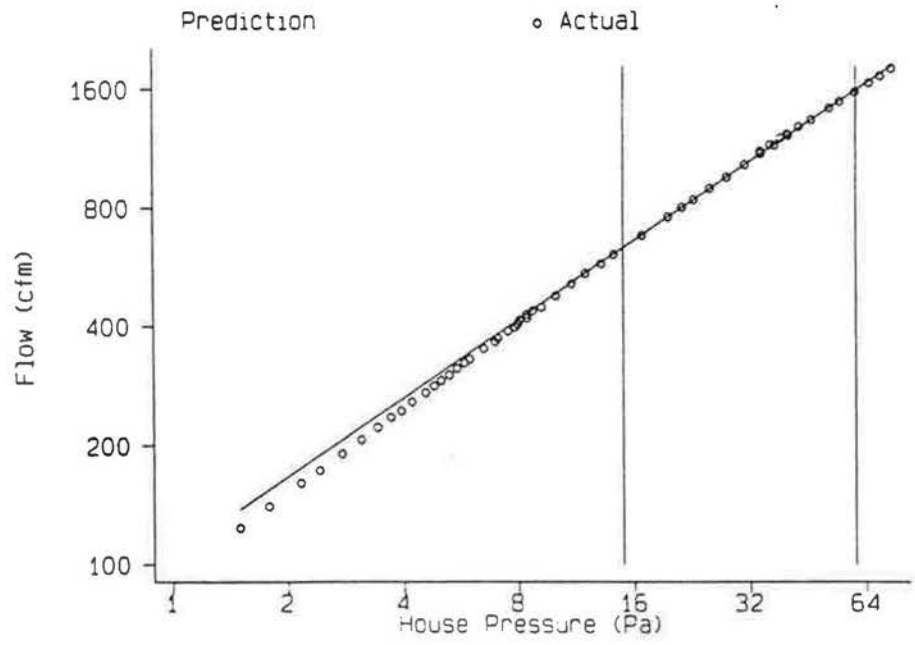

Figure E-2
Results from blower door test at Site 1, using pres e across the ceiling as envelope pressure

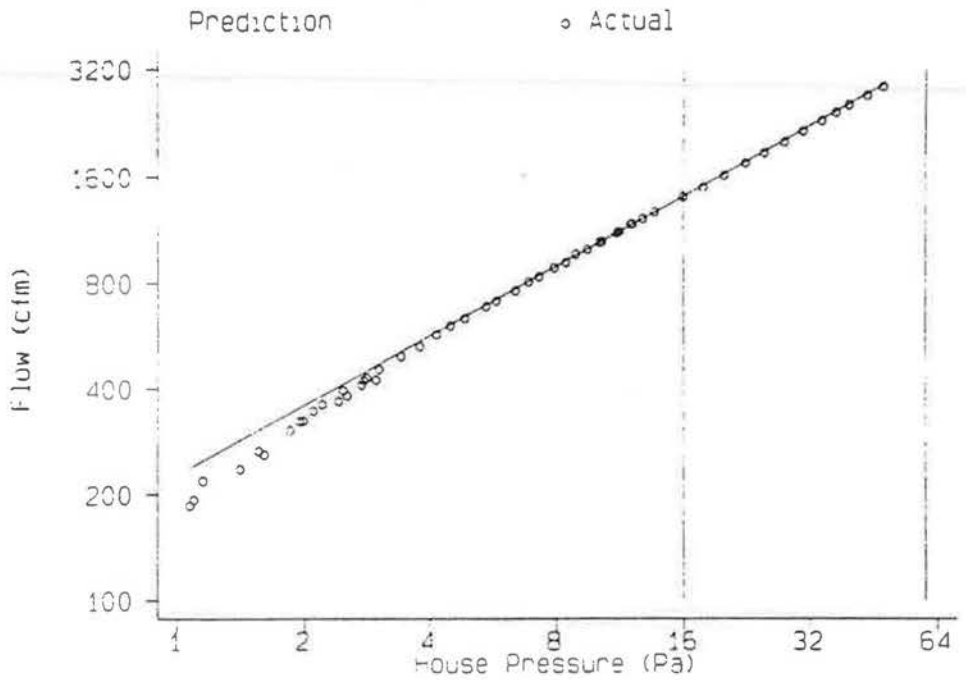

Figure E-3
Results from blower door test at Site 2

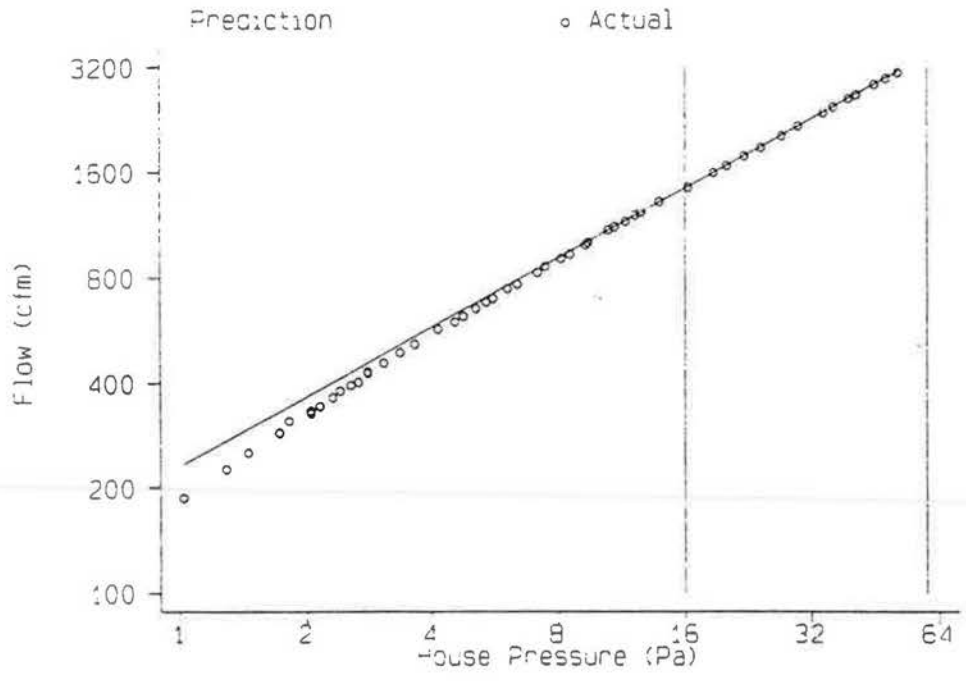

Figure E-4
Results from blower door test at Site 3

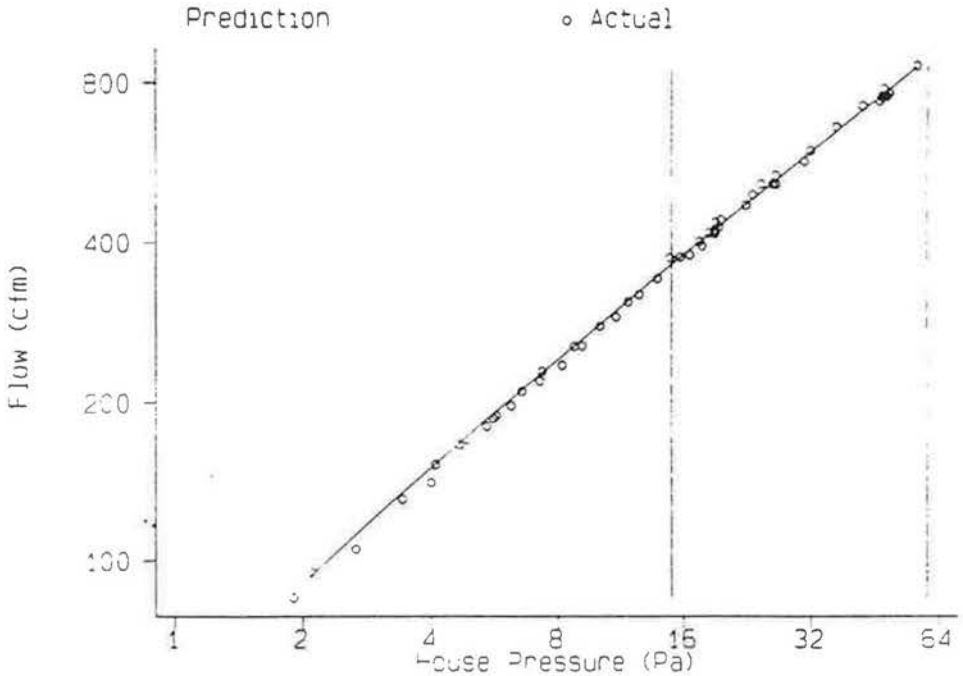

Figure E-5
Results from blower door test at Site 4

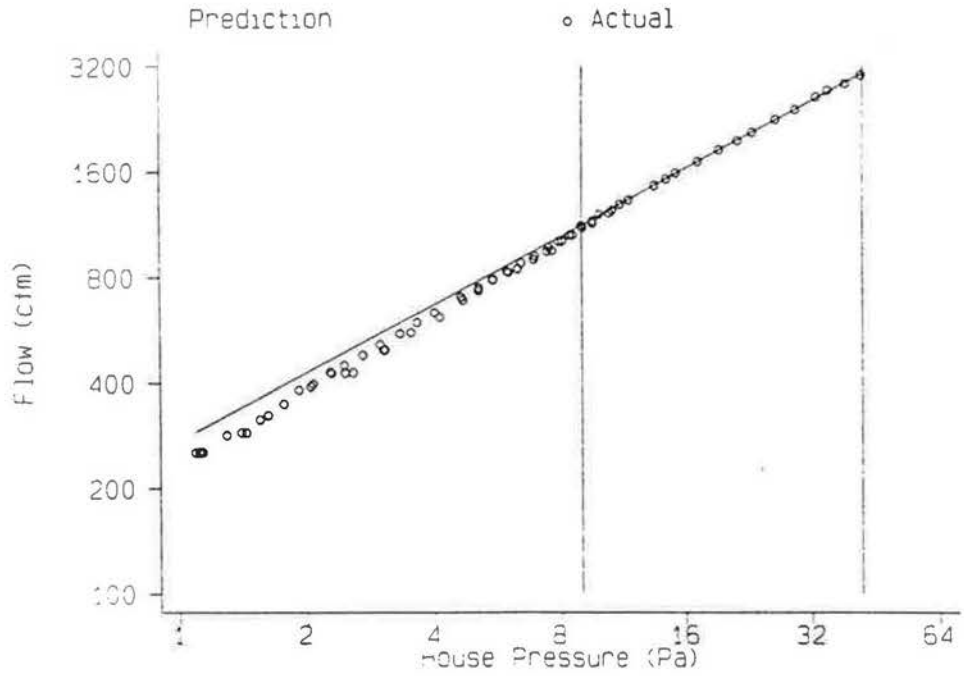

Figure E-6
Results from blower door test at Site 5

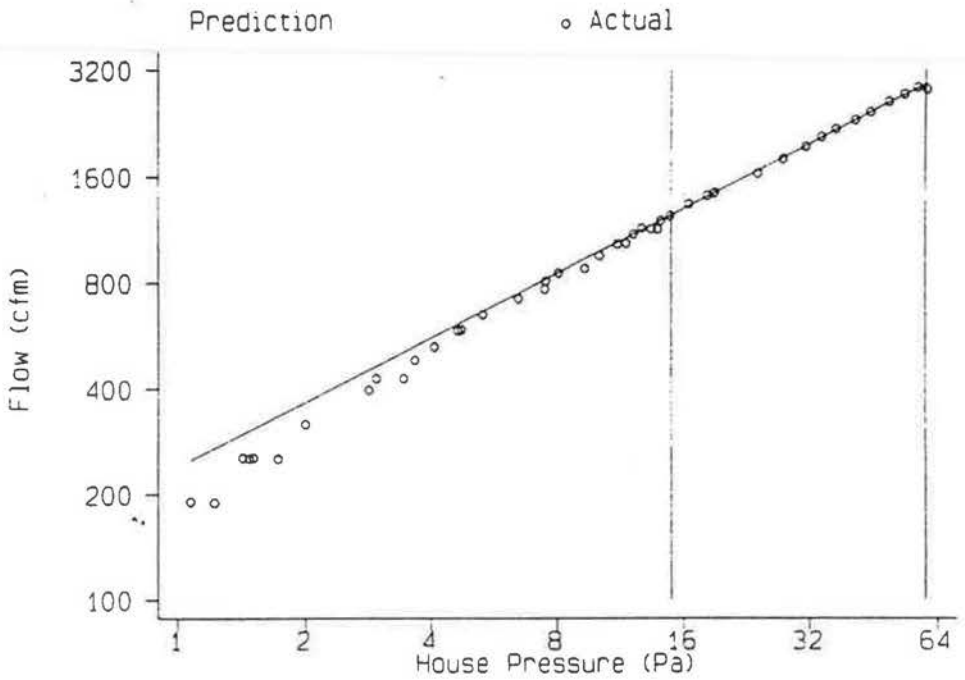

Figure E-7
Results from blower door test at Site 6

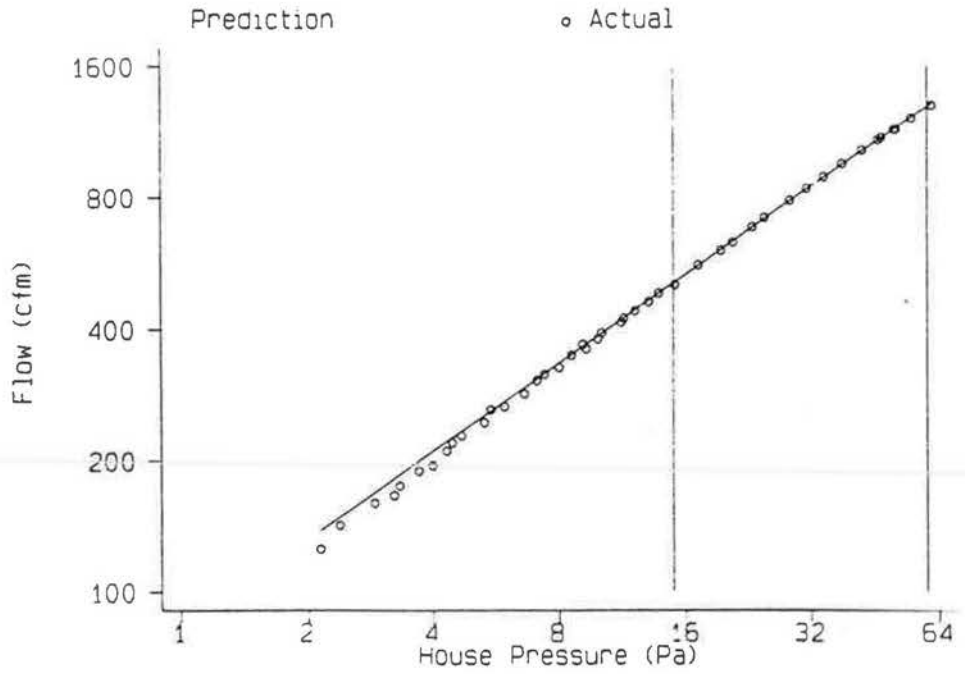

Figure E-8
Results from blower door test at Site 7

APPENDIX F. LBL AND AIM MODELS

Definitions

Building characteristics

n Building leakage exponent from blower door test

C Building leakage coefficient from blower door test ($m^3/s \cdot Pa^n$)

A_o Total leakage area (Effective Leakage Area from blower door test, m^2) defined as

$$C(\Delta P_{ref})^n \sqrt{\frac{\rho_{ref}}{2\Delta P_{ref}}}$$

where ΔP_{ref} is 4 Pa and ρ_{ref} is a reference density; 1.2 kg/m^3 was used for these homes.

A_c Leakage area in ceiling (m^2)

A_f Leakage area in floor (m^2)

h Average stack height (m)

The distribution of leakage in a building is expressed by two variables:

R Fraction of leakage area in floor and ceiling, or

$$R = \frac{A_c + A_f}{A_o}$$

X Leakage distribution parameter, given by

$$X = \frac{A_c - A_f}{A_o}$$

Wea r and site conditions

C'	Generalized shielding coefficient for LBL model; shielding classes are listed in Table F-1
g	Gravitational acceleration (m/s^2)
ρ_o	Outdoor density (kg/m^3)
T_i	Indoor temperature (K)
T_o	Outdoor temperature (K)
ΔT	$T_i - T_o$ (K)
S_w	Local d shelter co ient for IM-2 model
v	Wind s d at site (m/

LBL Model

Stack Effect

$$Q_s = \frac{A_o}{3}\sqrt{gh\frac{|\Delta T|}{T_i}}\left(1+\frac{R}{2}\right)\left(1-\frac{X^2}{(2-R)^2}\right)^{3/2} \qquad \text{(F-1)}$$

Wind Effect (Standard LBL Model)

$$Q_w = A_o v(1-R)^{1/3} C' \qquad \text{(F-2)}$$

Wind Effect (Modified LBL Model)

$$Q_w = A_o v(1-R)^{0.8} C' \qquad \text{(F-3)}$$

Site wind speed

The site wind speed v can be related to v', the wind speed at the airport, by

$$v = v'\left(\frac{\alpha(h/10)^{\gamma}}{\alpha'(h'/10)^{\gamma'}}\right) \qquad \text{(F-4)}$$

where α and γ are given for each terrain class in Table F-2 and h is the height of the wind tower; the primed quantities are from a wind measurement site such as an airport.

Combined LBL Model

$$Q_f = \sqrt{Q_s^2 + Q_w^2} \tag{F-5}$$

The tables below give the values of terrain and shielding parameters as defined in the LBL model (Sherman, 1980).

Table F-1
Generalized shielding coefficient versus local shielding

Shielding Class	C'	Description
1	0.324	No obstructions or local shielding whatsoever
2	0.285	Light local shielding with few obstructions
3	0.240	Moderate local shielding, some obstructions within two house heights
4	0.185	Heavy shielding, obstructions around most of perimeter
5	0.102	Very heavy shielding, large obstruction surrounding perimeter within two house heights

Table F-2
Terrain parameters for standard terrain classes

Class	γ	α	Description
1	0.10	1.30	Ocean or other body of water with at least 5 km of unrestricted expanse
2	0.15	1.00	Flat terrain with some isolated obstacles (e.g. buildings or trees well separated from each other)
3	0.20	0.85	Rural areas with low buildings, trees, etc.
4	0.25	0.67	Urban, industrial or forest areas
5	0.35	0.47	Center of large city (e.g. Manhattan)

The terrain and shielding classes have been changed from Roman to Arabic numerals.

AIM-2 Model

Stack Effect

$$Q_s = Cf_s(P_s)^n \tag{F-6}$$

where P_s, the stack pressure, is

$$P_s = \rho_o g h\left(\frac{T_i - T_o}{T_i}\right) \tag{F-7}$$

and f_s, the stack flow factor, is

$$f_s = \left(\frac{1+nR}{n+1}\right)\left(\frac{1}{2} - \frac{1}{2}\left(\frac{X^2}{2-R}\right)^{5/4}\right)^{n+1} \tag{F-8}$$

Wind Effect

$$Q_w = Cf_w(P_w)^n \tag{F-9}$$

where P_w, the wind pressure, is

$$P_w = \rho_o \frac{(S_w v)^2}{2} \tag{F-10}$$

The factor f_w differs for homes with crawl spaces and slab-on-grade foundations, because the entire floor of a home with a crawl space sees the pressure difference across the floor, whereas only the edges of the floor see this pressure difference in a slab-on-grade home.

For homes with crawl spaces,

$$f_w = 0.19(2-n)\left(1 - R\left(\frac{n}{2} + 0.2\right)\right)\left(1 - \left(\left(\frac{X - 0.2(1-R)}{2-R}\right)^2\right)^{0.75}\right) \tag{F-11}$$

and for homes with slab-on-grade or basement foundations,

$$f_w = 0.19(2-n)\left(1 - \left(\frac{X+R}{2}\right)^{1.5}\right) \tag{F-12}$$

The AIM-2 wind model also includes a method for extrapolating airport wind speeds to the site which is not presented here.

Combined AIM-2 Model

$$Q_f = \left(Q_s^{1/n} + Q_w^{1/n} - \frac{1}{3}(Q_s Q_w)^{1/2n} \right)^n \qquad \text{(F-13)}$$

where the factor of (-1/3) has been experimentally determined.